Politecnico di Milano

Facoltá di Ingegneria dei Processi Industriali

Corso di Laurea Specialistica in Ingegneria Nucleare

Dipartimento di Energia

Multiphysics models for new generation LWRs

Relatore: Prof. Antonio CAMMI

Correlatore: Ing. Davide PAPINI

Tesi di Laurea di:

Giovanna MALATESTA Matr. 734638

Anno accademico 2009-2010

Contents

Abstract **viii**

Estratto in lingua italiana **x**

Introduction **1**

1 Models for mixtures of water and steam in heated channels **4**

1.1 Introduction 5

1.2 The building up of the models 8

1.2.1 The building up of the one-dimensional model 9

1.2.2 The building up of the zero-dimensional model 19

1.3 The implementation of the models 25

1.3.1 The implementation of water thermodynamical and physical properties 26

1.3.2 The implementation of the one-dimensional model equations 28

1.3.3 The implementation of the zero-dimensional model equations 31

1.4 The validation of models 31

1.4.1 The collection of experimental data 32

1.4.2 The collection of simulated data 33

1.4.3 Comparison between experimental data and simulated data . 35

1.5 Conclusion 35

Nomenclature 41

Bibliography 43

2 A multi-physics zero-dimensional model for LWRs **44**

2.1 Introduction 45
2.2 A short description of SURE 46
2.3 The neutronics model 51
2.3.1 The Avery and Cohn formulation of the point kinetic theory 53
2.3.2 The application of the Avery and Cohn formulation of the point kinetic theory to SURE 55
2.3.3 The simulation results 57
2.4 The neutronics and thermo-hydraulics model 59
2.4.1 The application of the zero-dimensional thermo-hydraulics model to SURE 60
2.4.2 The deduction of coupling equations between the neutronics model and the thermo-hydraulics one 65
2.4.3 The simulation results 67
2.5 Conclusion 74
Nomenclature 75
Bibliography 78

3 A multi-physics one-dimensional model for LWRs 79
3.1 Introduction 80
3.2 A short description of MARS 82
3.3 The neutronics model 86
3.3.1 The two region and two group formulation of the diffusion theory 87
3.3.2 The application of the two region and two group formulation of the diffusion theory to MARS 91
3.3.3 The simulation results 96
3.4 The neutronics and thermo-hydraulics model 105
3.4.1 The application of the one-dimensional thermo-hydraulics model to MARS 106
3.4.2 The deduction of coupling equations between the neutronics model and the thermo-hydraulics one 108
3.4.3 The simulation results 113

3.5 Conclusion 119
Nomenclature 121
Bibliography 124

Conclusion **125**

A The one-dimensional thermo-hydraulics model **127**

B The zero-dimensional thermo-hydraulics model **130**

C The zero-dimensional neutronics model **134**

D The zero-dimensional neutronics and thermo-hydraulics model **135**

E The one-dimensional neutronics model **139**

F The one-dimensional neutronics and thermo-hydraulics model **141**

Nomenclature **146**

Bibliography **150**

List of Figures

1.1 The physical system considered 6
1.2 The one-dimensional scheme of the physical system considered . . . 7
1.3 The zero-dimensional scheme of the physical system considered . . . 7
1.4 The Moody diagram 11
1.5 The Nelson Martinelli diagram 15
1.6 Water viscosity dependence on pressure and enthalpy 28
1.7 The facility of the SIET thermo-hydraulics laboratories 33
1.8 Experimental pressure distributions and simulated ones with the one-dimensional model at 20 bar, 40 bar, and 60 bar 36
1.9 Experimental pressure distributions and simulated ones with the zero-dimensional model at 20 bar, 40 bar, and 60 bar 37
1.10 Comparison between experimental and simulated with the one-dimensional model pressure distributions at 20 bar, 40 bar, and 60 bar 38
1.11 Simulated temperature distributions with the one-dimensional model at 20 bar, 40 bar, and 60 bar 39
1.12 Simulated temperature distributions with the zero-dimensional model at 20 bar, 40 bar, and 60 bar 40

2.1 A pattern of the power plant in which SURE works 47
2.2 An axial section of the whole SURE reactor, of its core and of its single fuel element 48
2.3 Results of a previous work carried out on SURE here adopted . . . 52

2.4 SURE responses in a zero power condition to a positive reactivity steps of 1 % and a negative one determined respectively considering or not the precursors 57
2.5 SURE response in a zero power condition to positive reactivity steps of different entities determined considering the precursors 58
2.6 SURE response in a zero power condition to negative reactivity steps of different entities determined considering the precursors 58
2.7 SURE fuel properties versus temperature 65
2.8 SURE response in a normal operating condition to positive and negative inlet coolant mass flow rate steps of different entities 71
2.9 SURE response in a normal operating condition to positive and negative inlet coolant temperature steps of different entities 72
2.10 SURE properties variations in a normal operating conditions after a inlet coolant mass flow rate step of 1 % given 10 s after the beginning of the simulation 73
2.11 Coolant mass flow rate after a inlet perturbation of 1 % and coolant enthalpy after a inlet perturbation of 1 ℃ 74

3.1 The one-dimensional scheme of LWR considered 81
3.2 A pattern of the power plant in which MARS works 83
3.3 The MARS safety system SCCS 86
3.4 The MARS safety system ATTS 87
3.5 Effective multiplicative factor versus core macroscopic absorption cross section 95
3.6 Nominal spatial distributions of the MARS neutron fluxes 102
3.7 MARS response in a zero power condition to a negative core absorption macroscopic cross section step of 0.01 % given 5 s after the beginning of the simulation and a positive one of 0.01 % given 7 s after this time without the precursors 102

3.8 MARS response in a zero power condition to a negative core absorption macroscopic cross section step of 0.1 % given 5 s after the beginning of the simulation and a positive one of 0.1 % given 7 s after this time with the precursors 103
3.9 Stationary state reached by MARS after a negative core absorption macroscopic cross section step of 0.1 % and a positive one given 5 s and 7 s after the beginning of the simulation without the precursors 103
3.10 MARS response in a zero power condition to negative core absorption macroscopic cross section steps of different entities with the precursor 104
3.11 MARS response in a zero power condition to positive core absorption macroscopic cross section steps of different entities with the precursor 104
3.12 MARS nominal thermo-hydraulics condition 114
3.13 MARS response since its nominal condition to a core absorption macroscopic cross section step 116
3.14 MARS response since its nominal condition to a inlet coolant mass flux step 117
3.15 MARS response since its nominal condition to a inlet coolant temperature step 118
3.16 Coolant enthalpy after a inlet coolant temperature step of 1 ℃ . . . 120

List of Tables

2.1 Constructive features of SURE 49
2.2 Functional features of SURE 50
2.3 Results of a previous work carried out on SURE here adopted . . . 51
2.4 Delayed neutron fractions and decay constants for uranium 235 precursor groups 56
2.5 SURE geometrical features 65
2.6 SURE thermohydraulics nominal state 70

3.1 Constructive features of MARS 84
3.2 Functional features of MARS 85
3.3 Neutronic features of MARS 93
3.4 MARS uranium properties 101
3.5 MARS geometrical features 106
3.6 Fuel coefficients corresponding to different fuel feedback coefficients 111
3.7 Coolant coefficients corresponding to different coolant feedback coefficients 112
3.8 MARS fuel rod thermal conductivity coefficients and thermal resistances 113

Abstract

The object of the present work is the LWRs modeling by means of a multi-physics approach.

Modeling nuclear fission reactors requires to focus the attention both on the single physics taking part in their functioning and on the effects due to the interactions between them: such an aim is perfect to face with a multi-physics approach.

Two models has been so developed: a 0-D one for SURE (acronym for *Study on nUclear Reactor dEvolopment*), a Generation III+ BWR reactor conceived at *Politecnico di Milano*, and a 1-D for MARS (acronym for *Multipurpose Advanced Reactor inherently-Safe*), a Generation III+ PWR conceived at *LA SAPIENZA Università di Roma*.

Three steps have been accomplished. At first, a 0-D thermo-hydraulics model and a 1-D one have been deduced and implemented so as to reproduce the behavior of water and steam mixtures in heated channels; an important choice made in this first part concerns the physical model to adopt for the phase change: the *Equilibrium Drift Flux Model*. At second, a 0-D neutronics model and a 1-D one have been chosen and implemented so as to reproduce the zero power reactor dynamics and to do that the point kinetic theory and the diffusion one respectively have been adopted. Finally, the 0-D models and the 1-D ones have been opportunely coupled: the result has been a simulating tool, both 0-D and 1-D, able to reproduce the reactor dynamics in a normal operating condition. Several simulations have been performed in order to verify the validity of each model.

That has been possible thanks to two codes: *COMSOL Multiphysics*, used to implemented the equations, and *MATLAB*, used to implement the physical and thermodynamical water properties.

The result obtained can be considerer very good: indeed, on one hand all the simulations performed show a certain reliability and on the other hand the employing of a multi-physics approach, put in use by means of *COMSOL Multiphysics*, allows to reach such an aim in a relative simply way.

Estratto in lingua italiana

Il tema affrontato nel presente lavoro è la modelizzazione multi-fisica di reattori nucleari a fissione, in particolare di LWRs.

Con il termine "multi-fisica" si intende un nuovo modo di affrontare la modellizzazione e la simulazione di sistemi fisici complessi: la visione circoscritta ai singoli fenomeni che in essi si manifestano tipica di un approccio tradizionale, infatti, viene con esso sostituita da una visione più ampia che oltre ad essi ingloba anche gli effetti delle loro interazioni. Numerosi i vantaggi: primo fra tutti la possibilità di descrivere in modo più rigoroso il comportamento di tali sistemi fisici a fronte per altro di una riduzione dei tempi impiegati.

Sicuramente quello della produzione di energia elettrica da fonte nucleare è tra i settori indutriali che maggiormente può beneficiare di un tale approccio: in esso infatti convivono sia discipline per così dire tradizionali, come la termo-idraulica e la termo-meccanica, sia discipline più specifiche, come la neutronica e la radio-protezione, l'accoppiamento tra le quali è assolutamente imprescindibile. E ciò è tanto più vero nella modellizzazione e nella simulazione della dinamica dei reattori nucleari a fissione nella quale fisiche tanto diverse si intrecciano e si influenzano vicendevolmente.

Lo scopo del presente lavoro è proprio quello di creare modelli multi-fisici per due LWRs di nuova generazione: SURE, del quale ne è stato ideato uno zero-dimensionale, e MARS, del quale ne è stato ideato invece uno mono-dimensionale.

Qualche informazione a riguardo. SURE (acronimo per *Study on nUclear Reactor dEvolopment*) è un BWR di Generation III+ ideato presso il *Dipartimento di Energia* del *Politecnico di Milano*; oltre al particolare campo di applicazione, nasce infatti per alimentare stazioni spaziali, una sua caratteristica peculiare è rappre-

sentata dall'adozione di un sistema di controllo della potenza del tutto innovativo basato, invece che su inserimento e disinserimento di organi di controllo, sulle variazioni della portata in massa di refrigerante primario. Invece MARS (acronimo per *Multipurpose Advanced Reactor inherently-Safe*), ideato presso il *Dipartimento di Ingegneria Nucleare e Conversioni dell'Energia* de *LA SAPIENZA Università di Roma*, è un PWR di Generation III+ concepito nell'ottica di individuare il miglior compromesso tra un buon livello della sicurezza e una netta riduzione dei costi: in esso, infatti, tecniche di sicurezza basate sull'inevitabile manifestazione di fenomeni fisici naturali come la dilatazione termica e la circolazione naturale trovano posto accanto a soluzioni costruttive che consentono di smontare e sostituire anche quei componenti che sono maggiormente predisposti al danneggiamento.

Tre sono le fasi attraverso le quali il modello zero-dimensionale di SURE e quello mono-dimensionale di MARS sono stati creati.

Durante una prima fase si è proceduto alla deduzione di due modelli matematici di termo-idraulica, uno zero-dimensionale ed uno mono-dimensionale, capaci di descrivere il comportamento delle miscele di acqua e vapore all'interno di canali riscaldati. Per fare ciò, oltre ad assumere ovviamente le ipotesi di zero-dimensionalità nel primo caso e di mono-dimensionalità nel secondo, si è scelto di adottare il *Equilibrium Drift Flux Model*: una tale scelta rappresenta, infatti, il miglior compromesso tra la semplicità dei calcoli e la bontà dei risultati.

Si è poi passati in un secondo momento alla deduzione di due modelli matematici di neutronica, uno zero-dimensionale ed uno mono-dimensionale, capaci di descrivere la dinamica dei reattori nucleari a fissione a potenza zero. La necessità questa volta di ricercare il miglior compromesso tra la reperibilità dei dati e la bontà dei risultati ha condotto all'adozione per il primo di una formulazione a due regioni della teoria della cinetica puntiforme, quella di Avery and Cohn per l'esattezza, e per il secondo di una formulazione a due regioni e a due gruppi energetici della teoria della diffusione: come è noto, infatti, i parametri neutronici come le probabilità di trasferimento per i neutroni tra nocciolo e riflettore o come le sezioni d'urto macroscopiche relative ad un determinato intervallo di energie non sono facilmente calcolabili e, anzi, una loro determinazione richiederebbe pratica-

mente lo svolgimento di un lavoro a parte.

Neutronica e termo-idraulica sono state dunque adattate a SURE nel caso zero-dimensionale e a MARS nel caso mono-dimensionale per poi poter essere finalmente accoppiate: sono stati così dedotti dei modelli matematici capaci di descrivere la loro dinamica in condizioni normali di funzionamento. Tradizionale l'accoppiamento nel caso zero-dimensionale, molto interessante invece la procedura adottata per realizzarlo nel caso mono-dimensionale: l'andamento delle sezioni d'urto macroscopiche con la temperatura del combustibile e con quella del moderatore, infatti, è stato dedotto calcolando i valori del coefficiente di moltiplicazione effettivo corrispondenti a diverse composizioni del nocciolo, corrispondenti cioè a diversi valori delle temperature dette.

Tutti i modelli matematici dedotti, sia quelli disaccoppiati di termo-idraulica e di neutronica che quelli accoppiati, sono stati implementati e numerose simulazioni sono state effettuate al fine di verificarne l'attendibilità. In particolare poi di quelli di termo-idraulica è stato possibile effettuare una vera e propria validazione sperimentale: si avevano infatti a disposizione numerosi dati sperimentali relativi ad esperienze effettuate presso i laboratori di Piacenza della SIET su un generatore di vapore elicoidale.

Due gli strumenti che hanno reso possibile lo svolgimento del presente lavoro: *COMSOL Multiphysics* and *MATLAB*. Il primo, utilizzato per implementare le equazioni, è un codice capace di risolvere problemi matematici basati su equazioni differenziali alle derivate parziali utilizzando il metodo degli elementi finiti, caratteristica questa che lo rende particolarmente idoneo a risolvere problemi scientifici ed ingegneristici con un approccio di tipo multi-fisico. Il secondo, utilizzato invece per implementare le proprietà fisiche e termodinamiche dell'acqua, è un codice capace di risolvere sia numericamente sia simbolicamente problemi di calcolo matriciale.

Due importanti aspetti sono emersi dallo svolgimento del presente lavoro e, in particolar modo, dalla relatività semplicità con la quale è stato possibile implementare e simulare tutti i modelli matematici dedotti e dalla bontà dei risultati così ottenuti. Il primo è totalmente indipendente dalle considerazioni svolte sulla

modelizzazione e sulla simulazione multi-fisica e riguarda l'attendibilità dei modelli di termo-idraulica creati, soprattutto di quello mono-dimensionale: la validazione condotta su di esso, infatti, ha evidenziato la sua ottima consistenza con i dati sperimentali. Il secondo, invece, è una conferma proprio delle considerazioni fatte a tale proposito: i vantaggi che, sia in termini di semplicità che in termini di tempo, possono essere ottenuti quando nella modelizzazione e nella simulazione di sistemi fisici complessi come i reattori nucleari a fissione ci si avvale di un approccio multi-fisico sono infatti notevoli.

Tutto ciò rende possibile a questo punto prevedere anche possibili sviluppi futuri. Due sono le direzioni lungo le quali ci si potrebbe muovere: la prima è basata sui soli risultati ottenuti con il modello di termoidraulica monodimensionale e prevederebbe la modelizzazione della circolazione naturale all'interno di canali chiusi, tema quest'ultimo di grande interesse nello studio di eventuali situazioni incidentali all'interno di un nocciolo; la seconda prende invece spunto dal modello creato per MARS e prevederebbe, attraverso un adeguato calcolo dei valori delle sezioni d'urto macroscopiche, la realizzazione di un modello mono-dimensionale per BWRs.

Introduction

The object of the present work is the LWRs modeling by means of a multi-physics approach.

The term "multi-physics" indicates a new way to conceive the modeling and the simulating of complex physical systems based, rather on the only analysis of the single phenomena happening, also on the effects due to their interactions. Such a kind of modeling and simulating concerns all those physical systems the behavior of which is represented by coupled sets of partial or ordinary differential equations, as for example the nuclear fission reactors: indeed, in these ones equations representing the thermo-hydraulics phenomena and equations representing the neutronics ones are strongly coupled and require such an approach for a more rigorous description.

This is the context in which the present work has been conceived.

In particular, two different thermo-hydraulics and neutronics coupled model have been developed. The first is a zero-dimensional model for SURE, acronym for *Study on nUclear Reactor dEvolopment*. It is a Generation III+ BWR conceived at *Politecnico di Milano, Dipartimento di Energia* the main feature of which is represented by the innovative way to realize the power control: indeed, no control rods are present into the core the power variations of which are entirely entrusted to the primary coolant mass flow rate ones. Instead, the second one is a one-dimensional model of MARS, acronym for *Multipurpose Advanced Reactor inherently-Safe*. It is a Generation III+ PWR conceived at *LA SAPIENZA Università di Roma, Dipartimento di Ingneria Nucleare e Conversioni dell'Energia* with the aim to research the best compromise between safety and cost: indeed, it counts both the employing of innovative safety techniques based on the avoidability of the natural physical

laws and the adoption of planning solutions that allow for example to take to pieces and substitute even those components more subject to damage.

Three steps led to development of these models.

The first one has been the building up and the implementation of a only thermo-hydraulics model, both zero-dimensional and one-dimensional, able to describe the behavior of water and steam mixtures in heated channels. Besides the obvious hypothesis respectively of zero-dimensionally and one-dimensionally, a strong assumption has been made during this first part of the work adopting the *Equilibrium Drift Flux Model*.

The second one has been similarly the building up and the implementation of a only neutronics model, both zero-dimensional and one-dimensional, able to describe the zero power reactor dynamics. More precisely, in the first case such a model has been conceived using a two region formulation of the point kinetic theory, whereas in the second one a two region and two group formulation of the diffusion theory has been employed: indeed, this choice represents the best compromise between the availability of the neutronics data, otherwise very difficult to calculate, and the fairness of the results.

Finally, the zero-dimensional thermo-hydraulics and neutronics models and the one-dimensional ones, correctly adapted respectively to SURE and to MARS, have been coupled in order to realize a simulating tool able to reproduce their dynamics in a normal operating condition. Whereas for the coupling of the first ones the only choice of appropriate values of the reactivity feedback coefficients has been necessary, for that of the second ones a specific procedure has been adopted: indeed, the trend of the core macroscopic cross sections with the thermo-hydraulics properties have been determined calculating the values of the effective multiplicative factor corresponding to different core compositions.

A lot of simulations have been performed during the work in order to verify the validity of the models so built up and implemented. In particular, for the thermo-hydraulics ones an out and out experimental validation has been carried out being available several experimental data concerning experiences made at SIET thermo-hydraulics laboratories of Piacenza on an helically coiled steam generator.

Besides the employing of *MATLAB* for the implementation of the water physical and thermodynamical properties, a code named *COMSOL Multiphysics* has been used in virtue of its ability to solve, with a multi-physics approach, coupled sets of partial and ordinary differential equations.

The description of the overall work has been divided in three chapter. On the first one, a detailed statement of the first step, including also the experimental validation mentioned, is reported. Instead, on the other ones the development of the SURE model and of the MARS one respectively are widely explained.

Chapter 1

Models for mixtures of water and steam in heated channels

A description of the first part of the work is the subject of this chapter: the development of a one-dimensional model and a zero-dimensional one for mixtures of water and steam in heated channels.

It has been articulated in three step.

During the first one, two sets of equations able to reproduce the behavior of a mixture of water and steam in heated channels according respectively to a one-dimensional formulation or a zero-dimensional one have been deduced. To do that, besides obviously the hypothesis of one-dimensionally and zero-dimensionally, the *Equilibrium Drift Flux Model* has been adopted: in other words, it has been assumed that a mixture of water and steam is a single component system in which the phase change takes place in a thermodynamical equilibrium condition and in which the velocities of each phase are different but related by a slip ratio.

During the second one, these sets of equations have been implemented so as to compute their numerical solutions: indeed, they are formed by algebraic equations, ordinary differential equations and partial differential equations whose solution is difficult if not impossible to calculate. To do that, the code *COMSOL Multiphysics* has been used; moreover, the implementation of the water thermodynamical and physical properties required the use of *MATLAB*.

Finally, during the third one the reliability of the numerical solutions of these

sets of equations has been checked. To do that, these ones have been compared with experimental data collected at the SIET thermo-hydraulics laboratories for a previous work.

1.1 Introduction

The purpose of the first part of the work has been the development of a model, both one-dimensional and zero-dimensional, for mixtures of water and steam in heated channels.

Because of their complexity, the development of these models has been divided in three steps: the building up, the implementation and the validation. The first one consists in the deduction of a set of equations able to describe the behavior of a mixture of water and steam in heated channels assuring at the same time the respect of the fundamental physical laws. Since the set of equations so deduced is formed by algebraic equations, ordinary differential equations and partial differential equations, its analytic solution is very difficult to calculate: so the aim of the second one is just the compilation of a script able to calculate at least its numerical solution. The validity of the numerical solution so calculated is then checked during the third one by means of a comparison with experimental data.

In each of these steps, the physical system represented in Figure 1.1 has been considered. It is a cylindrical channel in which a water flow goes into in a subcooled condition, undergoes a phase change and goes out in a superheated condition; as Figure 1.1 shows, it is characterized by a length L, a diameter D and a slope angle θ and it is subject to a heat flux q''.

Different hypothesis have been assumed during the development of the one-dimensional model and the zero-dimensional one.

For the first one the following hypothesis has been introduced: the radial distribution of a property at a certain axial coordinate z and at a certain time t can be considered constant and equal to its mean value at the same time on the corresponding section. Consequently the physical system has been assimilated to an axis characterized by a length L and subject to a heat flux q''.

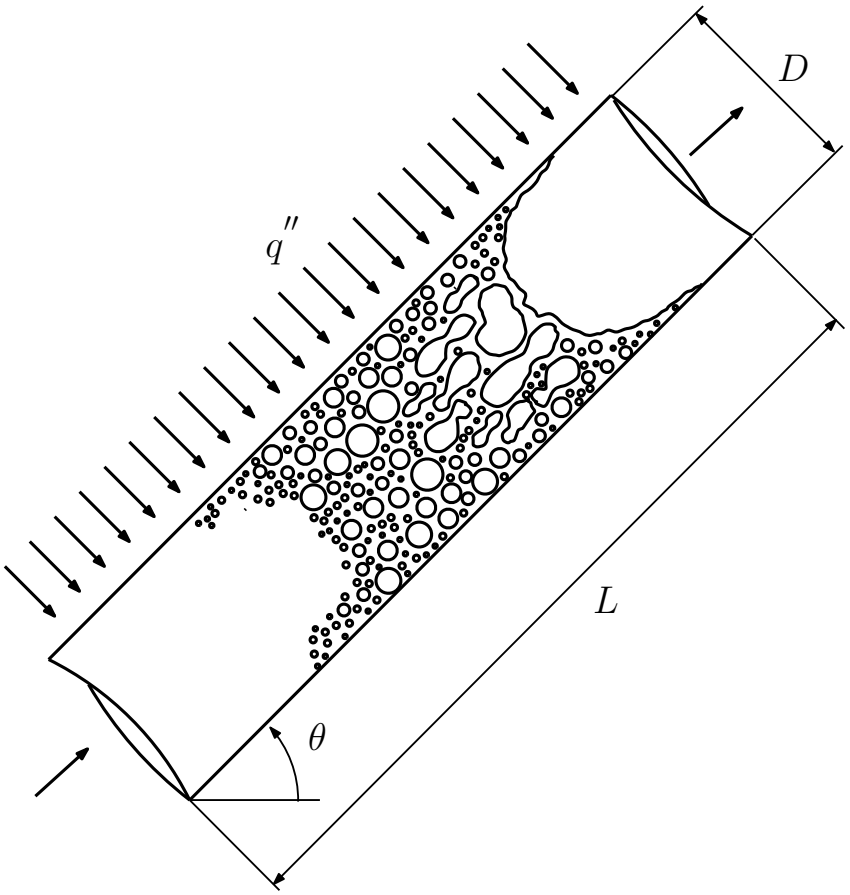

Figure 1.1: The physical system considered

Also for the second one the same hypothesis has been assumed. Moreover a further one has been introduced: the axial distribution of a property in the subcooled region, in the phase-change region or in the superheated region at a certain time t can be considered constant and equal to its mean value at the same time on the corresponding length. Consequently the physical system has been assimilated to three point regions: the first one represents the subcooled region, is characterized by a variable length L_1 and is subject to a heat flux q''; the second one represents the phase-change region, is characterized by a variable length L_2 and is subject to a heat flux q''; the third one represents the superheated region, is characterized by a variable length L_3 and is subject to a heat flux q''. Obviously, the length of the whole channel, sum of the lengths L_1, L_2 and L_3, has to be constant and equal to L.

Figure 1.2 and Figure 1.2 show a representation of the physical system considered in each of these approximations.

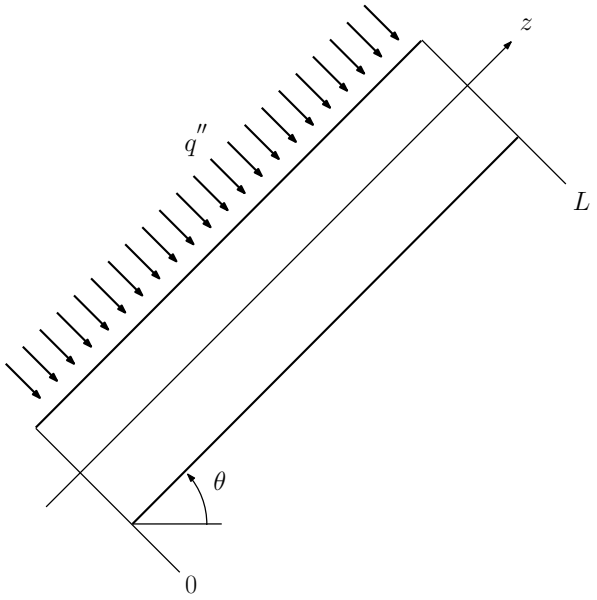

Figure 1.2: The one-dimensional scheme of the physical system considered

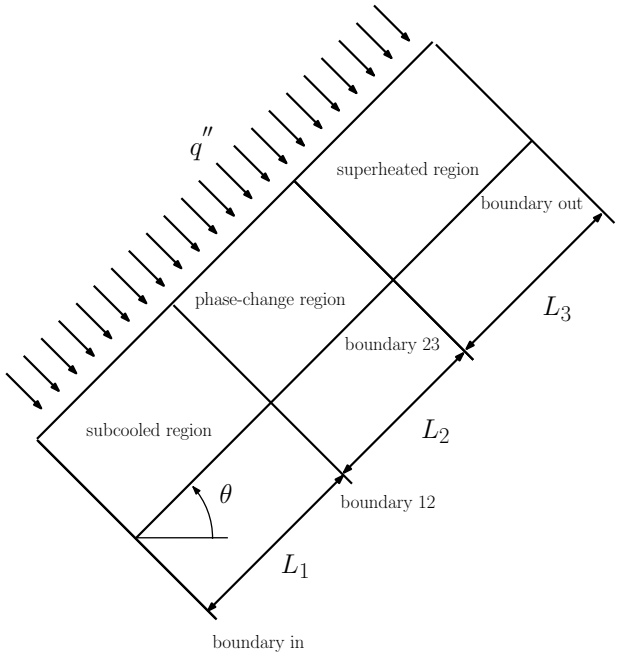

Figure 1.3: The zero-dimensional scheme of the physical system considered

Moreover, in both these cases the following hypothesis have been assumed:

- heat transmission along axial direction is neglected;
- heat losses to the environment are neglected.

Later on a detailed description of this first part of the work.

1.2 The building up of the models

The building up of the model of a physical system consists in the deduction of a set of equations whose solution describes its behavior.

Three different kind of equations have to be deduced: the conservation equations, the constitutive equations and the closure equations. The first ones include the mass balance equation, the momentum balance equation and the total energy balance equation. The second ones include both the state equations for the thermodynamical properties and the constitutive laws for the physical properties. Finally, the third ones include all the equations necessary to make the same the number of equations and the number of the unknown quantities.

This first step is surely the most important: indeed, the hypothesis here assumed outline irrevocably the application field of the model built up.

To this end an introduction is necessary before the beginning of the description of this step.

If in the physical system considered there is not any phase change, no specify hypothesis is necessary; instead if a phase change occurs, an hypothesis on the physical model is obligatory. Indeed, the evolution in space and in time of a two-phase mixture in a heated channel can be described by three different physical models:

- the *Equilibrium Homogeneus Model*, in which the physical system is considered as a single-component system; moreover, the phase change is assumed to take place in thermodynamical equilibrium conditions and the velocities of each phase is assumed to be the same;

- the *Equilibrium Drift Flux Model*, in which the physical system is considered as a single-component system; moreover, the phase change is assumed to take place in thermodynamical equilibrium conditions but the velocities of each phase is assumed to be different even if related by a slip ratio;

- the *Two Fluids Model*, in which the physical system is considered as a two-component system and both the temperatures and the velocities of each phase are assumed to be different.

In this work the second one has been chosen: indeed, this one represents the best compromise between the simplicity in the calculations and the precision in the results.

Later on the sets of equations deduced for the one-dimensional model and for the zero-dimensional model are illustrated and explained.

1.2.1 The building up of the one-dimensional model

The one-dimensional model has been built up deducting the conservation equations, the constitutive equation and the closure equations at first for a single-phase condition and for a two-phase condition and at second for a general condition connecting these ones previously deduced.

Single-phase conditions

Let us keep on adopting all the hypothesis mentioned for the one-dimensional model and assume that there is not a phase change.

Conservation equations

The mass balance equation, the momentum balance equation and the total energy balance equation take the following form for the considered physical system:

$$\frac{\partial}{\partial t}(\rho) + \frac{\partial}{\partial z}(g) = 0 \tag{1.1}$$

$$\frac{\partial}{\partial t}(g) + \frac{\partial}{\partial z}\left(\frac{g^2}{\rho}\right) = -a_g \sin\theta\, \rho - \frac{dp}{dz} - \left(\frac{\partial p}{\partial z}\right)_F \tag{1.2}$$

$$\frac{\partial}{\partial t}\left(\rho\, h - p + \frac{g^2}{2\,\rho}\right) + \frac{\partial}{\partial z}\left(g\, h + \frac{g^3}{2\,\rho^2}\right) = -a_g \sin\theta\, g + \left(\frac{\partial p}{\partial z}\right)_F \frac{g}{\rho} + q'' \frac{P_t}{A_h} \tag{1.3}$$

In these ones the term which represents the frictional pressure drops can be expressed by the following formula:

$$-\left(\frac{\partial p}{\partial z}\right)_F = -\left(\frac{\partial p}{\partial z}\right)_F^{SP} = -\frac{f_M^{SP}}{D_h}\,\frac{g^2}{2\,\rho} \tag{1.4}$$

where f_M^{SP} represents the Moody's factor for a single-phase mixture.

A consideration about the total energy balance equation. An enthalpy balance equation, more interesting for the purpose of this work, can be derived by the

momentum balance equation and the total energy balance equation and can be used in place of the latter. It is:

$$\frac{\partial}{\partial t}(\rho\, h - p) + \frac{\partial}{\partial z}(g\, h) = + \left(\frac{\partial p}{\partial z}\right)_F \frac{g}{\rho} + \left(\frac{\partial p}{\partial z}\right) \frac{g}{\rho} + q'' \frac{P_t}{A_h} \tag{1.5}$$

Constitutive equations

Among the thermodynamical properties, only density has to be specified. The constitutive equation for it takes the following form in the considered physical system:

$$\rho = \rho(p, h) \tag{1.6}$$

Indeed, in these conditions it has two degrees of freedom and its thermodynamical properties depend on two other ones.

Among the physical properties, only viscosity has to be specified. The constitutive equation for it takes the following form:

$$\mu = \mu(p, h) \tag{1.7}$$

Closure equations

Only one equation is necessary to close the set of equations: that for the Moody's factor.

Let us discern the condition of laminar flow by that of turbulent flow.

In the first one the velocity profiles can be deduced by solving the Navier Stokes equation and therefore the Moody's factor can be expressed by the following exactly relation [1]:

$$f_M^{SP} = \frac{64}{Re} \tag{1.8}$$

Instead, in the second one the velocity profiles can be deduced only by semi-empirical methods and therefore the Moody's factor can be expressed only by empirical relations, in particular by three different empirical relations. The first one is the Karman-Nikuradse relation; it is valid without any restrictions and is given by:

$$\frac{1}{\sqrt{f_M^{SP}}} = -0.80 + 0.87\, \ln(Re\, \sqrt{f_M^{SP}}) \tag{1.9}$$

The second one is the Mac-Adams relation; it is valid for smooth tubes and is given by:

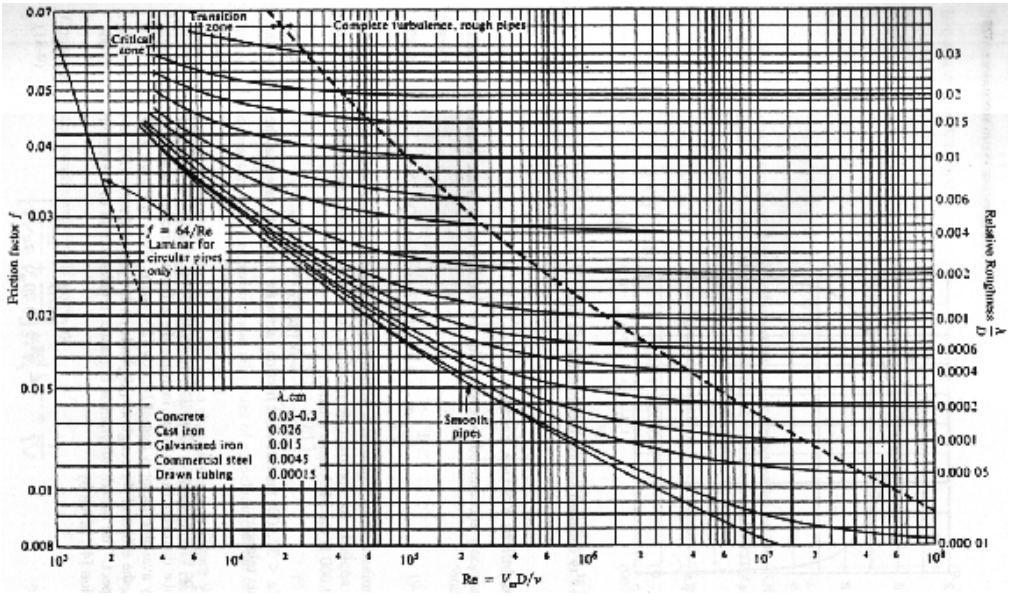

Figure 1.4: The Moody diagram

$$f_M^{SP} = \begin{cases} 0.315\, Re^{-0.25} & Re \leq 30\,000 \\ \\ 0.184\, Re^{-0.20} & 30\,000 \leq Re \leq 1\,000\,000 \end{cases} \tag{1.10}$$

The third one is the Colebrook relation, analytic translation of the Moody Diagram illustrated in Figure 1.3; it is valid for rough tubes and is given by:

$$\frac{1}{\sqrt{f_M^{SP}}} = -2\,\log_{10}\left(\frac{l/D_h}{3.70} + \frac{2.51}{Re\,\sqrt{f_M^{SP}}}\right) \tag{1.11}$$

as can be see, for Colebrook the effects of the tube roughness on the frictional pressure drops can be expressed in term of the ratio of depth of surface protusions to the tube diameter.

Model of a single-phase water mixture in a heated channel

Summarizing, without a phase change, the model searched is represented by equations (1.1), (1.2), (1.3) or (1.5), equation (1.4), equations (1.6) and (1.7) and one among the equations (1.8), (1.9), (1.10) e (1.11).

Two-phase conditions

Let us keep on adopting all the hypothesis mentioned for the one-dimensional model and assume that there is a phase change.

Conservation equations

The mass balance equation, the momentum balance equation and the total energy balance equation take the following form for the considered physical system:

$$\frac{\partial}{\partial t}(\rho_m) + \frac{\partial}{\partial z}(g_m) = 0 \tag{1.12}$$

$$\frac{\partial}{\partial t}(g_m) + \frac{\partial}{\partial z}\left(\frac{g_m^2}{\rho_m^+}\right) = -a_g \sin\theta\, \rho_m - \frac{dp}{dz} - \left(\frac{\partial p}{\partial z}\right)_F \tag{1.13}$$

$$\begin{aligned}\frac{\partial}{\partial t}\left(\rho_m h_m - p + \frac{g_m^2}{2\,\rho_m^+}\right) + \frac{\partial}{\partial z}\left[g_m h_m^+ + \frac{g_m^3}{2\,(\rho_m^2)^+}\right] = \\ = -a_g \sin\theta\, g_m + \left(\frac{\partial p}{\partial z}\right)_F \frac{g_m}{\rho_m} + q'' \frac{P_t}{A_h}\end{aligned} \tag{1.14}$$

In these equations the term which represents the frictional pressure drops can be expressed by means of two different approaches. According to the first one this term is related to the frictional pressure drops of an identical channel in which a liquid mass flux equal to the real mixture mass flux, sum of the liquid one and the vapor one, flows:

$$-\left(\frac{\partial p}{\partial z}\right)_F = -\left(\frac{\partial p}{\partial z}\right)_F^{TP} = -\phi_{LO}^2 \frac{f_M^{TP-LO}}{D_h} \frac{g_m^2}{2\,\rho_m^+} \tag{1.15}$$

where f_M^{TP-LO} represents the Moody's factor for the single-phase mixture described and ϕ_{LO} represents a possible single-phase/two-phase corrective factor. Instead, according to the second one this term is related to the frictional pressure drops of an identical channel in which a liquid mass flux equal to the only real liquid mass flux flows:

$$-\left(\frac{\partial p}{\partial z}\right)_F = -\left(\frac{\partial p}{\partial z}\right)_F^{TP} = -\phi_L^2 \frac{f_M^{TP-L}}{D_h} \frac{g_m^2\,(1-x)}{2\,\rho_m^+} \tag{1.16}$$

where f_M^{TP-L} represents the Moody's factor for the single-phase mixture described and ϕ_L represents another single-phase/two-phase corrective factor.

A consideration about the total energy balance equation similar to the one made for a single-phase mixture can be make. The enthalpy balance equation so obtained is:

$$\frac{\partial}{\partial t}\left(\rho_m h_m - p\right) + \frac{\partial}{\partial z}\left(g_m h_m^+\right) = + \left(\frac{\partial p}{\partial z}\right)_F^{TP} \frac{g_m}{\rho_m} + \left(\frac{\partial p}{\partial z}\right) \frac{g_m}{\rho_m} + q'' \frac{P_t}{A_h} \tag{1.17}$$

Constitutive equations

Among the thermodynamical properties, the density of each phase and the enthalpy of each phase have to be specified. Constitutive equations for these ones take the following form in the considered physical system:

$$\rho_L = \rho_L(p) \tag{1.18}$$

$$\rho_V = \rho_V(p) \tag{1.19}$$

$$h_L = h_L(p) \tag{1.20}$$

$$h_V = h_V(p) \tag{1.21}$$

Indeed, in these conditions it has only one degree of freedom and its thermodynamical properties depend on only another one.

Among the physical properties, the viscosity of each phase and the surface tension have to be specified. Constitutive equations for these one take the following form:

$$\mu_L = \mu_L(p) \tag{1.22}$$

$$\mu_V = \mu_V(p) \tag{1.23}$$

$$s = s(p) \tag{1.24}$$

Closure equations

A lot of equations are necessary to close the set of equations: the ones for the static density, the dynamic density and the static enthalpy; the ones for the void fraction and the volumetric ratio; the ones for the Moody's factor and the single-phase/two-phase corrective factor; the ones for the slip ratio and its terms.

The static density, the dynamic density and the static enthalpy are defined as:

$$\rho_m = \alpha\,\rho_L + (1-\alpha)\,\rho_V \tag{1.25}$$

$$\rho_m^+ = \left[\frac{x^2}{\alpha\,\rho_V} + \frac{(1-x)^2}{(1-\alpha)\,\rho_L}\right]^{-1} \tag{1.26}$$

$$h_m = \frac{\alpha\,\rho_V\,h_L + (1-\alpha)\,\rho_L\,h_L}{\rho_m} \tag{1.27}$$

The void fraction and the volumetric ratio can be expressed by the following formulas:

$$\alpha = \left[1 + \frac{1-x}{x}\,\frac{\rho_V}{\rho_L}\,S\right]^{-1} \tag{1.28}$$

$$\beta = \left[1 + \frac{1-x}{x}\,\frac{\rho_V}{\rho_L}\right]^{-1} \tag{1.29}$$

About the Moody's factor and the single-phase/two phase corrective factor there is something to say.

The Moody's factor can be expressed by one of the equation (1.8), (1.9), (1.10) and (1.11). However, it is important to adopt the correct values of the Reynolds number.

For the first type of the single-phase/two-phase corrective factor, three different empirical relations can be used. The first one is the Becker relation [2]; it is valid only when the dynamic quality is smaller than 0.30 and when the pressure is greater than 70 bar and takes the following form:

$$\phi_{LO}^2 = 1 + 10\,x\,\frac{p_{critical}\,[bar]}{p\,[bar]} \tag{1.30}$$

The second one is the Jones relation [1], analitic traslation of the Nelson-Martinelli Diagram illustrated in Figure 1.4; it is valid without any restriction and takes the following form:

$$\phi_{LO}^2 = \Omega(p, g_m)\,\left[1.2\,x^{0.824}\,\left(\frac{\rho_L}{\rho_V} - 1\right)\right] + 1.0 \tag{1.31}$$

where

$$\Omega(p; g_m) = \begin{cases} 1.36 + 0.0005\,p\,[\text{psi}] + 0.1\,10^{-6}\,g_m\,[\text{lb}\,\text{ft}^{-2}\,\text{h}^{-1}] + \\ -0.000714\,p\,[\text{psi}]\;10^{-6}\,g_m\,[\text{lb}\,\text{ft}^{-2}\,\text{h}^{-1}] \\ \text{for} \quad g_m\,[\text{lb}\,\text{ft}^{-2}\,\text{h}^{-1}]\;10^{-6} \leq 0.7 \\ \\ 1.26 - 0.0004\,p\,[\text{psi}] + 0.119\,10^{6}\,\dfrac{1}{g_m\,[\text{lb}\,\text{ft}^{-2}\,\text{h}^{-1}]} + \\ +0.00028\,p\,[\text{psi}]\;10^{6}\,\dfrac{1}{g_m\,[\text{lb}\,\text{ft}^{-2}\,\text{h}^{-1}]} \\ \text{for} \quad g_m\,[\text{lb}\,\text{ft}^{-2}\,\text{h}^{-1}]\;10^{-6} > 0.7 \end{cases} \tag{1.32}$$

as can be see, it can be used when the flow rate effects have to be considered. The third one is the Armand-Treshev relation [1]; it is valid for rough tubes when

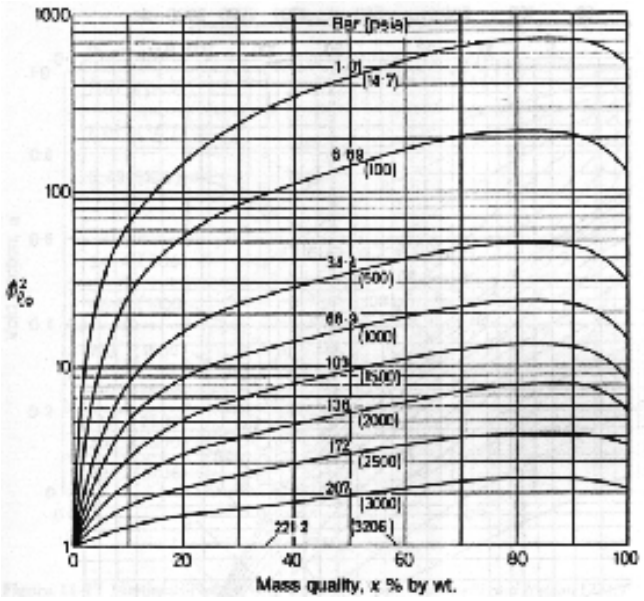

Figure 1.5: The Nelson Martinelli diagram

the pressure is greater than 1 Mpa and smaller than 18 Mpa and when the channel diameter is greater than 25.5 mm and smaller than 56.0 mm and takes the following form:

$$\phi_{LO}^2 = \begin{cases} \dfrac{(1-x)^{1.75}}{(1-\alpha)^{1.2}} & \text{for} \quad \beta \leq 0.9 \quad \text{and} \quad \alpha \leq 0.5 \\ \dfrac{0.48\,(1-x)^{1.75}}{(1-\alpha)^{n}} & \text{for} \quad \beta \leq< 0.9 \quad \text{and} \quad \alpha > 0.5 \\ \dfrac{0.025\,p\,[\text{MPa}] + 0.055}{(1-\beta)^{1}.75}\,(1-x)^{1.75} & \text{for} \quad \beta > 0.9 \end{cases} \tag{1.33}$$

where:

$$n = 1.9 + 1.48\,10^{-2}\,p\,[\text{MPa}] \tag{1.34}$$

It can be used when the void fraction effects have to be considered.

For the second type of the single-phase/two-phase corrective factor, two different empirical relations can be used. The first one is the Lockhart-Martinelli relation [1]; it is valid without any restriction and is given by:

$$\phi_L^2 = 1 + \frac{20}{X} + \frac{1}{X^2} \tag{1.35}$$

where:

$$X^2 = \begin{cases} \left(\frac{\mu_L}{\mu_V}\right)^{0.25} \left(\frac{1-x}{x}\right)^{1.75} \left(\frac{\rho_V}{\rho_L}\right) & \text{for} \quad Re_L \leq 30\,000 \\ \left(\frac{\mu_L}{\mu_V}\right)^{0.20} \left(\frac{1-x}{x}\right)^{1.80} \left(\frac{\rho_V}{\rho_L}\right) & \text{for} \quad 30\,000 \leq Re_L \leq 1\,000\,000 \end{cases} \tag{1.36}$$

The second one is the Chilsom relation [1]; it is valid only when the pressure is greater than 3 MPa and is given by:

$$\phi_L^2 = 1 + \frac{C}{X} + \frac{1}{X^2} \tag{1.37}$$

if g_m is smaller than a reference mass flux g^* and by:

$$\phi_L^2 = \left(1 + \frac{\bar{C}}{X} + \frac{1}{X^2}\right) \Psi \tag{1.38}$$

if g_m is greater than that reference mass flux g^*. The term C and $\bar{C}$ which appear in these equations can be expressed by the following formulas:

$$C = \left[\lambda + (C_2 - \lambda) \left(\frac{v_V - v_L}{v_V}\right)^{0.5}\right] \left[\left(\frac{v_V}{v_L}\right)^{0.5} + \left(\frac{v_L}{v_V}\right)^{0.5}\right] \tag{1.39}$$

$$\bar{C} = \left(\frac{v_V}{v_L}\right)^{0.5} + \left(\frac{v_L}{v_V}\right)^{0.5} \tag{1.40}$$

where:

$$C_2 = \frac{g^*}{g^m} \tag{1.41}$$

$$\Psi = \frac{1 + \frac{C}{T} + \frac{1}{T^2}\frac{g^*}{g_m}}{1 + \frac{\bar{C}}{T} + \frac{1}{T^2}\frac{g^*}{g_m}} \tag{1.42}$$

$$T = \left(\frac{x}{1-x}\right)^{\frac{2-n}{2}} \left(\frac{\mu_L}{\mu_V}\right)^{\frac{n}{2}} \left(\frac{v_L}{v_V}\right)^{\frac{1}{2}} \tag{1.43}$$

and $g^* = 2000\,\mathrm{kg\,m^{-2}\,s^{-1}}$, $\lambda = 0.75$ and $n = 0.2$ for smooth tubes, $g^* = 1500\,\mathrm{kg\,m^{-2}\,s^{-1}}$, $\lambda = 1.0$ and $n = 0.0$ for rought tubes.

Finally, the slip ratio can be expressed by the following formula:

$$S = C_0 + \frac{(C_0 - 1)\, x\, \rho_L}{(1-x)\, \rho_V} + \frac{V_{vj}\, \rho_L}{(1-x)\, G_m} \tag{1.44}$$

in which the contribute due to non-uniform void distribution and that due to local velocity differential between liquid and vapor appear.

The term C_0 and the term V_{vj} have to be specified. For the term C_0 two different approaches can be chosen [1]; more precisely, Dix suggested for C_0 the following expression:

$$C_0 = \beta \left[1 + \left(\frac{1}{\beta} - 1 \right)^B \right] \tag{1.45}$$

where

$$B = \left(\frac{\rho_V}{\rho_L} \right)^{0.1} \tag{1.46}$$

for all the flow regimes, whereas Zuber and Findlay suggested for C_0 different values in different flow regimes: the value 0.0 when the void fraction is low, the value of 1.0 when the void fraction is hight and the value 1.2 in bubbly flow and in slug flow. Even for the term V_{vj} two different approaches can be chosen [1]; more precisely, Zuber and Findlay suggested for V_{vj} the following formula:

$$V_{vj} = (1 - \alpha)^n \, V_\infty \tag{1.47}$$

where:

- V_∞ is equal to:

$$V_\infty = \frac{a_g \, (\rho_L - \rho_V) \, d^2}{18 \, \mu_L} \tag{1.48}$$

  and $n = 3$ in a flow regime characterize by small bubbles;

- V_∞ is equal to:

$$V_\infty = 1.53 \left[\frac{s \, a_g \, (\rho_L - \rho_V)}{\rho_L^2} \right]^{\frac{1}{4}} \tag{1.49}$$

  and $n = 1.5$ in a flow regime characterize by large bubbles;

- V_∞ is equal to:

$$V_\infty = 1.53 \left[\frac{s \, a_g \, (\rho_L - \rho_V)}{\rho_L^2} \right]^{\frac{1}{4}} \tag{1.50}$$

  and $n = 0$ in a churn flow regime;

- V_∞ is equal to:

$$V_\infty = 0.35 \sqrt{a_g \, D_h \left(\frac{\rho_L - \rho_V}{\rho_L} \right)} \tag{1.51}$$

  and $n = 0$ for a slug flow regime.

whereas Ishii suggested for V_{vj} a null value in an annular flow regime.

Model of a two-phase water mixture in a heated channel

Summarizing, if in the physical system considered a physical change takes place, the model descriptive of its behavior is represented by equations (1.12), (1.13), (1.14) or (1.17), one among the equations (1.15) and (1.16), equations (1.18), (1.19), (1.20), (1.21), (1.22), (1.23) and (1.24), equations (1.25), (1.26), (1.27), (1.28) and (1.29), one among the equations (1.8), (1.9), (1.10) and (1.11), one among the equations (1.30), (1.31) and (1.33) or among the equations (1.35), (1.37) and (1.38), equation (1.44) and the equations for its terms.

General conditions

A general model can be deduced by those ones previously built up: indeed, conservation equations have the same form in both the conditions analyzed.

So, keeping on adopting all the mentioned hypothesis, this model can be deduced imposing that:

- when the dynamic quality is smaller than 0:

$$\begin{gathered} x = 0 \\ \alpha = 0 \\ \beta = 0 \\ \rho_m = \rho_m^+ = \rho_L(p,h) \\ h_m = h_m^+ = h_L(p,h) \\ -\left(\frac{\partial p}{\partial z}\right)_F \equiv -\left(\frac{\partial p}{\partial z}\right)_F^{SP} \\ \mu = \mu_L(p,h) \end{gathered} \tag{1.52}$$

- when the dynamic quality is smaller than 1 and greater than 0 equations (1.25), (1.26), (1.27), (1.28) and (1.29), equations (1.15) and (1.16) and equations (1.18), (1.19), (1.20), (1.21), (1.22), (1.23) and (1.24) remain all valid.

- when the dynamic quality is greater than 1:

$$\begin{gathered} x = 1 \\ \alpha = 1 \\ \beta = 1 \\ \rho_m = \rho_m^+ = \rho_V(p,h) \end{gathered} \tag{1.53}$$

$$h_m = h_m^+ = h_V(p,h)$$
$$-\left(\frac{\partial p}{\partial z}\right)_F \equiv -\left(\frac{\partial p}{\partial z}\right)_F^{SP}$$
$$\mu = \mu_V(p,h)$$

Indeed so doing, using the appropriate correlation for the Moody's factor, for the single-phase/two-phase corrective factor and for the slip ratio and introducing appropriate initial and boundary conditions, equations (1.12), (1.13) and (1.17) represent the model searched as shown in Appendix A.

Finally, to note that the term which represents the thermal flux does not show necessary a thermal flux imposed condition: if replace with an appropriate relation it can represent also a temperature imposed condition.

1.2.2 The building up of the zero-dimensional model

The zero-dimensional model has been built up deducting the conservation equations, the constitutive equations and the closure equations at first for the subcooled region, the saturated region[1] and the superheated region and at second for the whole physical system connecting the ones previously deduced.

In particular, the deduction of the conservation equations for each region has been carried out integrating the ones deduced for the one-dimensional model and then using the Leibniz's Law. More precisely, let us considered for example the equation (1.1); the mass balance equation for the subcooled region can be deduced integrating this one on the corresponding length:

$$\int_0^{L_1} \left[\frac{\partial(\rho A_h)}{\partial t} + \frac{\partial(g A_h)}{\partial z}\right] dz = 0 \tag{1.54}$$

and then applying to the formula so obtained the Leibniz's Law:

$$\frac{d}{dt}\int_0^{L_1} (\rho A_h)\, dz - \rho_{12} A_h \frac{dL_1}{dt} + G_{12} - G_{in} = 0 \tag{1.55}$$

Similar considerations allow the deduction of the other conservation equations for the other regions.

[1] The phase-change region will be named the saturated region in virtue of the choice done about the physical model.

The subcooled region

Let us keep on adopting all the hypothesis mentioned for the zero-dimensional model and consider the subcooled region.

Conservation equations

The mass balance equation, the momentum balance equation and the enthalpy balance equation take the following form in the subccoled region:

$$\frac{dM_1}{dt} = G_{in} + \rho_{12}\, A_h \frac{dL_1}{dt} - G_{12} \tag{1.56}$$

$$\begin{aligned}\frac{dG_1}{dt} = {} & \frac{G_{in}^2}{\rho_{in}\, A_h} + G_{12}\frac{dL_1}{dt} - \frac{G_{12}^2}{\rho_{12}\, A_h} + p_{in}\, A_h - p_{12}\, A_h \\ & -a_g\, \langle\rho\rangle_1\, A_h\, L_1 - \frac{f_{M_1}}{2\, D_h} \left\langle \frac{G^2}{\rho\, A_h} \right\rangle_1 L_1\end{aligned} \tag{1.57}$$

$$\frac{dE_1}{dt} = G_{in}\, h_{in} + \rho_{12}\, u_{12}\, A_h \frac{dL_1}{dt} - G_{12}\, h_{12} + q''\, P_t\, L_1 \tag{1.58}$$

where the mass M_1, the mass flow rate G_1 and the energy E_1 can be expressed by the following formulas:

$$M_1 = \int_0^{L_1} (\rho\, A_h)\, dz = \langle\rho\rangle_1\, A_h\, L_1 \tag{1.59}$$

$$G_1 = \int_0^{L_1} (g\, A_h)\, dz = \langle G\rangle_1\, L_1 \tag{1.60}$$

$$E_1 = \int_0^{L_1} [(\rho\, h - p)\, A_h]\, dz = \langle\rho\, h\rangle_1\, A_h\, L_1 - \langle p\rangle_1\, A_h\, L_1 \tag{1.61}$$

Constitutive equations

Among the thermodynamical properties, the density, the enthalpy and the energy relative to the moving boundary L_1 have to be specified. The constitutive equations for these ones take the following form:

$$\rho_{12} = \rho_L(p_{12}) \tag{1.62}$$

$$h_{12} = h_L(p_{12}) \tag{1.63}$$

$$u_{12} = u_L(p_{12}) \tag{1.64}$$

Among the physical properties, only the viscosity relative to the moving boundary L_1 has to be specified. The constitutive equation for it takes the following form:

$$\mu_{12} = \mu_L(p_{12}) \tag{1.65}$$

Closure equations

Eight equations are necessary to close the set of equations for the subcooled region: the equations for the mean values of the density, the mass flow rate, the kinetic energy term in the frictional pressure drops expressions, the viscosity, the volumetric specific enthalpy and the pressure, an equation for the Moody's Factor and an equation for the Reynolds number.

The first equations take the following form:

$$\langle \rho \rangle_1 = \frac{\rho_{in} + \rho_{12}}{2} \tag{1.66}$$

$$\langle G \rangle_1 = \frac{G_{in} + G_{12}}{2} \tag{1.67}$$

$$\left\langle \frac{G^2}{\rho\, A_h} \right\rangle_1 = \frac{\dfrac{G_{in}^2}{\rho_{in}\, A_h} + \dfrac{G_{12}^2}{\rho_{12}\, A_h}}{2} \tag{1.68}$$

$$\langle \mu \rangle_1 = \frac{\mu_{in} + \mu_{12}}{2} \tag{1.69}$$

$$\langle \rho\, h \rangle_1 = \frac{(\rho\, h)_{in} + (\rho\, h)_{12}}{2} \tag{1.70}$$

$$\langle p \rangle_1 = \frac{p_{in} + p_{12}}{2} \tag{1.71}$$

For the Moody's factor can be used one among the equations (1.8), (1.9), (1.10) and (1.11), whereas the Reynolds number can be expressed by the following relation:

$$Re_1 = \frac{\langle G \rangle_1\, D_h}{A_h\, \langle \mu \rangle_1} \tag{1.72}$$

The saturated region

Let us keep on adopting all the hypothesis mentioned for the zero-dimensional model and consider the saturated region.

Conservation equations

The mass balance equation, the momentum balance equation and the enthalpy balance equation take the following form in the saturated region:

$$\frac{dM_2}{dt} = G_{12} - \rho_{12}\, A_h\, \frac{dL_1}{dt} - G_{23} + \rho_{23}\, A_h\, \frac{d\,(L_1 + L_2)}{dt} \tag{1.73}$$

$$\frac{dG_2}{dt} = \frac{G_{12}^2}{\rho_{12}\,A_h} - G_{12}\,\frac{dL_1}{dt} - \frac{G_{23}^2}{\rho_{23}\,A_h} + G_{23}\,\frac{d\,(L_1+L_2)}{dt} + p_{12}\,A_h - p_{23}\,A_h \\ -a_g\,\langle\rho\rangle_2\,A_h\,L_2 - \phi_{LO_2}^2\,\frac{f_{M_2}}{2\,D_h}\left\langle\frac{G^2}{\rho_L\,A_h}\right\rangle_2 L_2 \tag{1.74}$$

$$\frac{dE_2}{dt} = G_{12}\,h_{12} - \rho_{12}\,u_{12}\,A_h\,\frac{dL_1}{dt} + \rho_{23}\,u_{23}\,A_h\,\frac{d\,(L_1+L_2)}{dt} - G_{23}\,h_{23} + q''\,P_t\,L_2 \tag{1.75}$$

where the mass M_2, the mass flow rate G_2 and the energy E_2 can be expressed by the following formula:

$$M_2 = \int_{L_1}^{L_1+L_2} (\rho\,A)\,dz = \langle\rho\rangle_2\,A_h\,L_2 \tag{1.76}$$

$$G_2 = \int_{L_1}^{L_1+L_2} (g\,A_h)\,dz = \langle G\rangle_2\,L_2 \tag{1.77}$$

$$E_2 = \int_{L_1}^{L_1+L_2} [(\rho\,h - p)\;A]\,dz = \langle\rho\,h\rangle_2\,A_h\,L_2 - \langle p\rangle_2\,A_h\,L_2 \tag{1.78}$$

Constitutive equations

Among the thermodynamical properties, the density, the enthalpy and the energy relative to moving boundary L_2 have to be specified. The constitutive equations for these ones take the following form:

$$\rho_{23} = \rho_V(p_{23}) \tag{1.79}$$

$$h_{23} = h_V(p_{23}) \tag{1.80}$$

$$u_{23} = u_V(p_{23}) \tag{1.81}$$

Among the physical properties, only the viscosity relative to the moving boundary L_2 has to be specified. The constitutive equation for it takes the following form:

$$\mu_{23} = \mu_V(p_{23}) \tag{1.82}$$

Moreover, since in the frictional pressure drops expression the liquid density and the liquid viscosity appear, two further equations are necessary for the saturated region:

$$\rho_{LO} = \rho_L(p_{23}) \tag{1.83}$$

$$\mu_{LO} = \mu_L(p_{23}) \tag{1.84}$$

Closure equations

Nine equations are necessary to close the set of equations for the saturated region: the equations for the mean values of the density, the mass flow rate, the kinetic energy term in the frictional pressure drops expressions, the viscosity, the volumetric specific enthalpy and the pressure, an equation for the Moody's Factor, an equation for the Reynolds number and an equation for the single-phase/two-phase corrective factor.

The first equations take the following form:

$$\langle \rho \rangle_2 = \frac{\rho_{12} + \rho_{23}}{2} \tag{1.85}$$

$$\langle G \rangle_2 = \frac{G_{12} + G_{23}}{2} \tag{1.86}$$

$$\left\langle \frac{G^2}{\rho\, A_h} \right\rangle_2 = \frac{\dfrac{G_{12}^2}{\rho_{12}\, A_h} + \dfrac{G_{23}^2}{\rho_{23}\, A_h}}{2} \tag{1.87}$$

$$\langle \mu \rangle_2 = \frac{\mu_{12} + \mu_{LO}}{2} \tag{1.88}$$

$$\langle \rho\, h \rangle_2 = \frac{(\rho\, h)_{12} + (\rho\, h)_{23}}{2} \tag{1.89}$$

$$\langle p \rangle_2 = \frac{p_{12} + p_{23}}{2} \tag{1.90}$$

For the Moody's factor can be used one among the equations (1.8), (1.9), (1.10) and (1.11), whereas the Reynold number can be expressed by the following relation:

$$Re_2 = \frac{\langle G \rangle_2\, D_h}{A_h\, \langle \mu \rangle_2} \tag{1.91}$$

At the end, for the single-phase/two-phase corrective factor can be used one among the equations (1.30), (1.31) and (1.33) or one among the equations (1.35), (1.37) and (1.38).

The superheated region

Let us keep on adopting all the hypothesis mentioned for the zero-dimensional model and consider the superheated region.

Conservation equations

The mass balance equation, the momentum balance equation and the enthalpy balance equation take the following form in the superheated region:

$$\frac{dM_3}{dt} = G_{23} - \rho_{23}\, A_h\, \frac{d\,(L_1 + L_2)}{dt} - G_{out} \tag{1.92}$$

$$\begin{aligned}\frac{dG_3}{dt} = \frac{G_{23}^2}{\rho_{23}\, A_h} - G_{23}\, \frac{d\,(L_1 + L_2)}{dt} - \frac{G_{out}^2}{\rho_{out}\, A_h} + p_{23}\, A_h - p_{out}\, A_h \\ -a_g\, \langle\rho\rangle_3\, A_h\, L_3 - \frac{f_{M_3}}{2\, D_h} \left\langle \frac{G^2}{\rho\, A_h} \right\rangle_3 L_3\end{aligned} \tag{1.93}$$

$$\frac{dE_3}{dt} = G_{23}\, h_{23} - \rho_{23}\, u_{23}\, A_h\, \frac{d\,(L_1 + L_2)}{dt} - G_{out}\, h_{out} + q''\, P_t\, L_3 \tag{1.94}$$

where the mass M_3, the mass flow rate G_3 and the energy E_3 can be expressed by the following formula:

$$M_3 = \int_{L_1+L_2}^{L} (\rho\, A_h)\, dz = \langle\rho_3\rangle\, A_h\, L_3 \tag{1.95}$$

$$G_3 = \int_{L_1+L_2}^{L} (g\, A_h)\, dz = \langle G_3\rangle\, L_3 \tag{1.96}$$

$$E_3 = \int_{L_1+L_2}^{L} [(\rho\, h - p)\, A_h]\, dz = \langle\rho\, h\rangle_3\, A_h\, L_3 - \langle p\rangle_3\, A_h\, L_3 \tag{1.97}$$

Constitutive equations

Among the thermodynamical properties, only the density relative to the boundary L has to be specified. The constitutive equation for it takes the following form:

$$\rho_{out} = \rho(p_{out}, h_{out}) \tag{1.98}$$

Among the physical properties, only the viscosity relative to the boundary L has to be specified. The constitutive equation for it takes the following form:

$$\mu_{out} = \mu(p_{out}, h_{out}) \tag{1.99}$$

Closure equations

Eight equations are necessary to close the set of equations for the superheated region: the equations for the mean values of the density, the mass flow rate, the kinetic energy term in the frictional pressure drops expressions, the viscosity, the volumetric specific enthalpy and the pressure, an equation for the Moody's Factor and an equation for the Reynolds number.

The first equations take the following form:

$$\langle \rho \rangle_3 = \frac{\rho_{23} + \rho_{out}}{2} \tag{1.100}$$

$$\langle G \rangle_3 = \frac{G_{23} + G_{out}}{2} \tag{1.101}$$

$$\left\langle \frac{G^2}{\rho\, A_h} \right\rangle_3 = \frac{\dfrac{G_{23}^2}{\rho_{23}\, A_h} + \dfrac{G_{out}^2}{\rho_{out}\, A_h}}{2} \tag{1.102}$$

$$\langle \mu \rangle_3 = \frac{\mu_{23} + \mu_{out}}{2} \tag{1.103}$$

$$\langle \rho\, h \rangle_3 = \frac{(\rho\, h)_{23} + (\rho\, h)_{out}}{2} \tag{1.104}$$

$$\langle p \rangle_3 = \frac{p_{23} + p_{out}}{2} \tag{1.105}$$

For the Moody's factor can be used one among the equations (1.8), (1.9), (1.10) and (1.11), whereas the Reynolds number can be expressed by the following relation:

$$Re_3 = \frac{\langle G \rangle_3\, D_h}{A_h\, \langle \mu \rangle_3} \tag{1.106}$$

The whole channel

The model for the whole channel can be obtained very simply. Indeed, it is formed by equations from (1.56) to (1.72) for the subcooled region, equations from (1.73) to (1.91) for the saturated region and equations from (1.92) to (1.106) for the superheated region, by appropriate expressions for the Moody's factor of each regions and for the single-phase/two-phase corrective factor of the saturated one, by appropriate initial conditions and by the following bond equation on the total length:

$$L = L_1 + L_2 + L_3 \tag{1.107}$$

as shown in Appendix B.

1.3 The implementation of the models

The implementation of the model of a physical system consists in the translation of the set of equations deduced in the previous phase from a mathematical language to an appropriate computer language so as to compute its numerical solution.

Two kinds of informations have to be compiled: at first the thermodynamical and physical properties of the physical system and at second the set of equations descriptive of its behavior.

In this second step a very important choice is represented by those one of the code to use: in the present work the implementation of the first kind of informations has been carried out by means of *MATLAB*, whereas for the implementation of the second one *COMSOL Multiphysics* has been adopted.

Later on the way used for implement the water thermodynamical and physical properties and those one used for implement the one-dimensional model equations and the zero-dimensional model ones are illustrated and explained: indeed, for the first ones a unique procedure can be used, whereas two different approaches are required for the second ones.

1.3.1 The implementation of water thermodynamical and physical properties

For the implementation of water thermodynamical and physical properties the data provided by IAPWS, acronym for Internazional Association for the Properties of Water and Steam, have been used.

An instrument available in *MATLAB* environment allowed the use of these data: *XSTEAM for MATLAB*. *XSTEAM for MATLAB* is an implementation of the data provided by IAPWS IF97[2], in which thermodynamical and physical properties for water at pressure between 1 bar and 1000 bar and at temperature between 0°C and 2000°C are collected: to be more precise, it includes some *MATLAB* functions that allow to calculate these properties in this pressure and temperature range.

The water thermodynamical and physical properties implementation has been divided in two phases.

At first, text files containing the values of water thermodynamical and physical properties has been created in *MATLAB* environment: indeed, *MATLAB* is able

[2]There is an exception: for water viscosity *XSTEAM for MATLAB* uses the data provided by the IAPWS document "Revised Releaseon the IAPWS Formulation 1985 for the Viscosity Ordinary Watwer Substance"

to write the data stored in the vectors obtained with *XSTEAM for MATLAB* in a text file. Later on the *MATLAB* script used for water properties depending only on a thermodynamical property:

```
p = [1:10:220];
rhoL_p = zeros(1,length(p));
for i = 1:length(p)
    rhoL_p(i) = XSteam('rhoL_p',p(i)) ;
end
postwriteinterpfile('rhoL_p.txt',p*1e5,rhoL_p)
```

and that used for properties depending on two thermodynamical properties:

```
p = [1:1:220];
h = [50:20:2000];
rho_ph = zeros(lenght(p),lenght(h));
for i = 1:length(p)
   for j = 1:length(h)
   rho_ph(i,j) = XSteam('rho_ph', p(i), h(j));
   end
end
[X,Y] = meshgrid(p,h);
postwriteinterpfile('rhoL_ph.txt',p*1e5,h*1e3,rho_ph)
```

At second, functions expressing the water thermodynamical and physical properties dependence on the thermodynamical ones has been created in *COMSOL Multihpysics* environment: indeed, *COMSOL Multihpysics* is able to interpolate the data stored in the text files obtained with *MATLAB* [3].

The following constitutive equation has been implemented with this procedure: equations (1.6), (1.18), (1.19), (1.20), (1.21) and (1.24) for the one-dimensional model and equations (1.62), (1.63), (1.64), (1.79), (1.80), (1.81), (1.83) and (1.98) for the zero-dimensional one.

A different procedure has been applied to the implementation of the water viscosity.

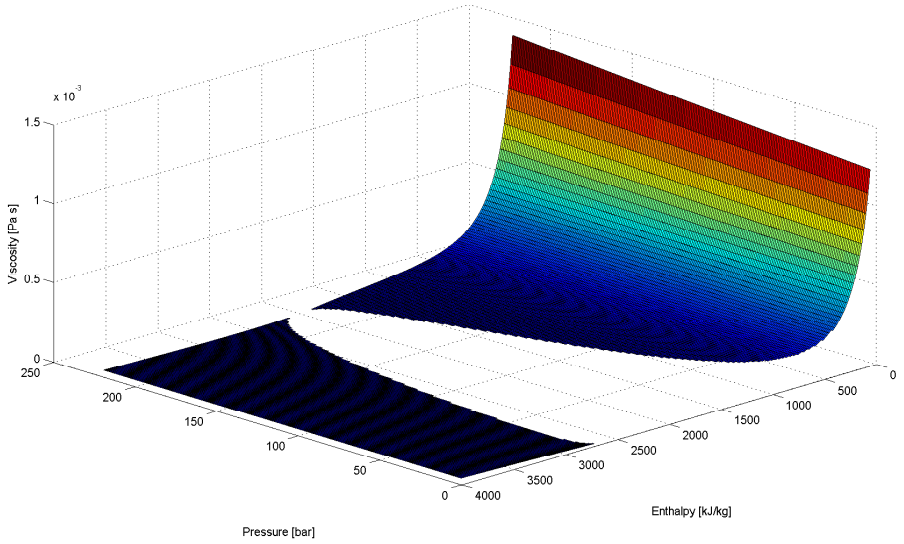

Figure 1.6: Water viscosity dependence on pressure and enthalpy

To describe it, let us discern a single-phase condition by a two-phase condition.

In the first case an accurate analysis of the IAPWS data allowed to conclude that the dependence of the water viscosity on the pressure can be ignored, as illustrated in Figure 1.6, and its implementation has been done using only the enthalpy as independent variable.

Instead, in the second case the implementation has been done using the data provided by Caruso [2]: indeed, *XSTEAM for MATLAB* does not provide water viscosity data for this condition.

1.3.2 The implementation of the one-dimensional model equations

For the implementation of the one-dimensional model equations the *COMSOL Multiphysics* module *PDE General Form* has been adopted.

The module *PDE General Form* solves both single equations taking the following form:

$$e_a \frac{\partial^2 u}{\partial t^2} + d_a \frac{\partial u}{\partial t} + \nabla \cdot \Gamma = F \tag{1.108}$$

if the coefficients e_a and d_a, the flux term Γ ,the known term F and an appropriate initial condition are provided it, and set of equations taking the following form:

$$\underline{\underline{e_a}} \frac{\partial^2 \underline{u}}{\partial t^2} + \underline{\underline{d_a}} \frac{\partial \underline{u}}{\partial t} + \nabla \cdot \underline{\Gamma} = \underline{F} \tag{1.109}$$

if the coefficient matrix $\underline{\underline{e_a}}$ and $\underline{\underline{d_a}}$, the flux term vector $\underline{\Gamma}$, the known term vector $\underline{F}$ and appropriate initial conditions are provided it [3]. Moreover, the *PDE General Form* module offers two different kinds of boundary conditions [3]:

- the first is a Dirichlet condition and is made available in the following form:

$$R = 0 \tag{1.110}$$

- the second is a Neumann condition and is made available in the following form:

$$-n \cdot \Gamma = G \tag{1.111}$$

The implementation of the one-dimensional model has been divided in five phases.

At first, a geometry as the one illustrated on Figure 1.2 has been created.

At second, unknown quantities have been chosen: the pressure p, the mass flux g_m and the enthalpy h_m^+.

At third, conservation equations have been implemented. To do that, equations (1.12), (1.13) and (1.17) have been reformulated in the form required by *PDE General Form* module just described, that is:

$$\underline{\underline{e_a}} = \begin{Bmatrix} 0 & 0 & 0 \\ 0 & 0 & 0 \\ 0 & 0 & 0 \end{Bmatrix} \tag{1.112}$$

$$\underline{\underline{d_a}} = \begin{Bmatrix} \dfrac{\partial \rho_m}{\partial p} & \dfrac{\partial \rho_m}{\partial g_m} & \dfrac{\partial \rho_m}{\partial h_m^+} \\ \dfrac{\partial g_m}{\partial p} & \dfrac{\partial g_m}{\partial g_m} & \dfrac{\partial g_m}{\partial h_m^+} \\ \dfrac{\partial}{\partial p}(\rho_m h_m - p) & \dfrac{\partial}{\partial g_m}(\rho_m h_m - p) & \dfrac{\partial}{\partial h_m^+}(\rho_m h_m - p) \end{Bmatrix} \tag{1.113}$$

$$\underline{\Gamma} = \left\{ \begin{array}{c} 0 \\ \\ \dfrac{g_m^2}{\rho_m^+} \\ \\ g_m\, h_m^+ \end{array} \right\} \tag{1.114}$$

$$\underline{F} = \left\{ \begin{array}{c} g_m \\ \\ -a_g\, \sin\theta\, \rho_m - \dfrac{dp}{dz} - \left(\dfrac{\partial p}{\partial z}\right)_F \\ \\ + \left(\dfrac{\partial p}{\partial z}\right) \dfrac{g_m}{\rho_m} + \left(\dfrac{\partial p}{\partial z}\right)_F \dfrac{g_m}{\rho_m} + q'' \dfrac{P}{A} \end{array} \right\} \tag{1.115}$$

and appropriate initial values have been imposed.

At fourth, constitutive equations and closure equations have been introduced. To do that a control variable has been defined in the following way:

$$v_c = \frac{h_m^+ - h_L}{h_V - h_L} \tag{1.116}$$

and conditions (1.52) and (1.54) have been imposed on the basis of value by this one assumed.

Finally boundary conditions, a Dirichlet one on the first boundary and a Neumann one on the second boundary, have been implemented fixing that:

$$R = \left\{ \begin{array}{c} p_{in} - u1 \\ \\ g_{in} - u2 \\ \\ h_{in} - u3 \end{array} \right\} \tag{1.117}$$

$$G = \left\{ \begin{array}{c} -\Gamma_1 \\ \\ -\Gamma_2 \\ \\ -\Gamma_3 \end{array} \right\} \tag{1.118}$$

1.3.3 The implementation of the zero-dimensional model equations

For the implementation of the zero-dimensional model equations a generic *COMSOL Multiphysics* module can be used: indeed, all its modules are provided of a section able to solve ordinary differential equations and named *Global Equations*.

The section *Global Equations* solves equations taking the following form:

$$f(u, \frac{du}{dt}, \frac{d^2u}{dt^2} ... \frac{d^nu}{dt^n}) = 0 \tag{1.119}$$

if appropriate initial conditions are provided it [3].

Also for the implementations of the zero-dimensional model the first step has been the choice of the unknown quantities: the mass flow rates G_{12}, G_{23} and G_{out}, the pressures p_{12}, p_{23} and p_{out}, the moving boundary L_1 and L_2 and the enthalpy h_{out}.

At second the conservation equations and their initial values have been implemented: no reformulation has been necessary in this case.

Finally the other equation have been introduced.

1.4 The validation of models

The validation of the model of a physical system consists in a comparison of the experimental data obtained in certain conditions with the ones obtained solving in same conditions the set of equations implemented in the previous phase so as to verify its validity.

This third step requires on one hand the collection of experimental data and on the other hand the collection of simulated data.

Because of the complexity of the facilities and the experimental experiences it is surely the most difficult. Fortunately in the present work no experimental data collection has been directly done having in our disposition the ones collected for a previous work.

Later on the collection of the experimental data and those one of the simulated ones are described. Moreover some considerations and their comparison are

reported.

1.4.1 The collection of experimental data

Measures collected during previous experiences at the facility of the SIET thermo-hydraulics laboratories of Piacenza have been used.

This facility is an electrical helically coiled steam generator.

In the eyes of constructive features, the experimental unit is made by two section: the supply section and the test section.

The first one assures the water to enter in the second one in desired conditions. It consists of a booster pump and a feed-water pump; moreover, a throttling valve and a by-pass line allow to control the mass flow rate.

The second one assures the collection of measures in different conditions. It is made by a stainless tube with an external diameter of 12.53×10^{-3} m, an internal diameter of 17.24×10^{-3} m and a length of 32.00 m; moreover, it is coled so as to form an helical shape with an external diameter of 1.00 m, a pinch of 8.00×10^{-1} m and a height of 8.00 m. A DC generator heats the first 24.00 m of this section by means of Joule effect.

In the eyes of functional features, the experimental unit is able to realized two experiences: the adiabatic experience and the diabatic experience.

The adiabatic one is realized bringing to the test section a two-phase water mixture characterize by a certain value of dynamic quality; a pre-heating system makes it possible. In this first case, the inlet mass flow rate, the inlet dynamic quality and the pressure in eight different points are measured.

Instead, in the diabatic one a single-phase water mixture characterized by a certain value of temperature is introduced in the test section and here is vaporized and superheated; the same pre-heating system and the DC generator make it possible. In this second case, the inlet mass flow rate, the inlet temperature, the thermal flux and the pressure in five different points are measured.

Some common characteristics. In both these experiences, data are collected during steady-state measures. Moreover, in both these experiences the pressure is measured using nine pressure taps located along the channel at a distance of about

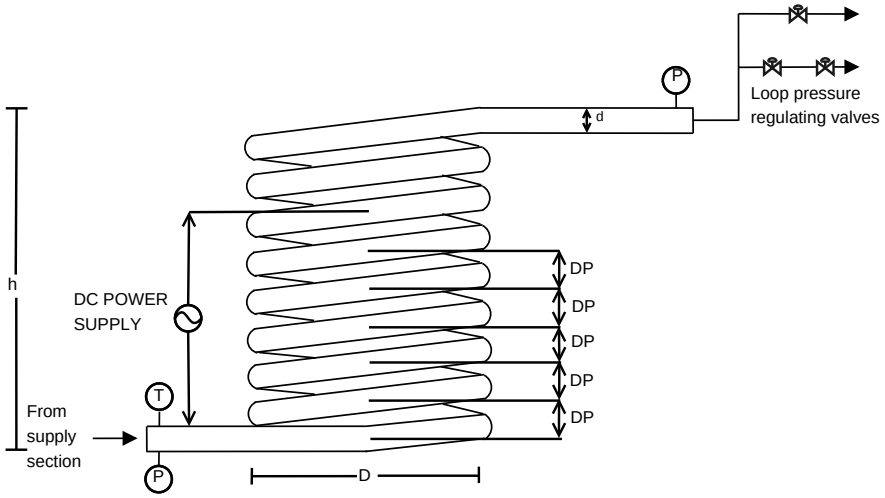

Figure 1.7: The facility of the SIET thermo-hydraulics laboratories

4.00 m and eight differential pressure trasducer that provide a maximum relative uncertainty of 0.4 %.

Figure 1.7 shows the facility described.

Obviously, experimental data collected during diabatic experiences are more interesting for the purpose of this work: for this reason only these ones have been considered.

1.4.2 The collection of simulated data

The collection of simulated data has been done at first adapting the models built up to the facility described and at second calculating its solution in the same conditions of the diabatic experiences made.

To adapt the models to the facility described, it has been necessary to insert the geometric features of the experimental unit, to insert a correct empirical correlation both for the Moody's factor and for the single-phase/two-phase corrective factor and to impose the stationary state.

With regard to the first aim, the following hypothesis has been assumed: the behavior of a helically coiled channel is the same of the behavior of a straight channel with a slope angle equal to the mean inclination of the helix.

With regard to the second aim, for the first one the Mac-Adams correlation has been adopted whereas for the second one the Friedel correlation suggested by [4]

has been chosen:

$$\phi_{LO}^2 = 0.2185\,E + \frac{0.2365\,F\,H}{Fr^{-0.0165}\,We^{-0.1318}} \tag{1.120}$$

in which:

- the term E is:

$$E = (1-x)^2 + x^2\,\frac{\rho_L\,f_{VO}}{\rho_V\,f_{LO}}; \tag{1.121}$$

- the term F is:

$$F = x^{0.78}\,(1-x)^{0.224}; \tag{1.122}$$

- the term H is:

$$H = \left(\frac{\rho_L}{\rho_V}\right)^{0.91}\,\left(\frac{\mu_V}{\mu_V}\right)^{0.19}\,\left(1-\frac{\mu_V}{\mu_L}\right)^{0.7}; \tag{1.123}$$

- the term Fr represents the Froude number and it is:

$$Fr = \frac{G^2}{a_g\,D\,\rho_m^2}; \tag{1.124}$$

- the term We represents Webber number and it is:

$$We = \frac{G^2\,d}{\rho_m\,s}. \tag{1.125}$$

Simulated data have been obtained calculating the numerical solution of the models built up in steady-state and in the following conditions:

- at the pressure of 20 bar, the conditions in which the heat flux is 50.74 $\mathrm{kW/m^2}$ and the mass flux is 198.15 $\mathrm{kg/(m^2\,s)}$, those ones in which the heat flux is 104.17 $\mathrm{kW/m^2}$ and the mass flux is 403.22 $\mathrm{kg/(m^2\,s)}$, those ones in which the heat flux is 161.40 $\mathrm{kW/m^2}$ and the mass flux is 602.29 $\mathrm{kg/(m^2\,s)}$ and those ones in which the heat flux is 212.78 $\mathrm{kW/m^2}$ and the mass flux is 796.17 $\mathrm{kg/(m^2\,s)}$ have been considered;

- at the pressure of 40 bar, the conditions in which the heat flux is 50.22 $\mathrm{kW/m^2}$ and the mass flux is 200.58 $\mathrm{kg/(m^2\,s)}$, those ones in which the heat flux is 104.76 $\mathrm{kW/m^2}$ and the mass flux is 402.08 $\mathrm{kg/(m^2\,s)}$, those ones in which the heat flux is 159.39 $\mathrm{kW/m^2}$ and the mass flux is 599.76 $\mathrm{kg/(m^2\,s)}$ and those ones in which the heat flux is 201.43 $\mathrm{kW/m^2}$ and the mass flux is 803.24 $\mathrm{kg/(m^2\,s)}$ have been considered;

- at the pressure of 60 bar, the conditions in which the heat flux is 50.74 kW/m^2 and the mass flux is 199.18 $kg/(m^2 s)$, those ones in which the heat flux is 104.72 kW/m^2 and the mass flux is 399.17 $kg/(m^2 s)$, those ones in which the heat flux is 159.13 kW/m^2 and the mass flux is 600.32 $kg/(m^2 s)$ and those ones in which the heat flux is 201.99 kW/m^2 and the mass flux is 803.30 $kg/(m^2 s)$ have been considered.

1.4.3 Comparison between experimental data and simulated data

In Figure 1.7 and Figure 1.8, pressure spatial distributions obtained both by experimental data and by simulated ones are illustrated for the one-dimensional model and for the zero-dimensional model. Moreover, Figure 1.9 shows a comparison between these distributions for the first one.

About the one-dimensional model, Figures 1.7 and 1.9 show the perfect overlap between experimental data and simulated ones in almost all the conditions considered: indeed, in the ones illustrated the error which could be commit using the model built up is at most 5%. Nevertheless, in Figures 1.7 and 1.9 results obtained when the pressure is low and the heat flux and the mass flow rate are hight are not illustrated: indeed, these ones are the only conditions in which the model developed shows numerical instabilities.

Instead, Figure 1.8 shows a worse overlap between experimental data and simulated ones for the zero-dimensional model.

To be complete, temperature spatial distributions obtained in the same conditions are illustrated in Figure 1.10 for the one-dimensional model and Figure 2.1 for the zero-dimensional model: these distributions, contrary to the pressure ones, are very similar.

1.5 Conclusion

Some final considerations are required to conclude the description of this first part of the work.

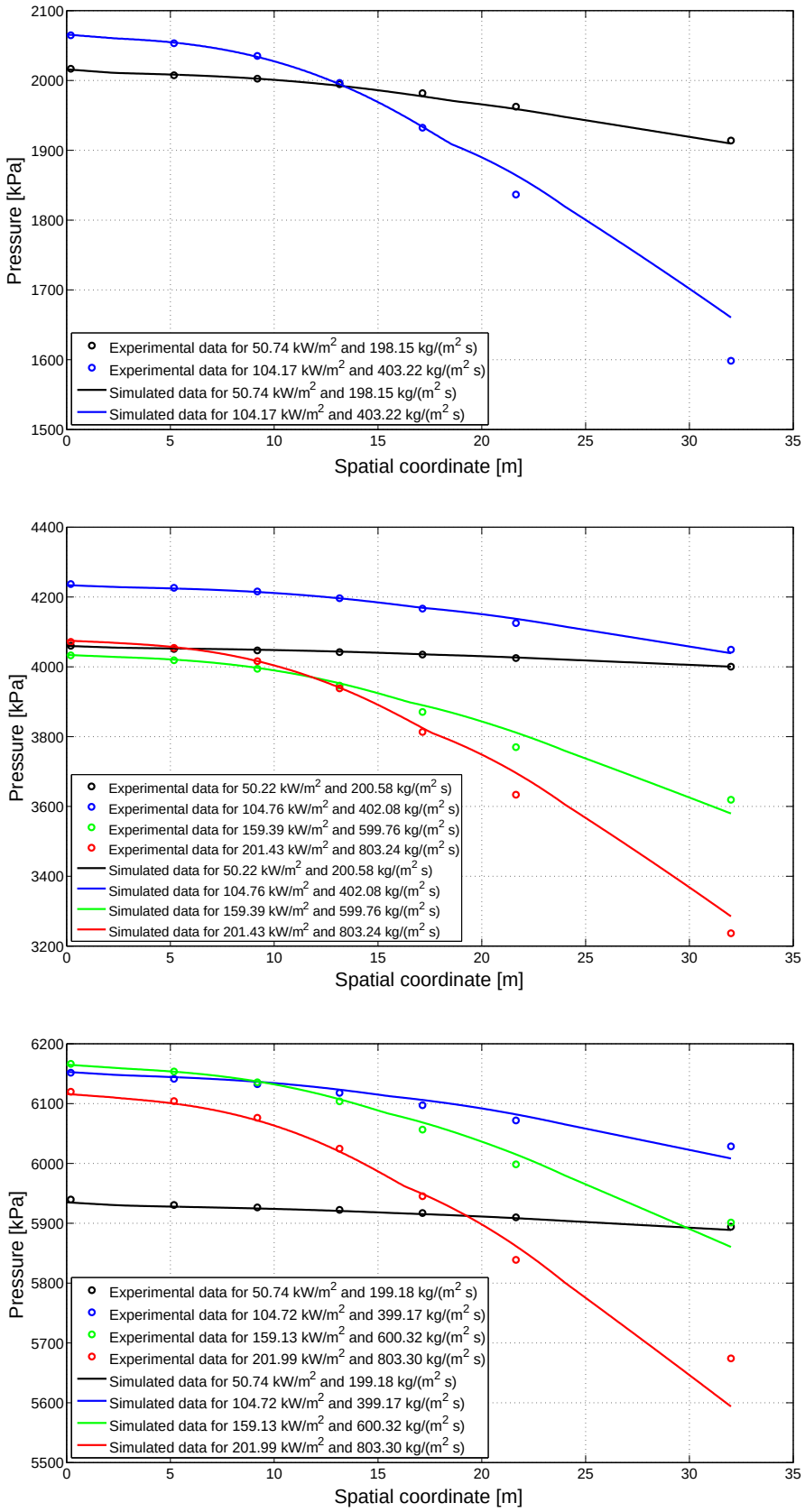

Figure 1.8: Experimental pressure distributions and simulated ones with the one-dimensional model at 20 bar, 40 bar, and 60 bar

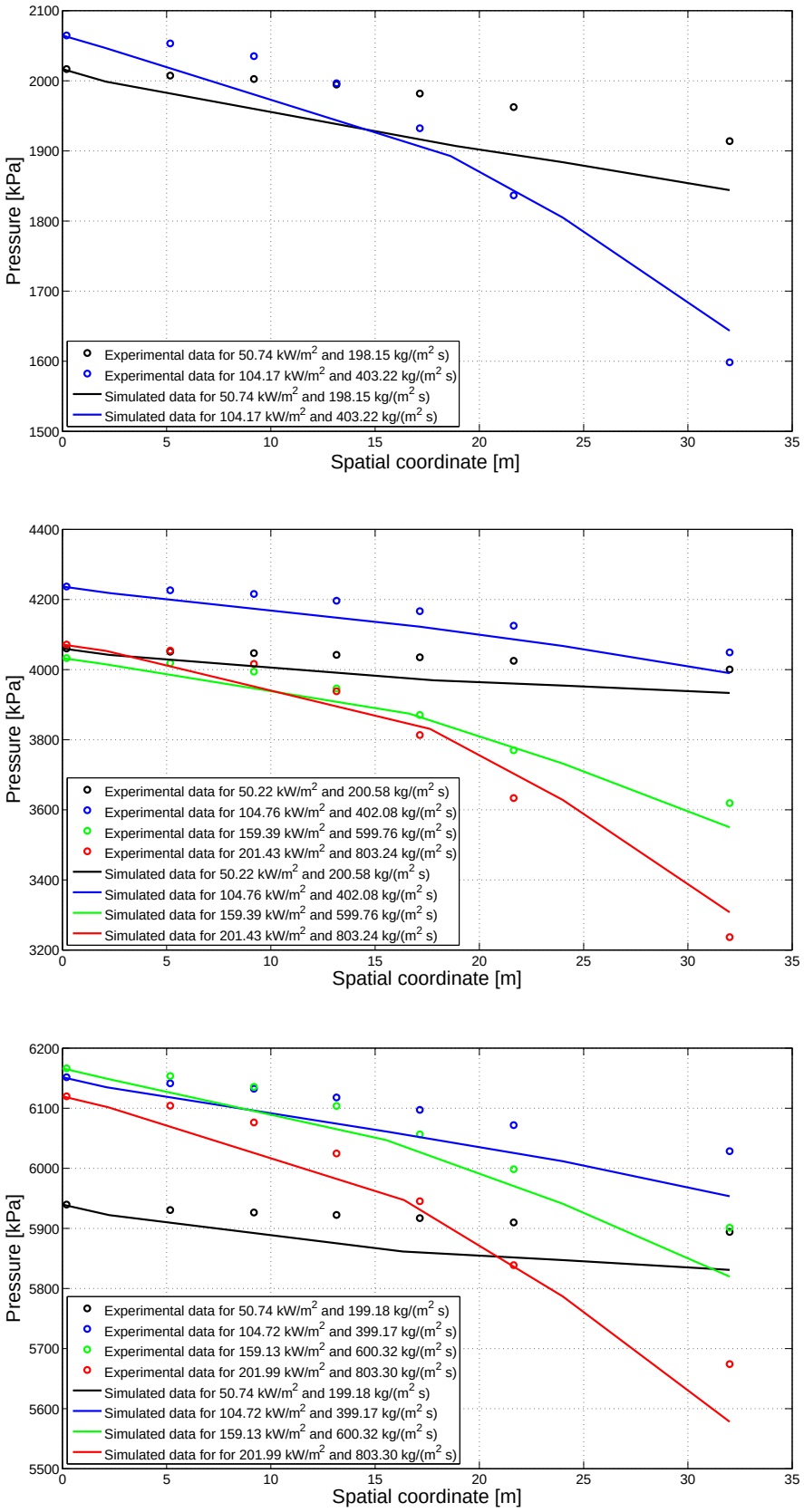

Figure 1.9: Experimental pressure distributions and simulated ones with the zero-dimensional model at 20 bar, 40 bar, and 60 bar

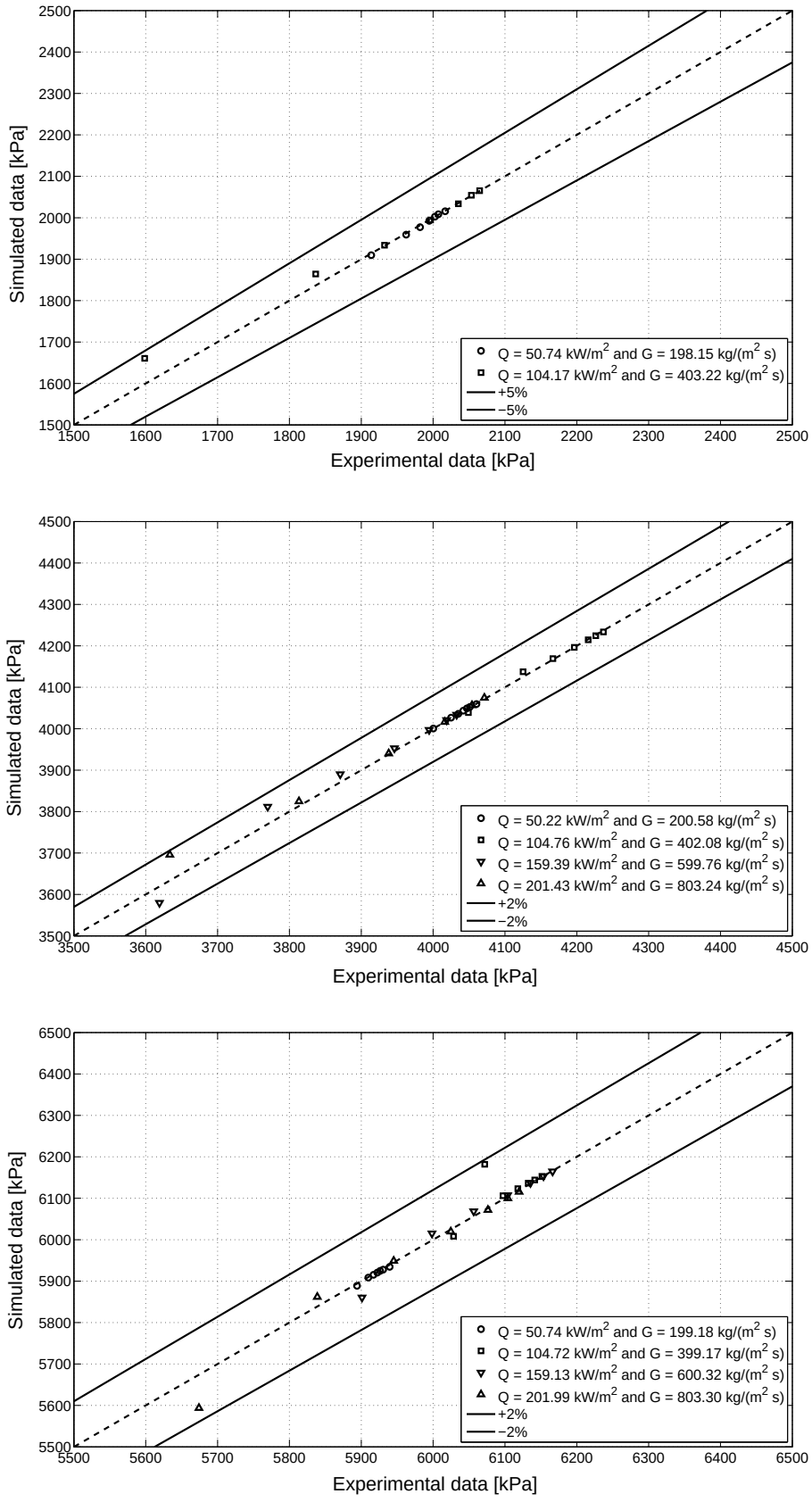

Figure 1.10: Comparison between experimental and simulated with the one-dimensional model pressure distributions at 20 bar, 40 bar, and 60 bar

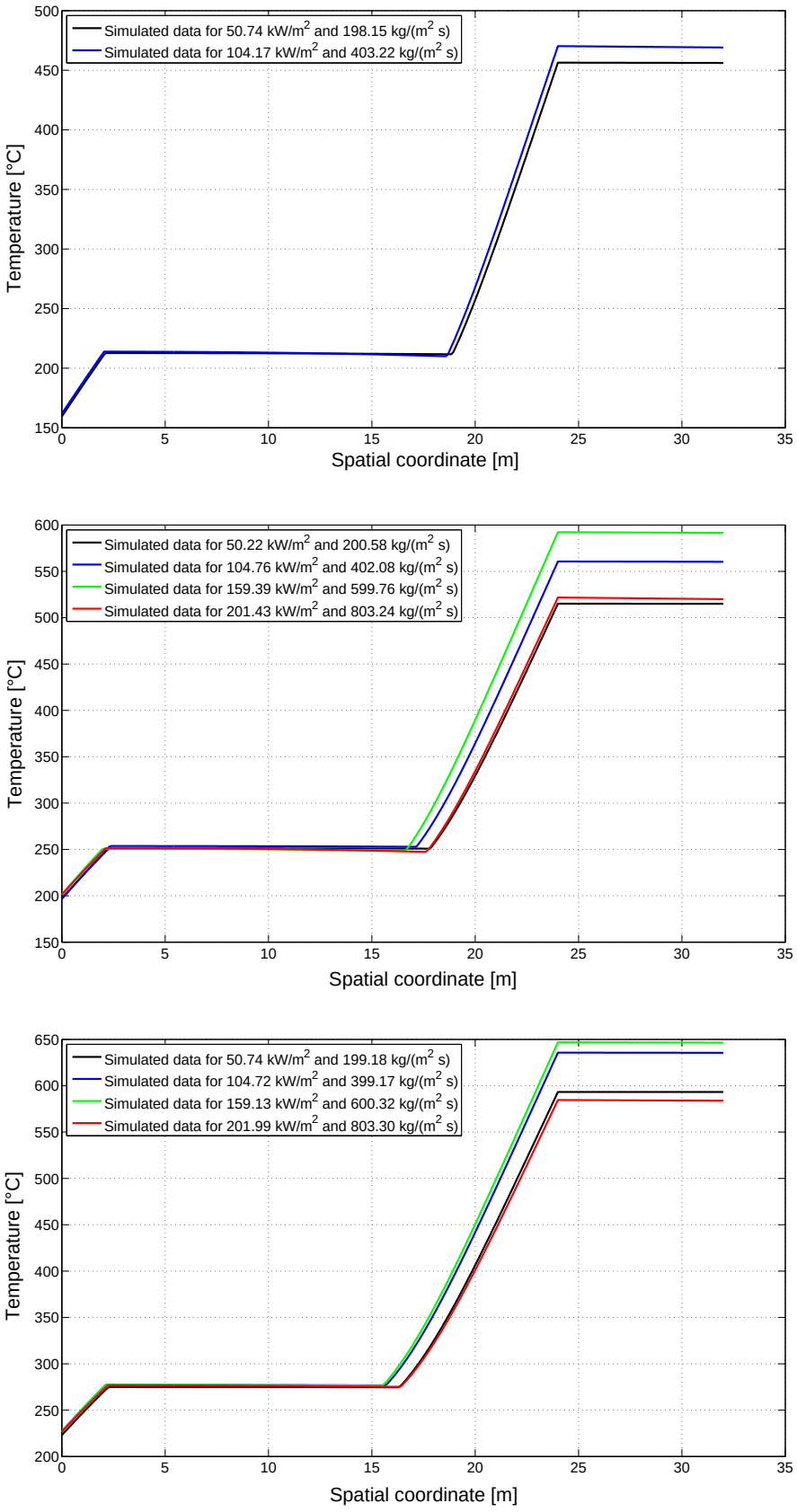

Figure 1.11: Simulated temperature distributions with the one-dimensional model at 20 bar, 40 bar, and 60 bar

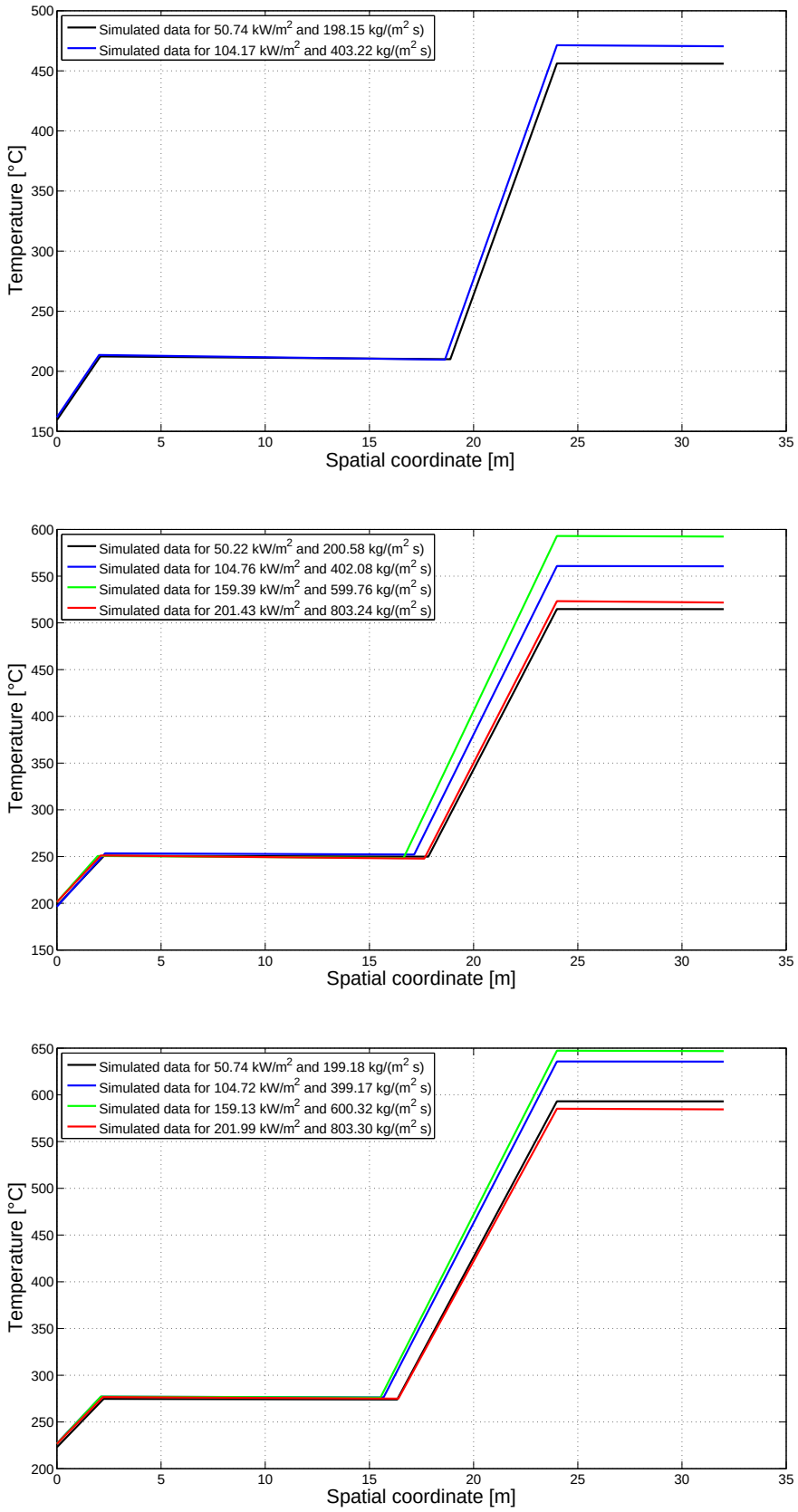

Figure 1.12: Simulated temperature distributions with the zero-dimensional model at 20 bar, 40 bar, and 60 bar

No particular remark has to be done on the building up of the models: indeed, a traditional approach has been used in the deduction of the sets of equations which describe the behavior of the physical systems by them represented.

Instead, an important conclusion can be drawn by their implementation: indeed, whereas the entire realization of a code able to solve this sets of equations would surely present more difficulties, require more time and supply results no so different, employing instruments as *MATLAB* and *COMSOL Multiphysics* allowed to implement them simply and quickly.

The result of the simulations so performed can be summarized in the two following points:

- about the pressure distributions, the comparison between experimental data and simulated ones showed the very good reliability of the one-dimensional model and the scarce fairness of the zero-dimensional model: indeed, as illustrated in Figures 1.7 and 1.9, the maximum error for the first one is lower than 5% and the only weakness appears for low values of pressure and hight values of heat flux and mass flow rate, values not of interest in this work;
- about the temperature distributions, the comparison between simulated data with the one-dimensional model and the ones with the zero-dimensional model underlined a perfect overlap.

That demonstrate how, whereas the zero-dimensional formulation are of interest to solve problems, like thermodynamical problems, in which the energy is the most important variable, the one-dimensional formulation are of interest to solve problems, like fluid dynamics problems, in which the pressure and the velocity is the most important variables.

Nomenclature

A area

a_g gravitational acceleration

D diameter

E	integrated energy (referred to the 0-D model)
	energy (referred to the 1-D model)
f_M	Moody's factor (Darcy's factor kind)
Fr	Froude number
g	mass flux
G	integrated mass flow rate (referred to the 0-D model)
h	enthalpy
l	surface protusion depth
L	channel length
M	integrated mass (referred to the 0-D model)
p	pressure
P	perimeter
q''	thermal flux
Re	Reynolds number
s	surface vapor tension
S	slip ratio
t	temporal coordinate
u	internal energy
v_C	single-phase/two-phase control variable
We	Webber number
x	dynamic quality
z	spatial coordinate

Greek symbols

α	void fraction
β	volumetric ratio
θ	channel slope angle
μ	viscosity
ρ	density
$\phi_{LO,L}$	two phase multiplier

Subscripts

F	frictional
h	hydraulic

in	channel inlet
L	liquid phase
m	mixture (referred to the 1-D model)
out	channel outlet
t	thermal
V	vapor phase
1	subcooled region (referred to the 0-D model)
2	saturated region (referred to the 0-D model)
3	superheated region (referred to the 0-D model)
12	moving boundary between the subcooled region and the saturated one (referred to the 0-D model)
23	moving boundary between the saturated region and the superheated one (referred to the 0-D model)

Superscripts

SP	single phase
TP	two phase
$+$	dynamic (referred to the 1-D model)

Mathematical symbols

$\langle\rangle$	mean value on a certain length

Bibliography

[1] Neil E. Todreas and Mujid S. Kazimi. *NUCLEAR SYSTEMS I - Thermal Hydraulic Fundamentals*. Taylor&Francis, 1989.

[2] Gianfranco Caruso. *Esercitazioni di Impianti Nucleari*. Aracne, 2003.

[3] *COMSOL Multiphysics User's Guide*.

[4] Private comunication.

Chapter 2

A multi-physics zero-dimensional model for LWRs

In this second chapter, the second part of the work is described: the creation of a multi-physics zero-dimensional model for LWRs.

Because of the availability of its data, the attention has been focused on SURE, a Generation III + LWR conceived at *Politecnico di Milano, Dipartimento di Energia* by Cammi et al.[1] and rethought by Memoli et al.[2] for spatial applications. Its principal characteristics are the feeding by a mixture of high enriched uranium and zirconium hydride, the cooling and the moderation by boiling water at high pressure and, above all, a power control entirely entrusted on the primary mass flow rate variations.

Three steps had to be accomplished to create the zero-dimensional model of SURE. At first, a zero-dimensional model for SURE neutronics has been built up and to do that the Avery and Cohn formulation, a theory able to describe the zero power reactor dynamics when a reflector is present, has been used. At second, a zero-dimensional model for its thermo-hydraulics has been built up and to do that those one deduced on the previous chapter, for less than some corrections, has been used: more precisely, because of the phase change mechanism manifesting in a BWR like SURE, by a three point region formulation a two point region one has been deduced. Finally at third, these models have been coupled introducing in the first one the effects due to the fuel temperature variations and the coolant density

ones and in the second one the effects due to the core neutron density variations.

Moreover, a lot of simulations have been performed with *COMSOL Multiphysics* and *MATLAB* so as to verify the validity of the models so developed. Initially, SURE response to reactivity steps of different entities in a zero power condition has been studied; then its response to inlet coolant mass flow rate and inlet coolant temperature steps of different entities in the nominal condition has been analyzed.

2.1 Introduction

During the second part of the work, the development of a multi-physics zero-dimensional model for LWRs has been carried out.

To this end, those one conceived at *Politecnico di Milano, Dipartimento di Energia* by Cammi et al.[1] and rethought by Memoli et al.[2] has been chosen: SURE. It is a Generation III + LWR destined to spatial applications; it is fed by a mixture of high enriched uranium and zirconium hydride and cooled and moderated by boiling water and its peculiar characteristic is represented by the power control entirely entrusted on the primary mass flow rate variations. The choice is feel on it because of the availability of its data: indeed, the aim of this second part was the creation of a model able to simulate, according to the inputs given it, the behavior of different kinds of LWRs.

Two steps led to the development of this model. At first, a zero-dimensional model for SURE neutronics, that is for SURE in a zero power condition, has been built up: to do that, equations of the two regions point kinetic formulation of Avery and Cohn have been used. At second, a zero-dimensional model for both its neutronics and its thermo-hydraulics, that is for SURE in a normal operating condition, has been built up: to do that, equations just mentioned and those ones of the zero-dimensional model deduced on the previous chapter opportunely adapted to SURE have been used; besides, apposite coupling equations between them had to be deduced.

In each of these steps a fundamental hypothesis has been assumed: the reactor chosen can be considered zero-dimensional. It implies for the neutronics the as-

sumption of all those hypothesis the validity of which allows to deduce the point kinetic theory from the diffusion one and for the thermo-hydraulics the assumption of all those hypothesis mentioned in the previous chapter.

Later on, a short description of SURE precedes the explanation of the way by means of which the zero-dimensional model for its neutronics and those one for both its neutronics and its thermo-hydraulics have been developed. Moreover, the result of some simulations performed with *COMSOL Multiphysics* and *MATLAB* so as to verify the validity of both these models are illustrated and explained.

2.2 A short description of SURE

SURE, acronym for *Study on nUclear Reactor dEvolopment* is a Generation III + LWR destined to spatial applications.

Even a short description of its main characteristics, both constructive and functional, requires the frame in the context in which it has been conceived.

The electric power production from nuclear font, especially those one that exploits the nuclear fission reaction, has a lot of undoubted advantages: by those ones concerning the environment problems due to the greenhouse gases emission to those ones concerning the social and political problems due to the fossil fuels exhaustibility. In particular one among its peculiar characteristics, the high energy density, makes it perfect to all those applications, like the spatial ones, in which a moderate weight and a long autonomy represent the most important demands. On the other hand, the differences between a terrestrial application and a spatial one, and consequently the complications which afflict the latter one, concern a lot of aspects: from the maintenance to the thermodynamical cycle.

This double side of a coin represents the context in which SURE has to be frame.

Figure 2.1 shows a pattern of the whole power plant in which SURE works.

Let us first of all considerer the constructive features.

It is an indirect cycle power plant constitute by a primary system and a secondary system: the first one is formed by a pump, the core and the channel between

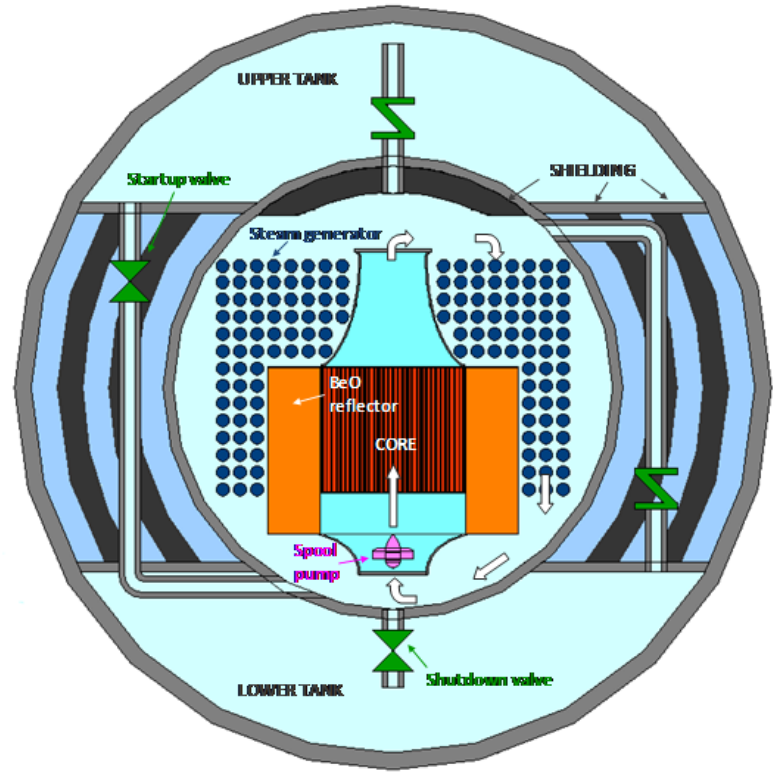

Figure 2.1: A pattern of the power plant in which SURE works

the barrel and the vessel and works according to a simple thermodynamical cycle of heating and cooling; instead, the second one is formed by an helically coiled steam generator, a turbine, a condenser and a pump and works according to a Rankine thermodynamical cycle. As Figure 2.1 shows, its peculiar constructive characteristics is represented by the integrated layout: indeed, the core, the primary pump and the helically coiled steam generator are all located into the vessel.

In particular, the core is composed by nineteen fuel elements; in each of them seven fuel rods are located according to an hexagonal lattice and the coolant is separately tuned by means of apposite orifices; moreover, it is surrounded by a reflector both in axial direction and in radial direction.

Figure 2.2 shows the axial section of the whole reactor, of the core and of the single fuel element.

Some informations about the materials. The fuel is represented by a metal matrix of high enriched uranium and zirconium hydride [3], choice made in order to guarantee a high value of the fuel feedback coefficient and consequently an inherent

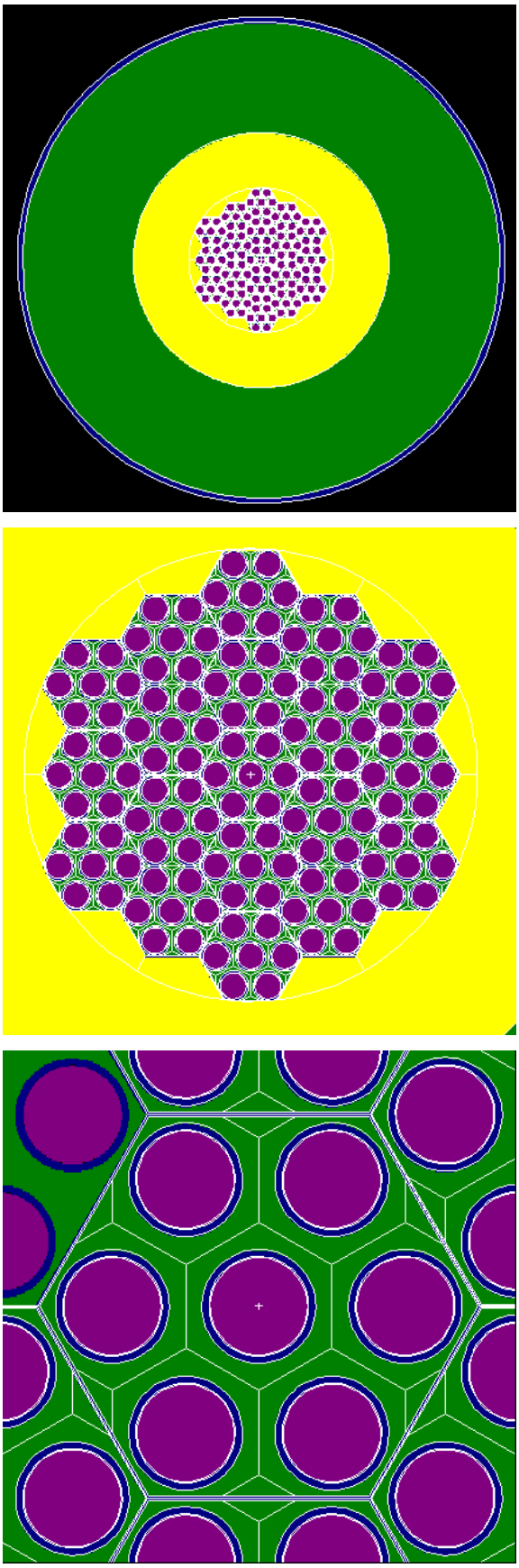

Figure 2.2: An axial section of the whole SURE reactor, of its core and of its single fuel element

Parameter	Value	Measure unit
Reactor height	4.810×10^{-1}	m
Reactor radius	4.250×10^{-1}	m
Core height	2.410×10^{-1}	m
Core radius	1.198×10^{-1}	m
Number of fuel elements	19	-
Number of fuel rods	133	-
Pitch between adjacent fuel rods	1.990×10^{-2}	m
External clad radius	8.910×10^{-3}	m
Internal clad radius	7.790×10^{-3}	m
External fuel radius	7.615×10^{-3}	m
Reflector height	3.210×10^{-1}	m
Reflector external radius	2.998×10^{-1}	m
Reflector internal radius	1.298×10^{-1}	m
Superior water layer height	4.000×10^{-2}	m
Inferior water layer height	1.200×10^{-1}	m
Superior water layer radius	4.139×10^{-1}	m
Inferior water layer radius	2.998×10^{-1}	m

Table 2.1: Constructive features of SURE

safety: indeed, with such a choice two different phenomenas, the broadening of the absorption cross section resonances and the reduction of the moderation ability of the hydrogen due to the variation of its energy level, attend with the increase of the fuel temperature. The primary coolant and the secondary one is represented by water; in particular, the core is cooled by boiling water so as to put into practice the power control mentioned. Finally, the reflector is represented by beryllium oxide in radial direction and by water in axial direction.

Let us now consider the functional features.

The primary water acquires a certain quantity of thermal energy flowing through the core and undergoing a phase change; then it yields the quantity of thermal

Parameter	Value	Measure unit
Nominal thermal power	800	kW
Fuel mass	47.8	kg
Uranium mass fraction in the fuel	0.4500	–
Uranium volumetric fraction in the fuel	0.1942	–
Weigh enrichment of uranium 235	0.93	-
Uranium 235 nucleus volumetric density	8.6695×10^{27}	$1/m^3$
Uranium 238 nucleus volumetric density	6.4487×10^{26}	$1/m^3$
Zirconium hydride mass fraction in the fuel	0.5500	–
Zirconium hydride volumetric fraction in the fuel	0.8058	–
Hydrogen/Zirconium ratio	1.7	-
Nominal inlet coolant pressure	155	bar
Nominal inlet coolant temperature	335	℃
Nominal inlet coolant mass flow rate	0.97	kg/s

Table 2.2: Functional features of SURE

energy so acquired to secondary water which, carrying out a Rankine thermodynamical cycle, produces electric energy.

An important characteristic of SURE, as just mentioned, is the innovative power control system in it adopted: indeed, its core is out of traditional control rods and the variations of the thermal power by it produced are entirely entrusted to the inlet mass flow rate, and consequently to the boiling boundary, ones. Such a choice, as can be easily deduced, is a consequence of the application field to which it is destined and, more precisely, to the necessity to reduce as much as possible the maintenance operations.

The principal constructive and functional data of SURE are reported on Tables 2.1 and 2.2.

A zero-dimensional model for SURE, quite different by the one realized in the

Parameter	Value	Measure unit
Uranium density	18 620	kg/m^3
Uranium thermal diffusion coefficient	1.1×10^{-5}	m^2/s
Uranium specific heat	120	J/(kg℃)
Uranium thermal conductivity coefficient	2.458	W/(m℃)
Fuel temperature feedback coefficient	−3	pcm/℃
Coolant density feedback coefficient	−30	$pcm/(kg/m^3)$
Total heat transfer coefficient between fuel and coolant	2.670×10^3	W/℃

Table 2.3: Results of a previous work carried out on SURE here adopted

present work, has been just developed in [4]. On Figure 2.3 and on Table 2.3 some results obtained during that work and here adopted are reported.

Just in [4] a more detailed description of SURE and also of the model for it developed mentioned can be found.

2.3 The neutronics model

The first step of this second part has been the development of a zero-dimensional neutronics model for SURE in a zero power condition.

Because of the presence of a reflector, the creation of such a model requires necessary the adoption of a two region formulation of the point kinetic theory and to this end a possible choice is represented by those one formulated by of Avery and Cohn [5], a theory initially conceived by Avery for a general two coupled regions system and then adapted by Cohn to the reflected cores: indeed, according to it, the overall system is composed by two different regions, the core and the reflector, the coupling of which can be realize introducing apposite coupling terms containing the probability that a neutron lost from one region will appear in the other one.

The use of the Avery and Cohn formulation of the point kinetic theory demands a short summary of its basics: it has been done before the description of its ap-

tb

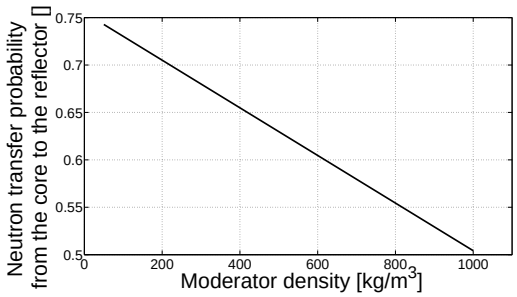

(a) Neutron transfer probability from the core to the reflector

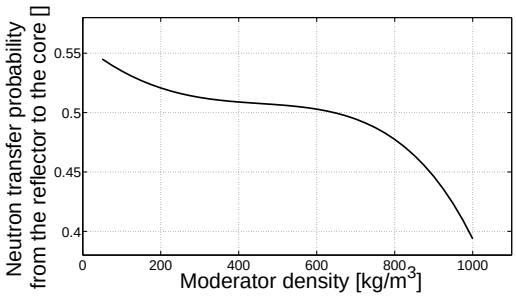

(b) Neutron transfer probability from the reflector to the core

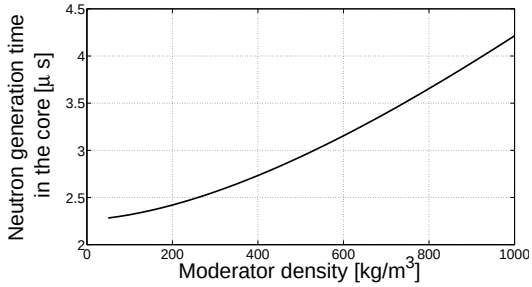

(c) Neutron generation times in the core

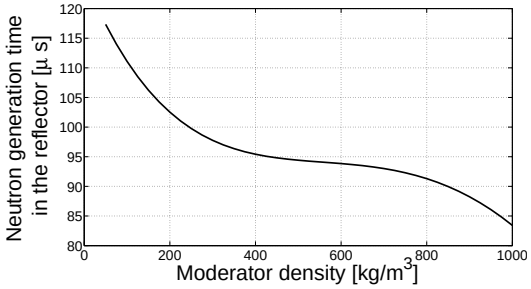

(d) Neutron generation times in the reflector

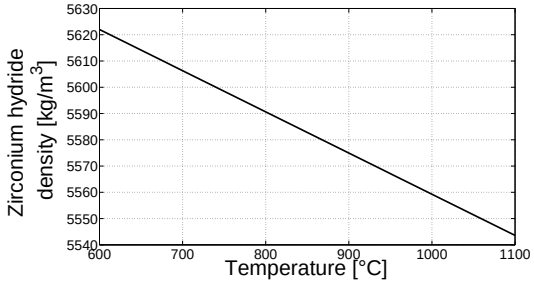

(e) Zirconium hydride density versus temperature

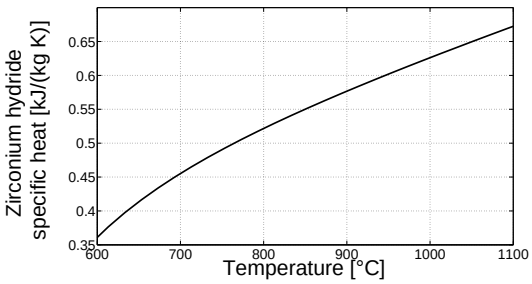

(f) Zirconium hydride specific heat versus temperature

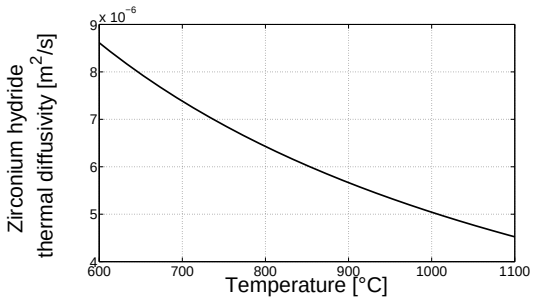

(g) Zirconium hydride thermal diffusivity versus temperature

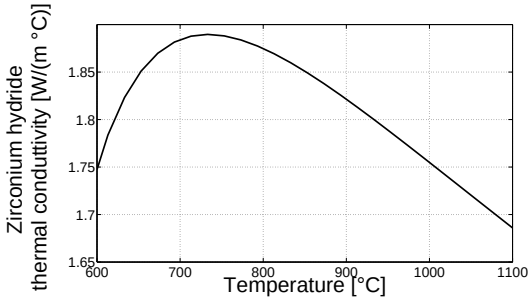

(h) Zirconium hydride thermal conductivity versus temperature

Figure 2.3: Results of a previous work carried out on SURE here adopted

plication to SURE. Moreover, the result of some simulations performed with the model so developed are reported and discussed.

2.3.1 The Avery and Cohn formulation of the point kinetic theory

The Avery and Cohn formulation of the point kinetic theory, summarized in Appendix C, is a formulation able to reproduce the zero power reactor dynamics when a reflector is present.

The application field of this theory is strongly defined by a large number of hypothesis the validity of which allows to deduced it. These hypothesis are the following:

- the reactor is constitute by two different regions: the core, a multiplying system formed by fuel materials, moderator materials and absorber materials, and the reflector, a non multiplying system formed by only the last two ones;
- the core is homogeneous, that is all the materials in it contained are intimately mixed;
- the reflector is homogeneous, that is that is all the materials in it contained are intimately mixed;
- both in the core and the reflector the neutrons have all the same energy, more precisely thermal energy;
- in the core all the spatial transient regime are exhaustive, that is the spatial distribution and the temporal trend of both the neutron density and the precursor density can be separated; moreover their spatial distribution can be assumed to be the same;
- in the reflector all the spatial transient regime are exhaustive, that is the spatial distribution and the temporal trend of the neutron density can be separated;
- the core is near to a critically condition;

- the neutron transfer from the core to the reflector and vive versa can be model, as hinted previously, using coupling terms containing the probability that a neutron loss from one will appear in the other one.

If the validity of these hypothesis is assumed, the equations able to reproduce the zero power reactor dynamics when a reflector is present are three.

The first one is a balance equation for neutrons in the core and can take both the following form:

$$\frac{dn_C}{dt} = \left[k_C\,(1-b)\right]\frac{n_C}{\tau_C} + f_{RC}\,\frac{n_R}{\tau_R} + \sum_{i=1}^{N}\lambda_i c_i \tag{2.1}$$

and the following one:

$$\frac{dn_C}{dt} = \frac{\varrho - b - f(1-b)}{f}\,\frac{n_C}{\Lambda_C} + f_{RC}\,\frac{1-\varrho}{1-f}\,\frac{n_R}{\Lambda_R} + \sum_{i=1}^{N}\lambda_i c_i \tag{2.2}$$

being the relation between Λ_C and τ_C:

$$\Lambda_C = \frac{\tau_C}{k_{eff}\,(1-f)} \tag{2.3}$$

and those one between Λ_R and τ_R:

$$\Lambda_R = \frac{\tau_R}{k_{eff}\,(1-f)} \tag{2.4}$$

The second one is a balance equation for neutrons in the reflector and can take both the following form:

$$\frac{dn_R}{dt} = f_{CR}\,\frac{n_C}{\tau_C} - \frac{n_R}{\tau_R} \tag{2.5}$$

and the following one:

$$\frac{dn_R}{dt} = f_{CR}\,\frac{1-\varrho}{1-f}\,\frac{n_C}{\Lambda_C} - \frac{1-\varrho}{1-f}\,\frac{n_R}{\Lambda_R} \tag{2.6}$$

being the relations between Λ_C and τ_C and between Λ_R and τ_R those ones of the equation (2.3) and equation (2.4).

Finally the third one is a balance equation for the precursors in the core and can take both the following form

$$\frac{dc_i}{dt} = k_C\,b_i\,\frac{n_C}{\tau_C} - \lambda_i\,c_i \tag{2.7}$$

and the following one:

$$\frac{dc_i}{dt} = b_i \Lambda_C n_C - \lambda_i c_i \tag{2.8}$$

being the relations between Λ_C and τ_C and between Λ_R and τ_R those ones of the equation (2.3) and equation (2.4).

In the present work, the second form has been chosen: indeed, the presence of the reactivity allows to couple the neutronics and the thermo-hydraulics using simply the reactivity feedback coefficients.

As can be seen from equation (2.2) and (2.6), the source term representing in the first one the neutrons loss from the reflector and appeared in the core and, vice versa, in the second one the neutrons loss from the core and appeared in the reflector containing the factors f_{CR}, f_{RC} and f: these terms represent just the probability that a neutron passes from the core to the reflector, that a neutron passes from the reflector to the core and that a neutron passed from the core to the reflector return behind.

To note finally that in a stationary state in which obviously the reactivity is null, the set of equations described are homogeneous and characterized by a singular coefficient matrix, that is it is undetermined. Therefore, possible initial conditions have to be calculated fixing for example a value of the neutron density in the core n_{C_0} able to guarantee a nominal thermal power production and determining then since it the following ones for the neutron density in the reflector:

$$n_{R_0} = \frac{1}{f_{CR} \Lambda_C \Lambda_R} n_{C_0} \tag{2.9}$$

and for the precursor density of each group in the core:

$$c_{i0} = \frac{b_i \Lambda_C}{\lambda_i} n_{C_0} \tag{2.10}$$

2.3.2 The application of the Avery and Cohn formulation of the point kinetic theory to SURE

In virtue of the hypothesis assumed the Avery and Cohn formulation led to a zero-dimensional model whereupon no particular calculations was so needed to applicate it to SURE: only the delayed neutron fractions of each precursor group

Group	Delayed neutron fraction [−]	Decay constant [s^{-1}]
1	$2.351\,921 \times 10^{-4}$	$1.259\,26 \times 10^{-2}$
2	$1.401\,961 \times 10^{-3}$	$3.126\,80 \times 10^{-2}$
3	$1.244\,881 \times 10^{-3}$	$1.135\,92 \times 10^{-1}$
4	$2.625\,081 \times 10^{-3}$	$3.074\,61 \times 10^{-1}$
5	$8.056\,541 \times 10^{-4}$	1.306 29
6	$2.093\,411 \times 10^{-4}$	3.560 20

Table 2.4: Delayed neutron fractions and decay constants for uranium 235 precursor groups

and of all the precursors, the decay constants of each precursor group and of all the precursors, the neutron generation times in the core and in the reflector and the neutron transfer probabilities between core and reflector have to be determinate or simply chosen.

For the delayed neutron fractions and for the decay constants the values reported in Table 2.4, characteristics of the uranium 235 precursor groups, have been chosen: otherwise, assuming that all the neutrons both in the core and in the reflector are thermal and being the SURE fuel a mixture of high enriched uranium and zirconium hydride, this is the isotope of interest.

Instead, for the other parameters the values corresponding to the nominal moderator density of about $390\,kg/m^3$, which can be deduced by the trend reported in Figure 2.3, have been fixed. The reasons of such a choice can be search in the simulations after done: indeed, these ones have been all lunched just by the nominal condition.

Besides the parameters referred above, the initial values of the neutron density in the core, the neutron density in the reflector and the precursor density of each group in the core have to be determined. To do that, the first one has been calculated using the following formula:

$$n_{C_0} = \frac{q'''}{v_n\,\sigma_{U_{235}}\,N_{U_{235}}\,E_{U_{235}}} \tag{2.11}$$

and the values of the uranium 238 nucleus volumetric density reported on Table

2.3: the reasons of such a choice have been just mentioned; then, by the value obtained of $3.775\,313 \times 10^{12}\,\mathrm{m}^{-3}$, the initial values of the other ones have been calculated using equations (2.9) and (2.10).

2.3.3 The simulation results

Before couple the neutronics model described and the zero-dimensional thermo-hydraulics one deduced on the previous chapter, some simulations have been performed so as to verify the availability of the first one: more precisely, a comparison between the SURE responses in a zero power condition to a certain perturbation determined considering or not the precursors and an analysis of its response always in a zero power condition to different perturbations considering the precursors have been done.

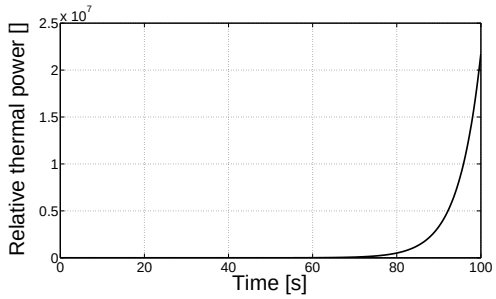

(a) Positive reactivity step of 1 % - Without precursors

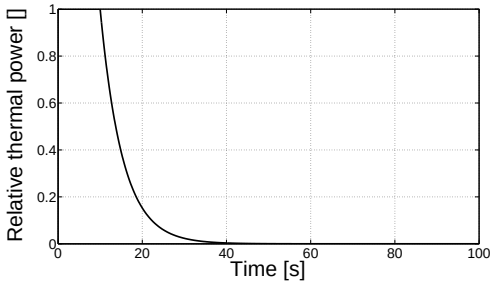

(b) Negative reactivity step of 1 % - Without precursors

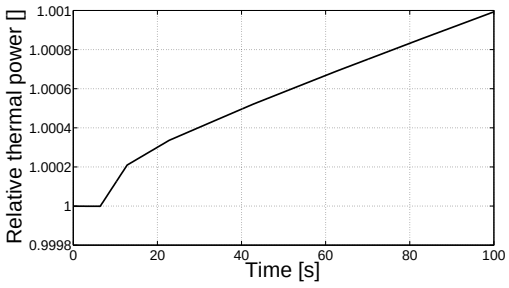

(c) Positive reactivity step of 1 % - With precursors

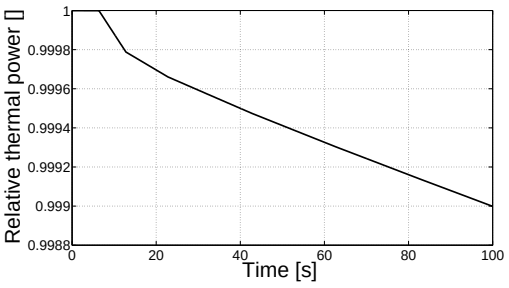

(d) Negative reactivity step of 1 % - With precursors

Figure 2.4: SURE responses in a zero power condition to a positive reactivity steps of 1 % and a negative one determined respectively considering or not the precursors

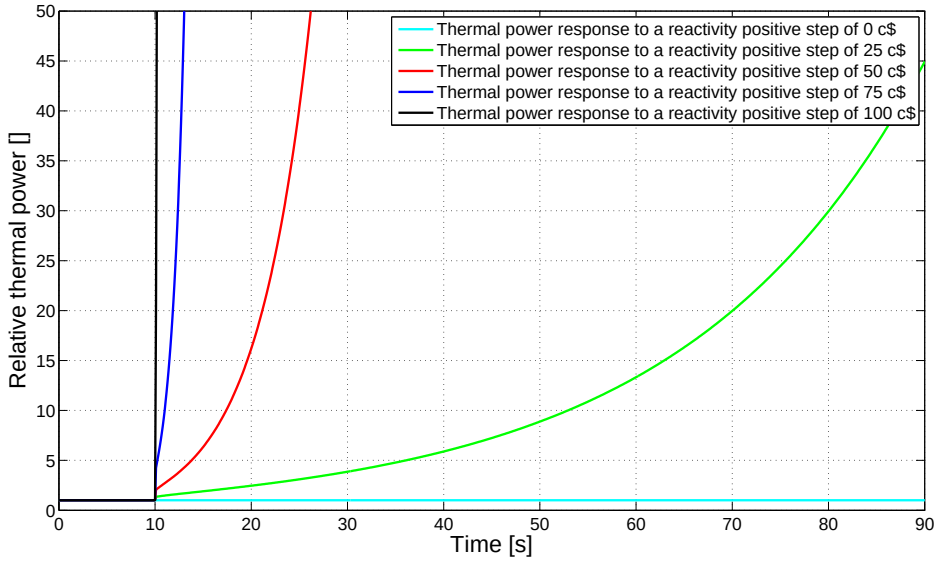

Figure 2.5: SURE response in a zero power condition to positive reactivity steps of different entities determined considering the precursors

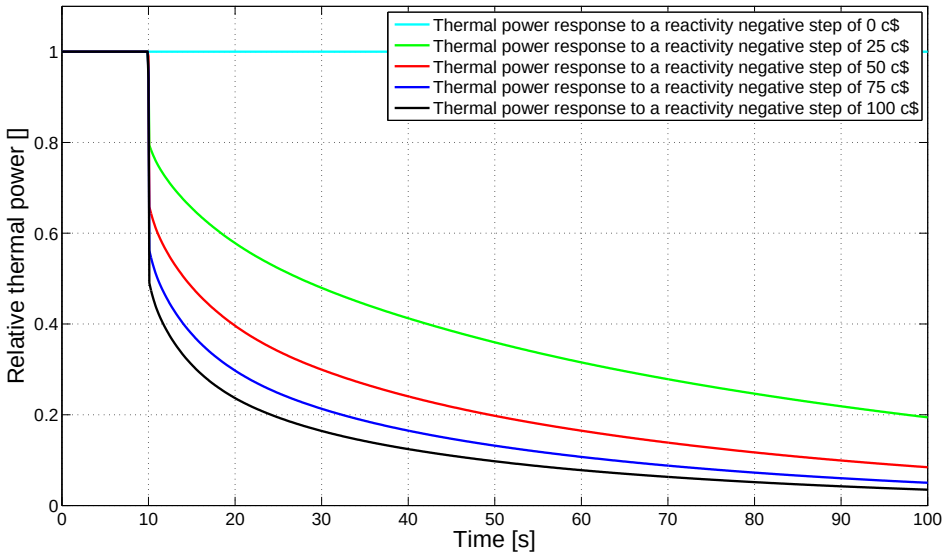

Figure 2.6: SURE response in a zero power condition to negative reactivity steps of different entities determined considering the precursors

To this end, the neutron balance equations in the core and in the reflector (2.2) and (2.6) and their relative initial conditions and, if necessary, the precursor balance equations of each group (2.8) and their relative initial conditions have been

implemented using the *COMSOL Multiphysics Global Equations* section. Moreover, the values choice for the delayed neutron fractions and the decay constants of each precursor group, for the neutron transfer probabilities from the core to the reflector and vice versa and for the neutron generation times in the core and in the reflector have been loaded.

On Figures 2.4 the SURE responses since the initial values referred above to a positive reactivity step of 1 % given 10 s after the beginning of the simulation and a negative one determined assuming a zero power condition and considering or not the precursors are illustrated. Whereas in a zero power condition in which the precursors are not considered also a modest reactivity insertion can induce neutron flux, and consequently thermal power production, variations of several magnitude orders, the same perturbation in the same condition induces variations of these variables of not even a percentage point if the precursors are considered; not only, because this increase or this descrease is as much rapid in the first case that the reactor dynamic is practically uncontrollable.

Instead, Figures 2.5 and 2.6 show the SURE response since the initial values referred above to positive or negative reactivity steps of 0$, 25$, 50$, 75$ and 100$ given 10 s after the beginning of the simulations determined assuming a zero power condition and considering the precursors. In both these figures, the prompt jump and the exponential trend the zero power reactors dynamic are visible and, moreover, as much marked as high is the entity of the reactivity insertions.

The simulation result, absolutely physically coherent, underlines the fairness of the neutronics model described.

2.4 The neutronics and thermo-hydraulics model

The second step of this second part has been the development of a zero-dimensional neutronics and thermo-hydraulics model for SURE in a normal operation condition.

Of fact, the availability of the neutronics model described and of the thermo-hydraulics one deduced on the previous chapter ratifies just its existence: indeed,

to create such a model it is sufficient to make on the second one some changes so as to adapt it to SURE and to determine apposite coupling equations between them. To note that, although the latter did not show a very good reliability in the reproduction of the experimental pressure distributions, it can be used to carry out the aim referred above: indeed, the active height of SURE core is 2.410×10^{-1} m and, consequently, the pressure drops don't affect so much its behavior, at least in a first approximation.

The subject of the following paragraph are the description both of the changes done on the thermo-hydraulics model deduced on the previous chapter so as to make it usable for SURE and of the coupling equations determined so as to couple this one to the neutronics one just described. Afterward, the result of some simulations performed with the model so obtained, summarized in Appendix D, are reported and discussed.

2.4.1 The application of the zero-dimensional thermo-hydraulics model to SURE

Two changes have to be done on the thermo-hydraulics model deduced on the previous chapter to applicate it to SURE: the first one concerns the phase change undergone by the water on one hand in the general heated channel and on the other hand in the SURE core; instead, the second one concerns the presence in the latter of the fuel, that is of a hot wall with which the water exchange thermal energy in a condition of temperature imposed. Moreover, a third one has to be done introducing the correct geometric features of SURE.

Let us considerer the first one.

The first change consisted of the passage from a three point region formulation to a two point region one: indeed, the model deduced on the previous chapter has been conceived with the intent that simulate the behavior of a water mixture in such a heated channel that it goes into in a subcooled condition and, after a phase change, goes out in a superheated condition; whereas that which happens in SURE is slightly different going into the primary water in a subcooled condition, undergoing an incomplete phase change and going out in a saturated condition.

This change has been carried out rethinking the physical system considered and repeating the same procedure by means of which in the first chapter the equations of each point region have been deduced.

More precisely, going on assume all the hypothesis mentioned in the previous chapter both on the physical system and on the physical mechanism of the phase change, two region has been so considered: the subcooled region and the saturated region. For the subcooled region the same conservation, constitutive and closure equations have been obviously deduced: equations from (1.56) to (1.72). Instead, for the saturated region constitutive equations take the following form:

$$\frac{dM_2}{dt} = G_{12} - \rho_{12}\, A_h\, \frac{dL_1}{dt} - G_{23} + \rho_{23} A_h \frac{d\,(L_1 + L_2)}{dt} \tag{2.12}$$

$$\begin{aligned}\frac{dG_2}{dt} = \frac{G_{12}^2}{\rho_{12}\, A_h} - G_{12}\, \frac{dL_1}{dt} - \frac{G_{23}^2}{\rho_{23}\, A_h} + G_{23}\, \frac{d\,(L_1 + L_2)}{dt} + p_{12}\, A_h - p_{23}\, A_h \\ -a_g\, \rho_2\, A_h\, L_2 - \phi_2\, \frac{f_{_{M_2}}}{2\, D_h} \left\langle \frac{G^2}{\rho_L\, A_h} \right\rangle_2 L_2\end{aligned} \tag{2.13}$$

$$\frac{dE_2}{dt} = G_{12}\, h_{12} - \rho_{12}\, u_{12}\, A_h\, \frac{dL_1}{dt} + \rho_{23}\, u_{23}\, A_h\, \frac{d\,(L_1 + L_2)}{dt} - G_{23}\, h_{23} + q^{''}\, P_t\, L_2 \tag{2.14}$$

where the mass M_2, the mass flow rate G_2 and the energy E_2 can be expressed by the following formulas:

$$M_2 = \int_{L_1}^{L_1+L_2} (\rho\, A_h)\, dz = \langle \rho \rangle_2\ A_h\, L_2 \tag{2.15}$$

$$G_2 = \int_{L_1}^{L_1+L_2} (g\, A_h)\, dz = \langle G \rangle_2\ L_2 \tag{2.16}$$

$$E_2 = \int_{L_1}^{L_1+L_2} [(\rho\, h - p)\ A_h]\, dz = \langle \rho\, h \rangle_2\ A_h\, L_2 - \langle p \rangle_2\ A_h\, L_2 \tag{2.17}$$

Constitutive equations, needed to define the outlet values of the density of each phase, the enthalpy of each phase and the viscosity of the only liquid phase, take the following form:

$$\rho_{L_{out}} = \rho_L(p_{out}) \tag{2.18}$$

$$\rho_{V_{out}} = \rho_V(p_{out}) \tag{2.19}$$

$$h_{L_{out}} = h_L(p_{out}) \tag{2.20}$$

$$h_{V_{out}} = h_V(p_{out}) \tag{2.21}$$

$$\mu_{L_{out}} = \mu_L(p_{out}) \tag{2.22}$$

Finally, closure equations expressing the mean value along the saturated region of the density, the mass flow rate, the kinetic energy term of the frictional pressure drops, the viscosity, the volumetric specific enthalpy and the pressure are needed:

$$\langle \rho \rangle_2 = \frac{\rho_{12} + \rho_{out}}{2} \tag{2.23}$$

$$\langle G \rangle_2 = \frac{G_{12} + G_{out}}{2} \tag{2.24}$$

$$\left\langle \frac{G^2}{\rho\, A_h} \right\rangle_2 = \frac{\dfrac{G_{12}^2}{\rho_{12}\, A_h} + \dfrac{G_{out}^2}{\rho_{out}\, A_h}}{2} \tag{2.25}$$

$$\langle \mu \rangle_2 = \frac{\mu_{12} + \mu_{out}}{2} \tag{2.26}$$

$$\langle \rho\, h \rangle_2 = \frac{(\rho\, h)_{12} + (\rho\, h)_{out}}{2} \tag{2.27}$$

$$\langle p \rangle_2 = \frac{p_{12} + p_{out}}{2} \tag{2.28}$$

Besides these ones, the following one for the Reynolds Number:

$$Re_2 = \frac{\langle G \rangle_2\, D_h}{A_h\, \langle \mu \rangle_2} \tag{2.29}$$

the Mac Adams correlation for the Moody's factor and the Jones correlation for the single-phase/two-phase corrective factor have to be added. Moreover, the exit density and the enthalpy density have to be so specify:

$$\rho_{out} = \rho_{L_{out}}\,(1 - \alpha_{out}) + \rho_{V_{out}}\,\alpha_{out} \tag{2.30}$$

$$h_{out} = h_{L_{out}}\,(1 - x_{out}) + h_{V_{out}}\,x_{out} \tag{2.31}$$

where the exit void fraction and the exit vapor quality are related by the following formula:

$$\alpha_{out} = \frac{1}{1 + \dfrac{1 - x_{out}}{x_{out}}\,\dfrac{\rho_{V_{out}}}{\rho_{L_{out}}}\,S_{out}} \tag{2.32}$$

being the slip ratio:

$$S_{out} = C_{0_{out}} + \frac{(C_{0_{out}} - 1)\,x_{out}\,\rho_{L_{out}}}{(1 - x_{out})\,\rho_{V_{out}}} \tag{2.33}$$

and:

$$C_{0_{out}} = B_{out}\left[1+\left(\frac{1}{\beta_{out}}-1\right)^{B_{out}}\right] \tag{2.34}$$

$$\beta_{out} = \frac{1}{1+\frac{1-x_{out}}{x_{out}}\frac{\rho_{V_{out}}}{\rho_{L_{out}}}} \tag{2.35}$$

$$B_{out} = \left(\frac{\rho_{V_{out}}}{\rho_{L_{out}}}\right)^{0.1} \tag{2.36}$$

Obviously, also in a two point region formulation a bond equation on the total length, that is:

$$L = L_1 + L_2 \tag{2.37}$$

has to be inserted.

As can be seen from equations deduced for the saturated region, the difference between a three point region formulation and a two point region one is that in the second, undergoing the water an incomplete phase change, all the properties characteristics of a two phase condition, like the void fraction, the vapor quality and the slip ratio, appear.

Let us now considerer the second one.

The second change consisted of the introduction of a energy balance equation for the fuel. This equation takes the following form

$$\frac{d}{dt}(m_{fuel}\,\chi_{fuel}\,T_{fuel}) = q'''\,m_{fuel}\,\rho_{fuel} - q''\,A_t \tag{2.38}$$

where for the density and the specific heat the relations found in [4] have been used. More precisely:

- the density can be expressed by the following formula:

$$\rho_{fuel} = \frac{f_{m_U}}{\rho_U} + \frac{f_{m_{ZrH_x}}}{\rho_{ZrH_x}} \tag{2.39}$$

  where the mass fractions f_{m_U} and $f_{m_{ZrH_x}}$ are characteristics of the mixture of uranium and zyrconium hydride adopted in SURE, the uranium density is a well known quantity and the zirconium hydride density takes the following form:

$$\rho_{ZrH_x} = \frac{1}{0.1706+0.0042\,x}\,[1-\xi_{ZrH_x}\,(T[K]-300)] \quad \mathrm{g/cm^3} \tag{2.40}$$

- the specific heat can be expressed by the following formula:

$$\chi_{fuel} = \frac{\kappa_{fuel}}{d_{fuel}\,\rho_{fuel}} \tag{2.41}$$

where the fuel thermal conductivity and thermal diffusivity are related to those one of the uranium and the zirconium hydride according to the following expressions:

$$\kappa_{fuel} = \kappa_U\, f_{v_U} + \kappa_{ZrH_x}\, f_{v_{ZrH_x}} \tag{2.42}$$

and

$$d_{fuel} = d_U\, f_{v_U} + d_{ZrH_x}\, f_{v_{ZrH_x}} \tag{2.43}$$

in which the volume fractions f_{v_U} and $f_{v_{ZrH_x}}$ are characteristics of the mixture of uranium and zirconium hydride adapted in SURE, the uranium thermal conductivity and thermal diffusivity are well known quantities and the zyrconium hydride thermal conductivity and thermal diffusivity are take the following form:

$$\kappa_{ZrH_x} = d_{ZrH_x}\,\chi_{ZrH_x}\,\rho_{ZrH_x} \quad \mathrm{W/(cmK)} \tag{2.44}$$

being

$$\begin{aligned}\chi_{ZrH_x} = {} & 25.02 + 4.746\,x + (3.103\,10^{-3} + 2.008\,10^{-2}\,x)\;T[K] + \\ & - (1.943\,10^{5} + 6.35\,10^{5}\,x)\;T[K]^{-2} \quad \mathrm{W/(molK)}\end{aligned} \tag{2.45}$$

and

$$d_{ZrH_x} = \frac{67.9}{T[K] + 1.62\,103\,(2-x) - 1.18\,10^{-2}} - 1.16\,10{-}2 \quad \mathrm{cm^{-2}/s} \tag{2.46}$$

Tables 3.2 and 2.3 report respectively the values of the mass and volumetric fractions of uranium and zyrconium hydride in the fuel and the values of the uranium physical properties; moreover, on Figure 2.3 the trend with the fuel temperature of the zirconium hydride properties are illustrated. The fuel density and the fuel specific heat so obtained are the ones of Figure 2.7.

Obviously, both the ordinary differential equations for the coolant in the subcooled region, that is equations from (1.56) to (1.58), and in the saturated region, that is equations from (2.12) to (2.14), and the one for the fuel, that is equation (2.38), have to be associated to appropriate initial values.

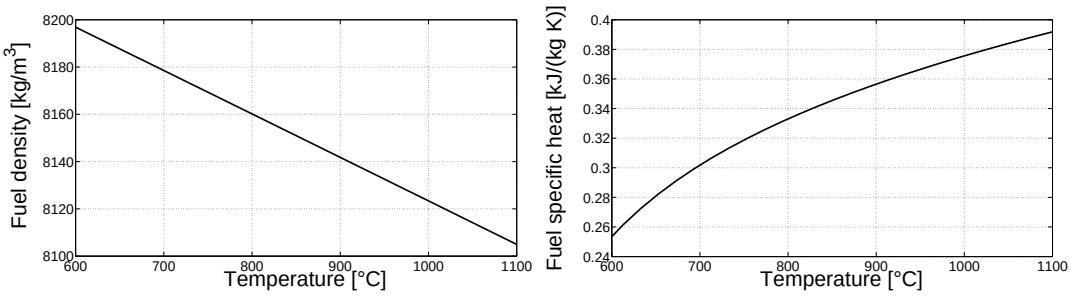

(a) Density **(b)** Specific heat

Figure 2.7: SURE fuel properties versus temperature

Parameter	Value	Measure unit
Hydraulic perimeter	1.085×10^{1}	m
Hydraulic area	1.450×10^{-2}	mm^2
Hydraulic diameter	5.3×10^{-3}	m
Thermal perimeter	7.446	m
Thermal area	1.794	m^2

Table 2.5: SURE geometrical features

Let us finally considerer the third one.

As mentioned previously, it is not an out and out change but rather an adaptation by means of the introduction of the correct geometrical features of SURE. The value referred above have been determined by those ones numerated on the previous paragraph and are reported in Table 2.5.

Finally, also the gravity acceleration has to be correctly chosen: in the present work the value of Mars has been fixed in virtue of the application field of SURE.

2.4.2 The deduction of coupling equations between the neutronics model and the thermo-hydraulics one

Two equations are necessary to couple the neutronics model just described and the thermo-hydraulics one deduced on the previous chapter and here corrected: the one expressing the effects of the fuel temperature variations and the coolant

density ones on the neutronics and the one expressing vice versa the effects of the core neutron density variations on the thermo-hydraulics.

The first one is an equation in which the trend of the reactivity with the fuel temperature and the coolant density is expressed and takes the following form:

$$\varrho = \alpha_{\varrho_{T_{fuel}}} \left(T_{fuel} - T_{fuel_{nom}}\right) - \alpha_{\varrho_{\rho_{cool}}} \left(\rho_{cool} - \rho_{cool_{nom}}\right) \tag{2.47}$$

where:

- the coefficient $\alpha_{\varrho_{T_{fuel}}}$ represents the feedback effects due to the fuel temperature changes which, as mentioned, are attributable both to the variation of the width of the uranium 238 absorption cross section resonances and to the variations of the distance between the hydrogen energy levels;

- the coefficient $\alpha_{\varrho_{\rho_c}}$ represents the feedback effects due to the coolant density changes which are attributable to the water nucleus density variations.

For both these coefficients the values reported on Table 2.3 have been fixed.

Instead, the second one is an equation by means of which the thermal power production due to the nuclear fission reactions can be inserted in the fuel energy balance and takes the following form:

$$q''' = n_C \, v_n \, \sigma_{U_{235}} \, N_{U_{235}} \, E_{U_{235}} \tag{2.48}$$

Indeed, as mentioned about the choice of an initial value for the neutron density in the core, the neutrons are all thermal and the SURE fuel is a mixture of high enriched uranium and hydride zirconium.

Really, another equation is necessary to couple the fuel dynamics and the coolant one. It is simply an equation in which the thermal flux term appearing both in the energy balance equations for the coolant in the subcooled region and in the satureted one and in the energy balance equation for the fuel is specify, that is:

$$q'' = U \left(T_{fuel} - T_{cool}\right) \tag{2.49}$$

where for the total heat transfer coefficient the value reported on Table 2.3 can be used.

At this point, a notation to explain how the nominal values of the coolant density appearing in equation (2.47) and the value of the coolant temperature appearing in equation (2.49) have been fixed has to be done: indeed, adopting a two point regions formulation for the thermo-hydraulics, it become necessary to establish a criteria on the base of which the mean value of a certain thermo-hydraulics property along the whole channel can be determined. The best idea appeared a weighted average in which the weights are represented by the region length, that is:

$$\langle x \rangle_{channel} = \frac{\langle x \rangle_1 \; L_1 + \langle x \rangle_2 \; L_2}{L_1 + L_2} \tag{2.50}$$

So, using this relation, the properties referred above takes the following form:

$$\rho_{cool_{nom}} = \frac{\langle \rho \rangle_1 \; L_1 + \langle \rho \rangle_2 \; L_2}{L_1 + L_2} \tag{2.51}$$

$$T_{cool} = \frac{\langle T \rangle_1 \; L_1 + \langle T \rangle_2 \; L_2}{L_1 + L_2} \tag{2.52}$$

being $\langle \rho \rangle_1$ and $\langle \rho \rangle_2$ expressing by equations (1.67) and (2.23) and $\langle T \rangle_1$ and $\langle T \rangle_2$ expressing by the following ones:

$$\langle T \rangle_1 = \frac{T_{in} + T_{sat}(p_{12})}{2} \tag{2.53}$$

$$\langle T \rangle_2 = \frac{T_{sat}(p_{12}) + T_{sat}(p_{out})}{2} \tag{2.54}$$

2.4.3 The simulation results

As for the neutronics one, some simulations have been performed so as to verify the validity of the neutronics and thermo-hydraulics model devoloped: more precisely, the SURE response in a normal operating condition since its nominal state to perturbations of different kinds and entities has been determined.

To do that, two steps have been accomplishes with the help of *COMSOL Multiphysics*. At first, the nominal state of its thermo-hydraulics has been calculated running a stationary simulation for the thermo-hydraulics model since arbitrary initial values; at second, its response in a normal operating condition since its nominal state to different inlet mass flow rate steps and inlet temperature ones

has been calculated running transient simulations for the neutronics and thermo-hydraulics model since the thermo-hydraulics nominal state determined and the neutronics one represented by equations (2.11), (2.9) and (2.10). In particular, for the first one a script has been implemented following these steps:

- the unknown quantities have been chosen: the mass flow rates G_{12} and G_{out}, the pressures p_{12} and p_{out}, the boiling level L_1 and the exit vapor quality x_{out};
- equations for the mass, the momentum and the energy balance in both the subcooled region and in the saturated one, that is equations (1.56), (1.57) and (1.58) and (2.12), (2.13) and (2.14), and those ones for their initial values have been implemented using the *COMSOL Multiphysics* module *Global Equations* described on the previous chapter;
- the water properties, in particular those ones expressed by equations (1.62), (1.63), (1.64) and (1.65) and (2.18), (2.19), (2.20), (2.21) and (2.22), and the fuel properties, in particular those ones expressed by equations (2.39) and (2.41), have been implemented by means of *COMSOL Multiphysics* and *MATLAB* using the same procedure described on the previous chapter;
- closure equations of both the subcooled region and the saturated one, that is equations from (1.66) to (1.72), equations from (2.23) to (2.36) and equation (2.37), and coupling ones between the fuel dynamics and the coolant one, that is equation (2.49), have been introduced;
- finally, the values fixed for the geometric features and for the total heat transfer coefficient between coolant and fuel have been loaded.

Instead, for the second one another script has been implemented following, besides these ones just mentioned, these steps:

- the unknown quantities have been chosen: the neutron density in the core n_C, the neutron density in the reflector n_R, the precursor in the core of each group c_i, the mass flow rates G_{12} and G_{out}, the pressures p_{12} and p_{out}, the boiling level L_1 and the exit vapor quality x_{out};

- equations for the neutrons balance in the core and in the reflector and for the precursors balance in the core, that is equations (2.2), (2.6) and (2.8), and those ones for their initial values, that is equations (2.9) and (2.10), have been implemented using the *COMSOL Multiphysics* module *Global Equations*;

- coupling equations between the neutronics and thermo-hydraulics, that is equations (2.47) and (2.48), have been introduced;

- finally, the values choice for the delayed neutron fractions and the decay constants of each precursor group, for the neutron transfer probabilities from the core to the reflector and vice versa, for the neutron generation times in the core and in the reflector and for the fuel temperature and the coolant density feedback coefficients have been loaded.

Obviously, no particular geometry had to be created and no particular module had to be chosen in a zero-dimensional formulation.

Table 2.6 shows the result of the stationary simulation mentioned, whereas on Figures 2.8 and 2.9 those ones of the transient simulations are illustrated.

The relative thermal power trends shown on 2.8 and 2.9 are physically consistent. Indeed, an increase of the inlet coolant mass flow rate or a decrease of the inlet temperature induces the boiling boundary advancing and, consequently, the coolant density rise with the result of a positive reactivity insertion the timetable and the entities of which depend on the coolant density feedback coefficient; the increase of the neutron flux and, consequently, of thermal power production induces in turn the fuel temperature growth with the result of a negative reactivity insertion the timetable and the entity of which depend on the fuel temperature feedback coefficient; this succession of events allows the reaching of a new stationary state the thermal power level of which depends on the feedback coefficients referred above. Vice versa obviously for a decrease of the inlet coolant mass flow rate and for an increase of the inlet coolant temperature.

Figure 2.10 shows just such a sequence for a positive inlet mass flow rate of 1% given 10 s after the beginning of the simulation and allows to trace what happens in SURE after such a perturbation:

Parameter	Value	Measure unit
Thermal power	800	kW
Coolant mass flow rate G_{in}	0.97	kg/s
Coolant mass flow rate G_{12}	0.97	kg/s
Coolant mass flow rate G_{out}	0.97	kg/s
Coolant mass flow rate $\langle G \rangle_1$	0.97	kg/s
Coolant mass flow rate $\langle G \rangle_2$	0.97	kg/s
Coolant mass flow rate $\langle G \rangle_{core}$	0.97	kg/s
Coolant density ρ_{in}	634.90	kg/m^3
Coolant density ρ_{12}	594.36	kg/m^3
Coolant density ρ_{out}	139.10	kg/m^3
Coolant density $\langle \rho \rangle_1$	614.63	kg/m^3
Coolant density $\langle \rho \rangle_2$	633.73	kg/m^3
Coolant density $\langle \rho \rangle_{core}$	390.13	kg/m^3
Coolant pressure p_{in}	155.0000	bar
Coolant pressure p_{12}	154.9986	bar
Coolant pressure p_{out}	154.9899	bar
Coolant pressure $\langle p \rangle_1$	154.9993	bar
Coolant pressure $\langle p \rangle_2$	154.9943	bar
Coolant pressure $\langle p \rangle_{core}$	154.9947	bar
Coolant temperature T_{in}	335.00	℃
Coolant temperature T_{12}	344.79	℃
Coolant temperature T_{out}	344.78	℃
Coolant temperature $\langle T \rangle_1$	339.89	℃
Coolant temperature $\langle T \rangle_2$	344.79	℃
Coolant temperature $\langle T \rangle_{core}$	344.32	℃
Fuel temperature	643.91	℃
Fuel specific heat	404.65	kJ/(kg℃)
Fuel density	8088.32	kg/m^3
Outlet void fraction	0.9245	-
Outlet vapor quality	0.7728	-
Outlet slip ratio	1.6209	-

Table 2.6: SURE thermohydraulics nominal state

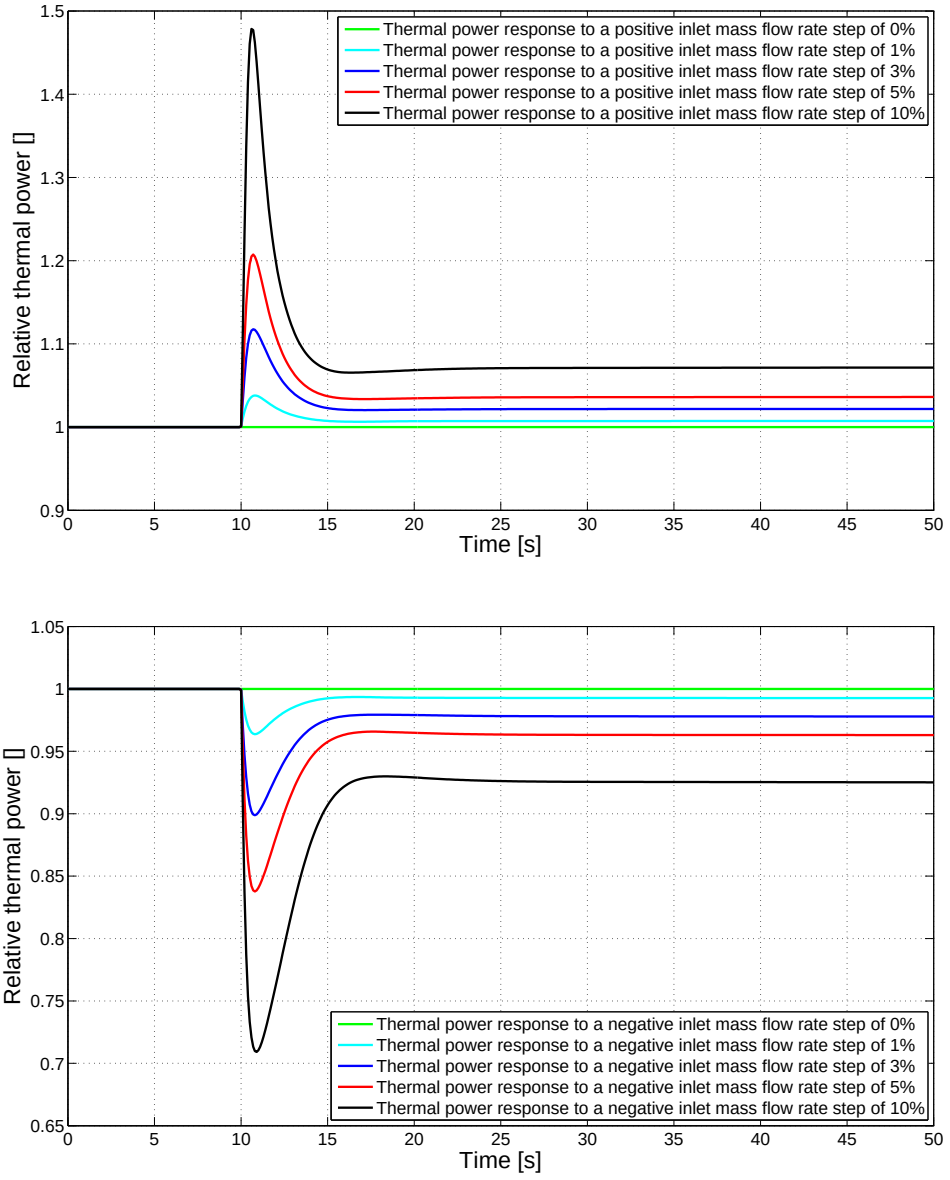

Figure 2.8: SURE response in a normal operating condition to positive and negative inlet coolant mass flow rate steps of different entities

- the inlet mass flow rate undergoes 10 s after the beginning of the simulation a sudden increase from its nominal power of about 0.97 kg/s to 0.9797 kg/s, as Figure 2.10a shows;
- the effect of this increase is an advancing of the boiling boundary of almost 1% and consequently, because of the reduction of the vapor phase, the growth of the coolant density of 0.2% as Figures 2.10c and 2.10d show: the result

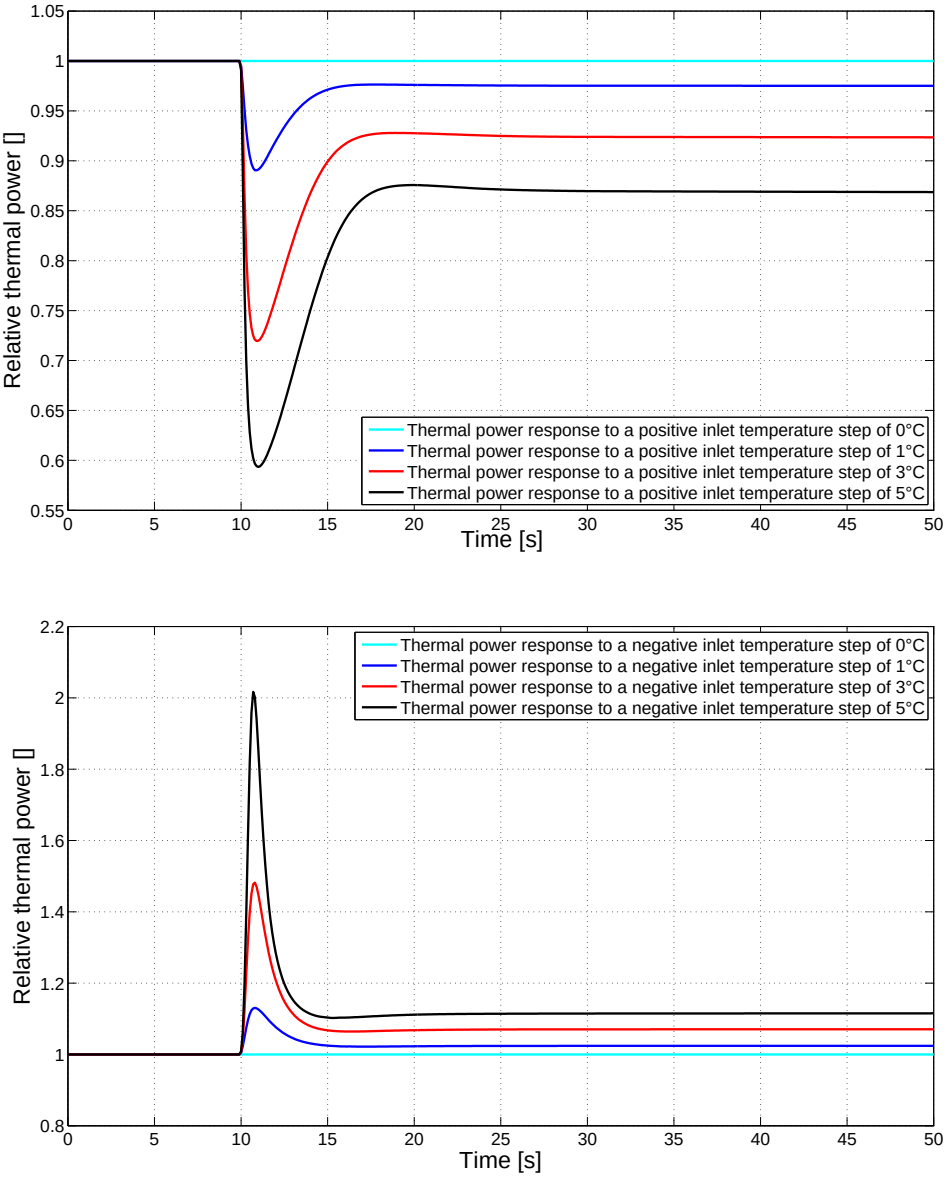

Figure 2.9: SURE response in a normal operating condition to positive and negative inlet coolant temperature steps of different entities

is a positive reactivity insertion because of the sign of the coolant density feedback coefficient;

- the effect of this insertion is the rise of the volumetric thermal power density of 4% and consequently the growth of the fuel temperature of 0.25% as as Figures 2.10e and 2.10f show: the result is vice versa a negative reactivity insertion because of the sign of the fuel temperature feedback coefficient;

- finally, the sequence of these positive and negative reactivity insertions allow to reach a new stationary state corresponding to a higher thermal power level: indeed, as Figure2.10b shows, the reactivity increase and decrease until to reach again a null value.

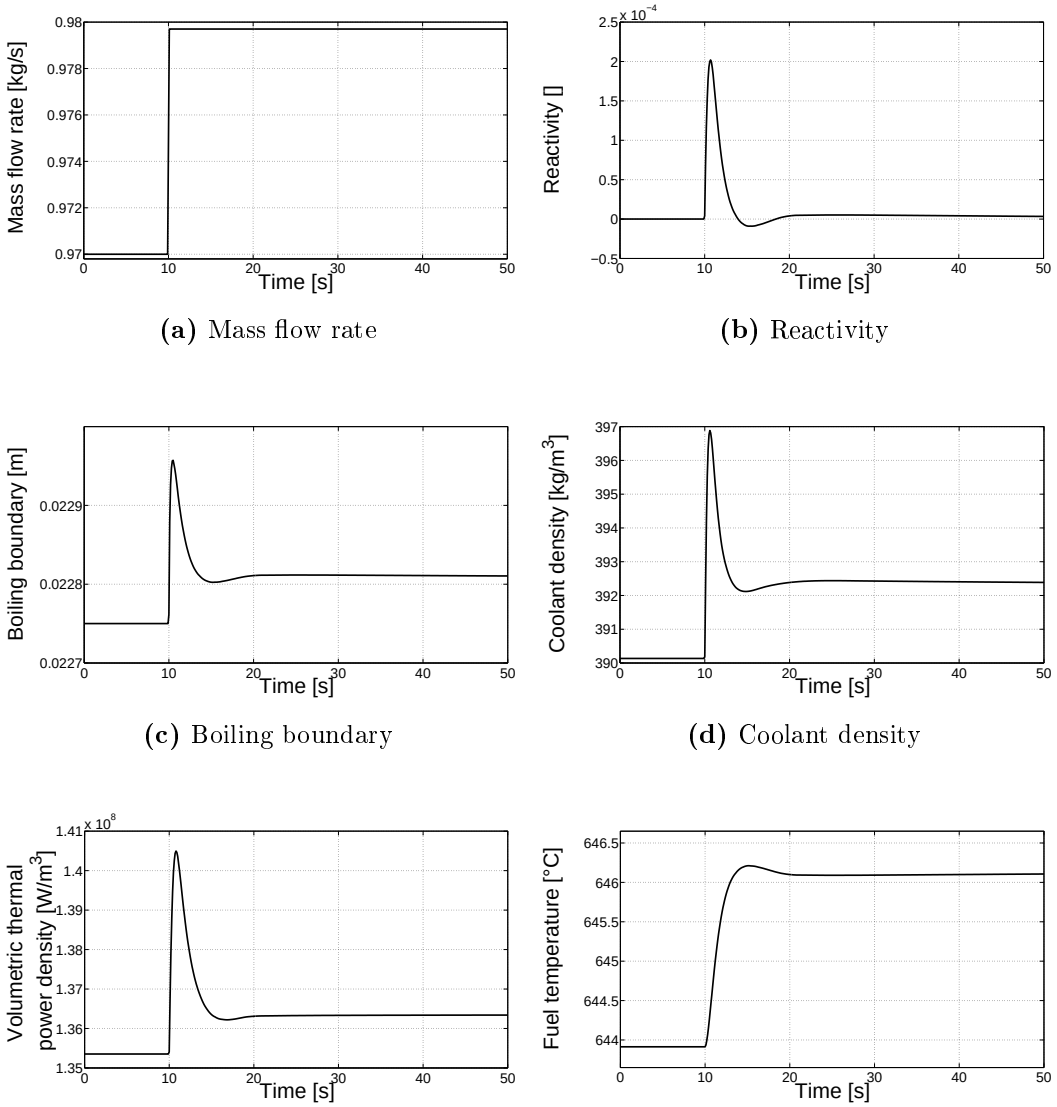

(a) Mass flow rate **(b)** Reactivity

(c) Boiling boundary **(d)** Coolant density

(e) Volumetric thermal power density **(f)** Fuel temperature

Figure 2.10: SURE properties variations in a normal operating conditions after a inlet coolant mass flow rate step of 1 % given 10 s after the beginning of the simulation

Although the simulations performed show the reliability of the neutronics and thermohydraulics model created, some inaccuracies typical of a zero-dimensional

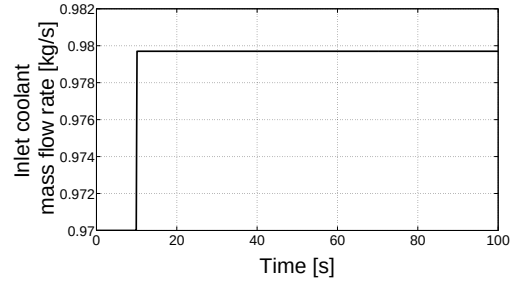

(a) Inlet coolant mass flow rate

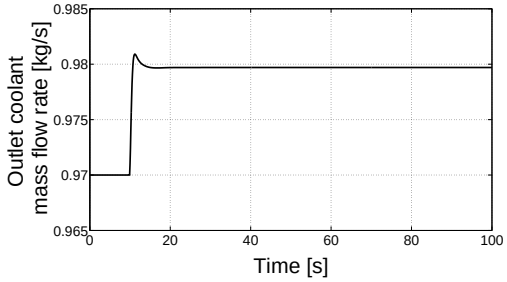

(b) Outet coolant mass flow rate

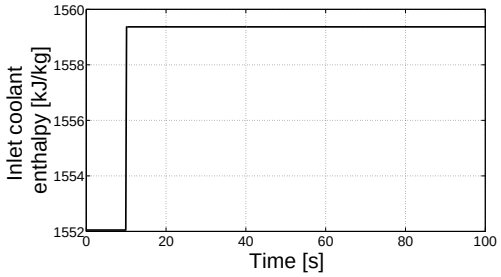

(c) Inlet coolant enthalpy

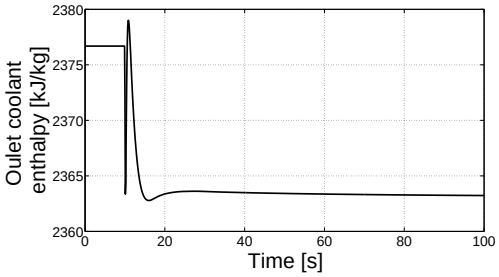

(d) Outlet coolant enthalpy

Figure 2.11: Coolant mass flow rate after a inlet perturbation of 1 % and coolant enthalpy after a inlet perturbation of 1 °C

approach appear when the outlet property trends after a inlet perturbation are investigated. About it, on Figure 2.11 the outlet mass flow rate after a inlet mass flow rate step of 1 % and the outlet enthalpy after a inlet temperature step of 1 °C are illustrated: as can be seen, the inlet perturbation of these variable reproduces oneself instantanely at the outlet of the core. Obviously, this results are not physically coherent: indeed, such a pertubation should employ a certain time, depending both on the channel lenght and on the conditions in force in it, to reach its outlet; rather it is due to all the hypothesis assumed so as to model the physical system considered as shown on Figure 1.3, that is so as to reduce it to three point regions or two ones.

2.5 Conclusion

The development of a neutronics and thermo-hydraulics model for SURE underlined some important aspect of the multi-physics modeling and not only.

Employing code based, as *COMSOL Multiphysics*, on a multi-physics approach turns out to be somewhat very efficient. To note however that such an efficiency becomes particularly important for a multi-dimensional formulation: indeed, being all the models here realize for SURE zero-dimensional, other codes like for example *Simulink* could be used.

Besides this one, some considerations on the reliability of all the models created, also the single-physics one, have to be done.

Both the neutronics one and the neutronics and thermo-hydraulics one showed a certain consistency: indeed, although no experimental data on SURE were available, its simulated responses to reactivity steps in a zero power condition, determined with the first one, and to inlet coolant mass flow rate and temperature steps in a normal operating conditions, determined with the second one, reflected the theoretical nuclear fission reactor dynamics. More precisely, by the first simulations the difference between such a dynamic with or without precursors and the typical trend of a zero power reactor thermal power after a reactivity insertion, given by the prompt jump and the exponential growth, can be noticed; instead, the second ones illustrates the role played by the feedback effects due to the fuel temperature and the coolant density variations.

Nevertheless, all the limitations characteristics of a zero-dimensional approach remain: an example is represented by the instant variation of the outlet mass flow rate after a inlet mass flow rate step and of the outlet enthalpy after a inlet temperature step discussed. It means that the adoption of such an approach is recommended only or in those problems in which the reactor dimensions are as much small that the spatial distribution of its properties can be neglected or in those ones in which their dynamics instead of their spatial distribution is of interest.

Instead, no particular attention is required by the procedure used to couple the neutronics model and the thermo-hydraulics one, absolutely traditional.

Nomenclature

- A area
- a_g gravitational acceleration

b precursor delayed neutron fraction

c precursor density

d thermal diffusion coefficient

D diameter

E energy

f neutron transfer probability

f_m mass fraction

f_M Moody's factor

f_v volume fraction

g mass flux

G integrated mass flow rate

h enthalpy

L channel length

k multiplicative factor

m mass

M integrated mass

n neutron density

N nucleus density

p pressure

P perimeter

q'' thermal flux

q''' thermal power volumetric density

Re Reynolds number

S slip ratio

t temporal coordinate

T temperature

u internal energy

U total heat transfer coefficient between the fuel and the coolant

v neutron velocity

x dynamic quality

Greek symbols

α void fraction

α_ϱ	reactivity feedback coefficient
β	volumetric ratio
θ	channel slope angle
κ	thermal conductivity coefficient
λ	precursor decay constant
Λ	neutron generation time
μ	viscosity
ξ	volumetric expansion coefficient
ρ	density
ϱ	reactivity
σ	microscopic cross section
τ	neutron life time
$\phi_{LO,L}$	two phase multiplier
χ	specific heat

Subscripts

C	core region
$cool$	coolant
eff	effective
$fuel$	fuel
h	hydraulic
i	precursor group
in	channel inlet
L	liquid phase
nom	nominal
out	channel outlet
R	reflector region
sat	saturation
t	thermal
U	uranium
U_{235}	uranium 235
U_{238}	uranium 238
V	vapor phase

ZrH_x	zyrconium hydride
0	initial
1	subcooled region
2	saturated region
12	moving boundary between the subcooled region and the saturated one

Mathematical symbols

$\langle\rangle$	mean value on a certain length

Bibliography

[1] A. Cammi, F. Finzi, C. Lombardi, M. E. Ricotti, and L. Santini. A "generation iii+" nuclear reactor for space needs. *Progress in nuclear energy*, 2009.

[2] Vito Memoli, Andrea Bigoni, Antonio Cammi, Marco Colombo, Carlo Lombardi, Davide Papini, and Marco Enrico Ricotti. Preliminar feasibility study of a water space reactor with an innovative reactivity control system. In *PHYSOR 2010 - Advances in Reactor Physics to Power the Nuclear Renaissance*, 2010.

[3] M. T. Simnad. The u-zrh$_x$ alloy: its properties and use in triga fuel. *Nuclear Engineering and design*, 1981.

[4] Vito Memoli. *Modeling approaches for analysis of innovative nuclear reactors.* PhD thesis, 2010.

[5] Gregory D. Spriggs, Robert D. Busch, and John G. William. Two-region kinetic model for reflected reactor. *Annals of nuclear energy*, 1997.

Chapter 3

A multi-physics one-dimensional model for LWRs

The subject of this third chapter is the last part of the work: the development of a multi-physics one-dimensional model for LWRs.

The same reasons that led in the previous part of the work to considerer SURE bring out the choice of MARS, a Generation III+ reactor conceived at *La SAPIENZA Università di Roma, Dipartimento di Ingegneria Nucleare e Conversioni dell'Energia*. It is a PWR characterized by innovative constructive solutions designed in order to increase as much as possible the safety minimizing at the same time the costs: indeed, its distinctive features are for example safety systems the functioning of which depends only on the unavoidability of the natural physical laws or structural components the disassembling and the substituting of which is simply feasible.

To do that, three steps analogous to the ones accomplished to develop the zero-dimensional model for SURE have been carried out. The first one has been the built up of a one-dimensional model for the MARS neutronics by means of a two regions two groups diffusion formulation, a theory able to describe the zero power reactor evolution in space and in time when two neutron energy groups are considered and a reflector is present. The second one has been the built up of a model for the MARS thermo-hydraulics by means of the one deduced on the first chapter opportunely corrected. Finally, the third one has been the coupling

of these models by means of apposite equations expressing both the effect of the thermo-hydraulics property variations on the neutronics and the effect, vice versa, of the neutronics property variations on the thermo-hydraulics; in particular, the equations in which the core macroscopic cross sections and the fuel temperature and the coolant one are related have been deduced using the procedure suggested by [1], a procedure based on the calculation of the effective multiplicative factor corresponding to different core compositions.

The use of *COMSOL Multiphysics* and *MATLAB* allows also this time to perform a lot of simulations, both in a zero power condition and in a normal operating one, since which verify the validity of all the models so developed.

3.1 Introduction

The object of the third part of the work has been the development of a one-dimensional model for light water reactor.

In particular the attention has been focused on MARS, a Generation III+ light water reactor conceived at *LA SAPIENZA Università di Roma, Dipartimento di Ingegneria Nucleare e Conversioni dell'Energia*. It is a PWR the peculiar characteristic of which is represented by the adoption of innovative safety systems based, rather on mechanisms the functioning of which requires both the availability of electric power and the presence of operators, on the unavoidability of the natural physical laws; moreover, planning solutions finalized to maximize the simplicity and the rapidity in construction and exercise and to minimize the production of radioactive wastes and the costs are its distinctive features. The reasons of such a choice are the same ones that led in the previous part of the work to considerer SURE: indeed, on one hand the only available macroscopic cross section data are those ones suggested by [2] for a generic PWR and on the other hand all the geometric and thermo-hydraulics features of MARS are widely illustrated on [3].

As for the development of the zero-dimensional model of SURE, two phases have been tackled. At first, a one-dimensional model for the neutronics of MARS in a zero power condition has been built up using a two regions and two groups

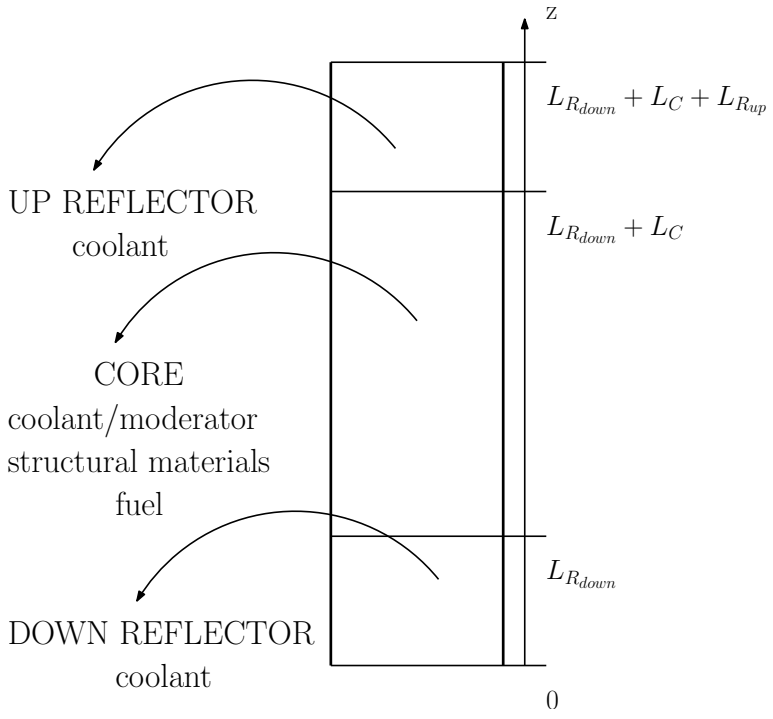

Figure 3.1: The one-dimensional scheme of LWR considered

diffusion formulation, a theory able to describe besides the reactor dynamics the space evolution of its properties when two neutron energy group are considered and a reflector is present. At second, a one-dimensional model for its neutronics and its thermo-hydraulics in a normal operating condition has been built up using the neutronics one just referred and the thermo-hydraulics one deduced on the first chapter and determining apposite coupling equations between them.

In each of these phases, the LWR illustrated on Figure 3.1 has been considered. It is an equivalent cylindrical channel constitute by three section:

- the first one is the down reflector and is representative of the coolant layer located at the inlet of the core; it is characterized by hydraulics equivalent area, perimeter and diameter A_h, P_h and D_h and by a length $L_{R_{down}}$;
- the second one is the core and is representative of the fuel, the coolant/moderator and the structural materials contained in it; it is characterized by hydraulics equivalent area, perimeter and diameter A_h, P_h and D_h, by thermal equivalent area and perimeter A_q and P_q and by a length L_C;
- the third one is the up reflector and is representative of the coolant layer

located at the outlet of the core; it is characterized by hydraulics equivalent area, perimeter and diameter A_h, P_h and D_h and by a length $L_{R_{up}}$.

Later on, a description of the built up and the validation of both the models referred above are reported. Before, a patch of the principal constructive and functional features of MARS is accounted.

3.2 A short description of MARS

MARS, acronym for *Multipourpose Advanced Reactor inherently-Safe*, is a Generation III+ LWR conceived since 1983 at *LA SAPIENZA Università di Roma, Dipartimento di Ingegneria Nucleare e Conversioni dell'Energia.*

It has been design in order to increase the safety reducing at the same time as much as possible the costs: indeed, in its planning aspects like the adoption of innovative safety techniques took place near aspects like the optimization of the pre-assemblage, the assemblage and the reparation of the components.

Figure 3.2 shows a pattern of the whole power plant in which MARS works.

It is an indirect cycle power plant formed by a primary system, constituted by a pump, the channel between the barrel and the vessel, the core and a steam generator working in natural circulation, and a secondary system, in which by means of a Rankine thermodynamical cycle electric power is produced. The reactor is a PWR; its core is composted by eighty-nine fuel elements each of which has a square shape and accommodates two hundred and eighty-nine positions and two hundred and sixty-four fuel rods. The coolant is represented by sub cooled water at a pressure of 75 bar, whereas the fuel is represented by uranium dioxide.

On Tables 3.1 and 3.2 the principal constructive and functional characteristics of MARS are reported.

Peculiar characteristic of MARS is an innovative way to think the safety: indeed, all the safety systems of which it is provided base their functioning on the inescapable manifestation of the natural physical laws.

These safety systems are three: SCCS, ATSS and CPP.

SCCS, acronym for *Safety Core Cooling System*, is a safety system conceived

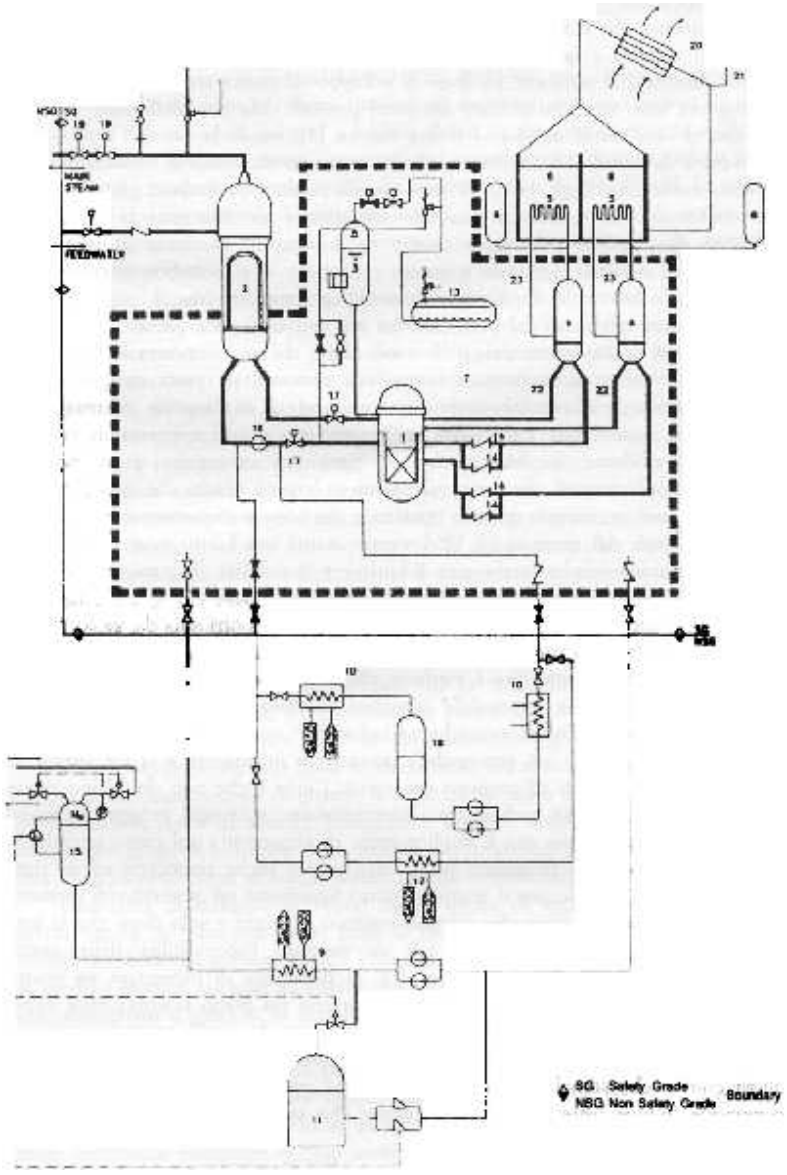

Figure 3.2: A pattern of the power plant in which MARS works

in order to remove the residual thermal power produced by the core even after its power off. It is articulated in three different circuits having the following characteristics:

- the first one is crossed by the primary coolant in a natural circulation condition, allowed in a first moment by the quota difference between its two legs and in a second moment by the temperature difference between them, and exchanges thermal power with the second one by means of a heat exchanger; a valve, the opening of which is regulated by the pressure difference between vessel internal and external, blocks its functioning during normal operating

Parameter	Value	Measure unit
Core height	2.600	m
Core radius	1.200	m
Number of fuel elements	289	-
Number of positions for fuel elements	289	-
Number of fuel rods for fuel elements	264	-
Number of fuel rods	23 496	-
Number of traditional control rods	36	-
Number of innovative control rods	9	-
Active fuel rod height	2.600	m
Pitch between adjacent fuel rods	1.197×10^{-2}	m
External clad radius	4.750×10^{-2}	m
Internal clad radius	4.120×10^{-2}	m
External fuel radius	4.020×10^{-2}	m

Table 3.1: Constructive features of MARS

conditions;

- the second one is crossed by another coolant, always represented by water, in a natural circulation condition, allowed also this one by a quota difference and a temperature one between its two legs, and exchanges thermal power with the first one by means of the heat exchanger referred above and with the third one by means of a second one;

- finally, the third one is a water pool in which the second heat exchanger is immersed and that exchanges thermal power with the atmosphere by means of a complex mechanism of evaporating and condensing allowed by the natural circulation.

Figure 3.3 shows a pattern of this safety system.

ATSS, acronym for *Additional Temperature-actuated Scram System*, is a safety system conceived, in addition to the traditional scram system, in order to power

Parameter	Value	Measure unit
Nominal thermal power	600	MW
Nominal electric power	170	MW
Fuel mass	32 121	kg
Fuel density	10 310	kg/m^3
Fuel enrichment	2.3	%
Nominal inlet coolant pressure	75	bar
Nominal inlet coolant temperature	214	℃
Nominal inlet coolant mass flow rate	3227	kg/s

Table 3.2: Functional features of MARS

off the reactor as soon as the operating conditions differs by a fixed threshold. It is constitute by nine control rods the insertion into the core of which is guarantee by a mechanism based on the thermal dilatation due to the primary coolant temperature variations. Figure 3.4 shows a pattern of this safety system.

Finally, CPP, acronym for *Containment for Primary system Protection*, is a safety system conceived in order at first to preserve a null pressure difference between internal and external of the primary system so as to reduce the arise of intense stresses and consequently of break and at second to face an eventually primary coolant loss. It is a container in which the pump, the vessel, the steam generator and a part of SCCS are located and that accommodates water at the same pressure of the primary coolant.

Other important characteristics distinguish MARS. For example, the modest electric power possible to install allows on one hand its adoption both by little electric societies and by bigger ones and on the other hand the realization of a whole power plant increasing gradually the potentiality. Moreover, the possibility to take to pieces and substitute all the components, even those ones like the vessel mainly subject to damage, allows to extend the reactor life and to simplify the decomissioning.

The result of all these features is a strong reduction of the costs.

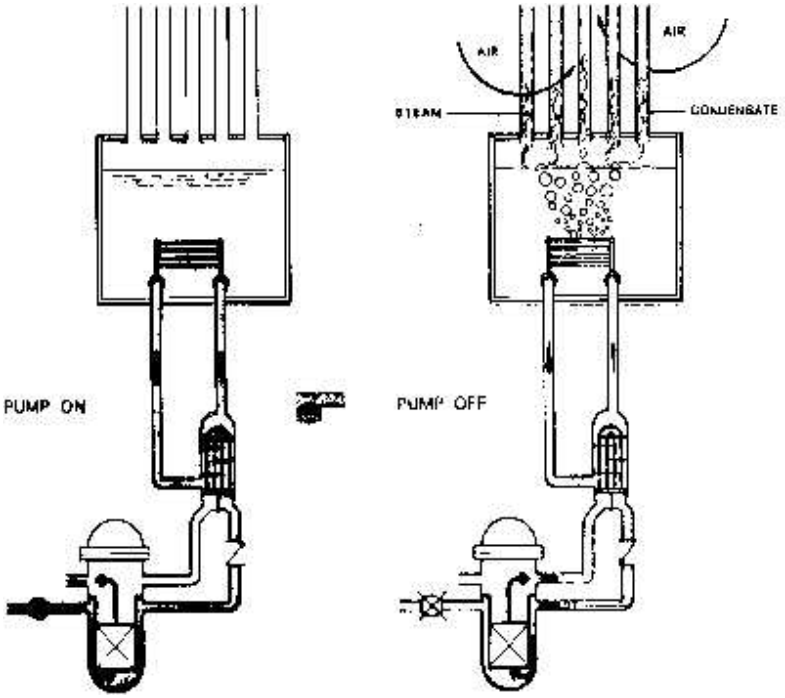

Figure 3.3: The MARS safety system SCCS

However, a more widened description of MARS can be found on [4].

3.3 The neutronics model

During this third part of the work, a first steps has been the development of a one-dimensional neutronics model for MARS in a zero power condition.

This step has been carried out adopting a two region and two group formulation of the diffusion theory according to which the reactor is formed by two different region, the core and the reflector, coupled between themselves by apposite boundary conditions and the neutrons in it contained belong to two different energetic group, the fast one and the thermal one, coupled between themselves by apposite transfer macroscopic cross sections. To note that this choice has been led on order to reach the best compromise between the fairness of the model and the availability of the data: indeed, [2] make available all the necessary neutronics properties, otherwise very difficult to calculate.

This theory is illustrated and explained on the next paragraph before the description of its application to MARS. Moreover, the verify of the validity of the

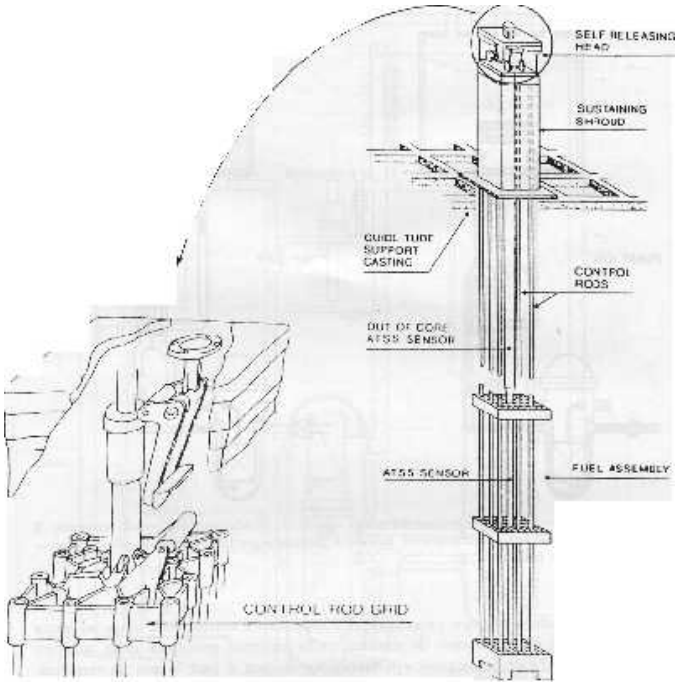

Figure 3.4: The MARS safety system ATTS

neutronics model so developed are reported.

3.3.1 The two region and two group formulation of the diffusion theory

The two region and two group formulation of the diffusion theory is a formulation able to reproduce the evolution in space and time of a zero power reactor when a reflector is present.

The hypothesis which define its application field are several. Some of them are the same ones just assumed for the zero-dimensional neutronics model described on the previous chapter: those ones concerning the presence of a multiplying region, the core, and a non multiplying region, the reflector, and their homogeneity. Moreover, there are the following ones:

- the neutrons, as suggested by [2], can belong to two different energetic groups: the fast group corresponding to a velocity of $1 \times 10^7\,\mathrm{m/s}$, the neutrons with energy comprised between the value E_1 =0 eV and the value E_2 =1 eV fall into which, and the thermal group corresponding to a ve-

locity of 2200 m/s, the neutrons with energy comprised between the value E_2 =1 eV and E_3 =10 MeV fall into which;

- the neutron flux relative to the fast group and those one relative to the thermal group can be expressed by the following relations:

$$\Phi_1 = \int_{E_2=1\,eV}^{E_3=10\,MeV} \Phi \, dE \tag{3.1}$$

$$\Phi_2 = \int_{E_1=0\,eV}^{E_2=1\,eV} \Phi \, dE \tag{3.2}$$

- the neutron properties relative to the fast group and those ones relative to the thermal group, that is the macroscopic cross sections and the diffusion coefficients, can be expressed by means of weighted average in which the weights are represented by the neutron flux:

$$x_1 = \frac{\int_{E_2=1\,eV}^{E_3=10\,MeV} \Phi \, x \, dE}{\int_{E_2=1\,eV}^{E_3=10\,MeV} \Phi \, dE} \tag{3.3}$$

$$x_2 = \frac{\int_{E_1=0\,eV}^{E_2=1\,eV} \Phi \, x \, dE}{\int_{E_1=0\,eV}^{E_2=1\,eV} \Phi \, dE} \tag{3.4}$$

- the neutrons can pass from the fast group to the thermal one but cannot do vice versa: indeed, the cut off energy for the second one has been chosen sufficiently high such that the upscattering out of it can be ignored; in particular, the passage from the fast group to the thermal one can be model using coupling macroscopic cross sections containing the scattering probability for a neutron from the first one to the second one.

Assuming these hypothesis and referring to the LWR scheme illustrated in Figure 3.1, two different sets of equations can be used to reproduce the zero power reactors behavior.

The first set of equations are formed by six partial differential equations and allows to determine the evolution in space and in time of the system referred above.

The first one is a balance equation for fast neutrons in the core and takes the following form:

$$\frac{1}{v_1}\frac{\partial \Phi_1}{\partial t} + \frac{\partial}{\partial z}\left(-\mathcal{D}_{C1}\frac{\partial \Phi_1}{\partial z}\right) = \left[-\mathcal{D}_{C1}\,B^2 - \Sigma_{C1a} - \Sigma_{Ct} + (\nu\,\Sigma_f)_{C1}\,(1-b_1)\right]\,\Phi_1 + \left[+\,(\nu\,\Sigma_f)_{C2}\,(1-b_2)\right]\,\Phi_2 + \sum_{i=1}^{N}\lambda_i\,c_i \tag{3.5}$$

The second one is a balance equation for thermal neutrons in the core and takes the following form:

$$\frac{1}{v_2}\frac{\partial \Phi_2}{\partial t} + \frac{\partial}{\partial z}\left(-\mathcal{D}_{C2}\frac{\partial \Phi_2}{\partial z}\right) = (+\Sigma_{Ct})\,\Phi_1 + \left(-\mathcal{D}_{C2}\,B^2 - \Sigma_{C2a}\right)\,\Phi_2 \tag{3.6}$$

The third one is a balance equation for precursors in the core and takes the following form:

$$\frac{\partial c_i}{\partial t} = (\nu\,\Sigma_f)_{C1}\,b_{1_i}\,\Phi_1 - \lambda_i\,c_i \tag{3.7}$$

for the precursors produced by the fast fission reactions, and:

$$\frac{\partial c_i}{\partial t} = (\nu\,\Sigma_f)_{C2}\,b_{2_i}\,\Phi_2 - \lambda_i\,c_i \tag{3.8}$$

for the precursors produced by the thermal fission ones. The fourth one is a balance equation for fast neutrons in the reflector and takes the following form:

$$\frac{1}{v_1}\frac{\partial \Phi_1}{\partial t} + \frac{\partial}{\partial z}\left(-\mathcal{D}_{R1}\frac{\partial \Phi_1}{\partial z}\right) = \left(-\mathcal{D}_{R1}\,B^2 - \Sigma_{R1a} - \Sigma_{Rt}\right)\,\Phi_1 \tag{3.9}$$

The fifth one is a balance equation for thermal neutrons in the reflector and takes the following form:

$$\frac{1}{v_2}\frac{\partial \Phi_2}{\partial t} + \frac{\partial}{\partial z}\left(-\mathcal{D}_{R2}\frac{\partial \Phi_2}{\partial z}\right) = (+\Sigma_{Rt})\,\Phi_1 + \left(-\mathcal{D}_{R2}\,B^2 - \Sigma_{R2a}\right)\,\Phi_2 \tag{3.10}$$

Finally, the sixth one is a balance equation for precursors in the reflector and takes the following form:

$$c_i = 0 \tag{3.11}$$

for the precursors produced by both the fast fissions reactions and the thermal ones.

To those equations, apposite boundary and initial conditions for the fast neutron flux, the thermal neutron flux and the precursor density have to be associated.

The boundary conditions can be fixed imposing the annulment of the fast neutron flux and the thermal one at the extremities of the reflector, that is referring to Figure 3.1:

$$\begin{aligned} \Phi_1(0,t) &= 0 \\ \Phi_1(L_{R_{down}} + L_C + L_{R_{up}}, t) &= 0 \\ \Phi_2(0,t) &= 0 \\ \Phi_2(L_{R_{down}} + L_C + L_{R_{up}}, t) &= 0 \end{aligned} \tag{3.12}$$

the continuity of the fast neutron current and the thermal one at the interface between core and the the reflector, that is referring to Figure 3.1:

$$\begin{aligned} -\mathcal{D}_{R1} \left.\frac{\partial \Phi_1(L_{R_{down}}, t)}{\partial z}\right|_R &= -\mathcal{D}_{C1} \left.\frac{\partial \Phi_1(L_{R_{down}}, t)}{\partial z}\right|_C \\ -\mathcal{D}_{C1} \left.\frac{\partial \Phi_1(L_{R_{down}} + L_C, t)}{\partial z}\right|_R &= -\mathcal{D}_{R1} \left.\frac{\partial \Phi_1(L_{R_{down}} + L_C, t)}{\partial z}\right|_C \\ -\mathcal{D}_{R2} \left.\frac{\partial \Phi_2(L_{R_{down}}, t)}{\partial z}\right|_R &= -\mathcal{D}_{C2} \left.\frac{\partial \Phi_2(L_{R_{down}}, t)}{\partial z}\right|_C \\ -\mathcal{D}_{C2} \left.\frac{\partial \Phi_2(L_{R_{down}} + L_C, t)}{\partial z}\right|_R &= -\mathcal{D}_{R2} \left.\frac{\partial \Phi_2(L_{R_{down}} + L_C, t)}{\partial z}\right|_C \end{aligned} \tag{3.13}$$

and the annulment of the precursor density both at the extremities of the reflector and at the interfaces between the core and the reflector, that is referring to Figure 3.1:

$$\begin{aligned} c_i(0,t) &= 0 \\ c_i(L_{R_{down}}, t) &= 0 \\ c_i(L_{R_{down}} + L_C, t) &= 0 \\ c_i(L_{R_{down}} + L_C + L_{R_{up}}, t) &= 0 \end{aligned} \tag{3.14}$$

Instead, the initial conditions of the fast neutron flux and the thermal one can be arbitrarily fixed being the solution of the equations (3.5), (3.6), (3.9) and (3.10) defined for less than a multiplicative constant: for example, as for the zero-dimensional neutronics model deduced on the previous chapter, the values in corresponding of which the thermal power production is nominal can be chosen; since these ones, the initial value of the precursor density can be fixed using equations (3.7) and (3.8) for the core, that is:

$$c_{i_0} = \frac{(\nu \Sigma_f)_{C1} \, (1 - b_i)}{\lambda_i} \, \Phi_{1_0} \tag{3.15}$$

$$c_{i_0} = \frac{(\nu \Sigma_f)_{C2} \, (1 - b_i)}{\lambda_i} \, \Phi_{2_0} \tag{3.16}$$

for the precursors produced respectively by the fast fission reactions and the thermal ones and equation (3.10) for the reflector, that is:

$$c_{i_0} = 0 \tag{3.17}$$

The second set of equations are formed by four eigenvalues and eigenfunctions equations and allows to determine the condition, sub-critical, critical or super-critical, of a reactor in corresponding of a certain composition.

The first one is a balance equation for fast neutrons in the core and takes the following form:

$$\begin{aligned} &-\frac{\partial}{\partial z}\left(-\mathcal{D}_{C1}\,\frac{\partial \Phi_1}{\partial z}\right) - \mathcal{D}_{C1}\,B^2\,\Phi_1 - \Sigma_{C1a}\,\Phi_1 - \Sigma_{Ct}\,\Phi_1 \\ &+\frac{1}{k_{\text{eff}}}\left[(\nu\,\Sigma_f)_{C1}\;(1-b_1)\;\Phi_1 + (\nu\,\Sigma_f)_{C2}\;(1-b_2)\;\Phi_2\right] = 0 \end{aligned} \tag{3.18}$$

The second one is a balance equation for thermal neutrons in the core and takes the following form:

$$-\frac{\partial}{\partial z}\left(-\mathcal{D}_{C2}\,\frac{\partial \Phi_2}{\partial z}\right) - \mathcal{D}_{C2}\,B^2\,\Phi_2 - \Sigma_{C2a}\,\Phi_2 + \Sigma_{Ct}\,\Phi_1 = 0 \tag{3.19}$$

The third one is a balance equation for fast neutrons in the reflector and takes the following form:

$$-\frac{\partial}{\partial z}\left(-\mathcal{D}_{R1}\,\frac{\partial \Phi_1}{\partial z}\right) - \mathcal{D}_{R1}\,B^2\,\Phi_1 - \Sigma_{R1a}\,\Phi_1 - \Sigma_{Rt}\,\Phi_1 = 0 \tag{3.20}$$

The fourth one is a balance equation for thermal neutrons in the reflector and takes the following form:

$$-\frac{\partial}{\partial z}\left(-\mathcal{D}_{R2}\,\frac{\partial \Phi_2}{\partial z}\right) - \mathcal{D}_{R2}\,B^2\,\Phi_2 - \Sigma_{R2a}\,\Phi_2 + \Sigma_{Rt}\,\Phi_1 = 0 \tag{3.21}$$

Also to these equations apposite boundary condition have to associated. To this end, the same fixed for the first set of equations, that is equations (3.11), (3.12) and (3.13) can be used.

3.3.2 The application of the two region and two group formulation of the diffusion theory to MARS

The application of the two region and two group formulation of the diffusion theory to MARS has been carried out fixing at first opportune values of the geo-

metric features, that is the ones illustrated on Table 3.1, and choosing at second appropriate values for the neutronics ones.

In particular, for the neutronic features the values of the delayed neutron fractions and the precursor decay constants reported on table 2.4[1] and those ones of the macroscopic cross sections and diffusion coefficients suggested for a generic PWR by [2] and reported on Table 3.3 have been choice.

The one choice for the thermal absorption macroscopic cross section in the core deserves a deepening.

The values illustrated on Table 3.4 have been calculated referring to dimensions and compositions typical of a PWR and using an iterative procedure during which the neutron fluxes corresponding to certain values of the macroscopic cross sections are determined by means of equations (3.1) and (3.2) and vice versa the macroscopic cross sections corresponding to certain values of the neutron fluxes are determined by means of equations (3.3) and (3.4). Therefore, it is evident that the application of such values to a PWR characterized by own dimensions and own compositions is not really correct and the result is a condition or highly sub-critical or highly super-critical: indeed, it is known [5] that in a diffusion-reaction problem as this one there is a unique value of the system dimensions able to guarantee, in correspondence to certain diffusion and reaction coefficients, the reaching of a stationary regime and vice versa there is a unique value of both the diffusion coefficient and the reaction coefficient able to guarantee, in correspondence to certain system dimensions, the same aim.

To counter this problem, a fictitious thermal absorption macroscopic cross section, representative for example of a control rod group, has been added to the one suggested by [2] for the core so as to guarantee in correspondence of the MARS dimensions the reaching of a critical condition since which verify its response to eventually perturbations.

To do that equations (3.18), (3.19), (3.20) and (3.21), conveniently implemented by means of *COMSOL Multiphysics*, have been used. More precisely, *COMSOL*

[1] Only the precursor of the uranium 235 has been considered in this analysis being MARS a thermal reactor.

Parameter	Value	Measure unit
Fast diffusion coefficient in the core	1.263×10^{-2}	m
Thermal diffusion coefficient in the core	3.543×10^{-3}	m
Fast diffusion coefficient in the reflector	1.300×10^{-2}	m
Thermal diffusion coefficient in the reflector	1.600×10^{-2}	m
Fast absorption macroscopic cross section in the core	1.207	m^-1
Thermal absorption macroscopic cross section in the core	2.410×10^{1}	m^-1
Fast absorption macroscopic cross section in the reflector	4.000×10^{-2}	m^-1
Thermal absorption macroscopic cross section in the reflector	1.970	m^-1
Fast fission macroscopic cross section in the core	8.476×10^{-2}	m^-1
Thermal fission macroscopic cross section in the core	1.851	m^-1
Transfer macroscopic cross section from the fast group to the thermal one in the core	1.412×10^{1}	m^-1
Transfer macroscopic cross section from the fast group to the thermal one in the core	4.940	m^-1

Table 3.3: Neutronic features of MARS

Multiphysics arranges a module, the *PDE Coefficient Form*, able to solve if set on the *Stationary Solver* or the *Transient Solver* both single equations taking the following form:

$$e_a \frac{\partial u^2}{\partial t^2} + d_a \frac{\partial u}{\partial t} + \nabla \cdot \left(-c\nabla u - \underline{\alpha} u + \underline{\gamma}\right) + a\, u + \underline{\beta} \cdot \nabla u = f \tag{3.22}$$

if the scalar e_a, d_a, c, a and f, the vectors α, γ and β and appropriate initial and boundary conditions are provided it, and set of equations taking the following

form:

$$\underline{\underline{e_a}}\,\frac{\partial \underline{u}^2}{\partial t^2} + \underline{\underline{d_a}}\,\frac{\partial \underline{u}}{\partial t} + \nabla\cdot\left(-\underline{\underline{c}}\nabla\underline{u} - \underline{\underline{\alpha}}\underline{u} + \underline{\gamma}\right) + \underline{\underline{a}}\,\underline{u} + \underline{\underline{\beta}}\cdot\nabla\underline{u} = \underline{f} \tag{3.23}$$

if the vectors γ and f, the matrix e_a, d_a, c, a and β and appropriate initial and boundary condition are provided it [6]; moreover this module, if set of the *Eigenvalue Solver*, is able to determinate the eigenvalues λ and the relative eigenfunctions associated to both single equations taking the following form:

$$\nabla\cdot\left(-c\nabla u - \underline{\alpha}u + \underline{\gamma}\right) + a\,u + \underline{\beta}\cdot\nabla u = d_a\,\lambda\,u - e_a\,\lambda^2\,u \tag{3.24}$$

and set of equations taking the following form:

$$\nabla\cdot\left(-\underline{\underline{c}}\nabla\underline{u} - \underline{\underline{\alpha}}\underline{u} + \underline{\gamma}\right) + \underline{\underline{a}}\,\underline{u} + \underline{\underline{\beta}}\cdot\nabla\underline{u} = \underline{\underline{d_a}}\,\lambda\,\underline{u} - \underline{\underline{e_a}}\,\lambda^2\,\underline{u} \tag{3.25}$$

if the same parameters are provided it [6]. So, creating a geometry as the one illustrated on Figure 3.1 and reformulating equations (3.18), (3.19), (3.20) and (3.21) in the following way:

$$\underline{\underline{e_a}} = \left\{\begin{array}{cc} 0 & 0 \\ 0 & 0 \end{array}\right\} \tag{3.26}$$

$$\underline{\underline{d_a}} = \left\{\begin{array}{cc} (\nu\Sigma_f)_{C1} & (\nu\Sigma_f)_{C2} \\ 0 & 0 \end{array}\right\} \tag{3.27}$$

$$\underline{\underline{c}} = \left\{\begin{array}{cc} \mathcal{D}_{C1} & 0 \\ 0 & \mathcal{D}_{C2} \end{array}\right\} \tag{3.28}$$

$$\underline{\underline{\alpha}} = \left\{\begin{array}{cc} 0 & 0 \\ 0 & 0 \end{array}\right\} \tag{3.29}$$

$$\underline{\gamma} = \left\{\begin{array}{c} 0 \\ 0 \end{array}\right\} \tag{3.30}$$

$$\underline{\underline{a}} = \left\{\begin{array}{cc} (+\mathcal{D}_{C1}\,B^2 + \Sigma_{C1a} + \Sigma_{Ct}) & 0 \\ (-\Sigma_{Ct}) & (+\mathcal{D}_{C2}\,B^2 + \Sigma_{C2a}) \end{array}\right\} \tag{3.31}$$

$$\underline{\underline{\beta}} = \left\{\begin{array}{cc} 0 & 0 \\ 0 & 0 \end{array}\right\} \tag{3.32}$$

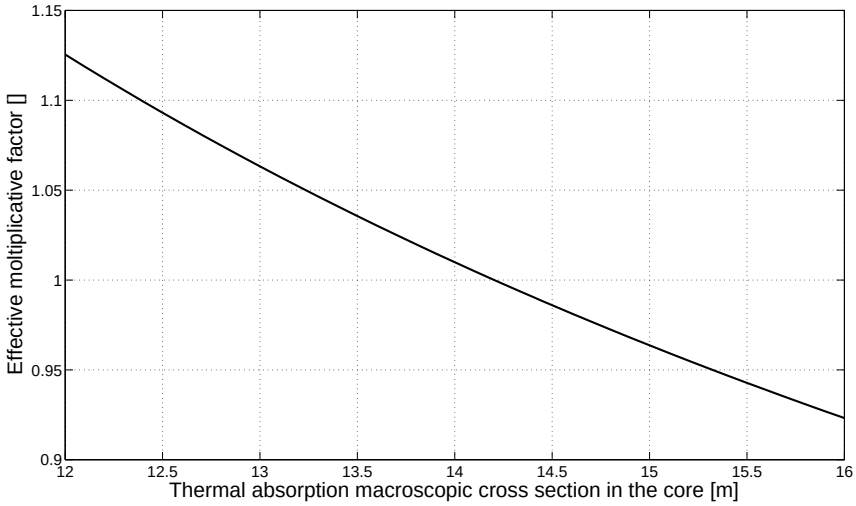

Figure 3.5: Effective multiplicative factor versus core macroscopic absorption cross section

$$\underline{f} = \left\{ \begin{array}{c} 0 \\ 0 \end{array} \right\} \tag{3.33}$$

for the core and:

$$\underline{\underline{e_a}} = \left\{ \begin{array}{cc} 0 & 0 \\ 0 & 0 \end{array} \right\} \tag{3.34}$$

$$\underline{\underline{d_a}} = \left\{ \begin{array}{cc} (\nu\Sigma_f)_{R1} & (\nu\Sigma_f)_{R2} \\ 0 & 0 \end{array} \right\} \tag{3.35}$$

$$\underline{\underline{c}} = \left\{ \begin{array}{cc} \mathcal{D}_{R1} & 0 \\ 0 & \mathcal{D}_{R2} \end{array} \right\} \tag{3.36}$$

$$\underline{\underline{\alpha}} = \left\{ \begin{array}{cc} 0 & 0 \\ 0 & 0 \end{array} \right\} \tag{3.37}$$

$$\underline{\gamma} = \left\{ \begin{array}{c} 0 \\ 0 \end{array} \right\} \tag{3.38}$$

$$\underline{\underline{a}} = \left\{ \begin{array}{cc} (+\mathcal{D}_{R1}\, B^2 + \Sigma_{R1a} + \Sigma_{Rt}) & 0 \\ (-\Sigma_{Rt}) & (+\mathcal{D}_{R2}\, B^2 + \Sigma_{R2a}) \end{array} \right\} \tag{3.39}$$

$$\underline{\underline{\beta}} = \left\{ \begin{array}{cc} 0 & 0 \\ 0 & 0 \end{array} \right\} \tag{3.40}$$

$$\underline{f} = \left\{ \begin{array}{c} 0 \\ 0 \end{array} \right\} \tag{3.41}$$

for the reflector, imposing the boundary conditions equations (3.12), (3.13) and (3.14) and loading all the values choice for the neutronic properties, the trend of the MARS multiplicative factor with the thermal absorption macroscopic cross section in the core can be simply determined.

Figure 3.5 shows just this trend: as can be seen, the value able to guarantee a critical condition is 14.20 $\mathrm{m}^{-}1$ rather than a value of 12.10 $\mathrm{m}^{-}1$ suggested by [2].

3.3.3 The simulation results

In order to verify the validity of the neutronics model just described and applied to MARS two different analyses have been performed: at first, its responses in a zero power condition to a certain perturbation determined considering or not the precursors have been compared; at second, its responses in a zero power condition to different perturbations determined considering the precursors have been analyzed.

To do that, the *COMSOL Multiphysics* module *PDE Coefficient form* set on the *Transient Solver* has been used. More precisely, the following step have been carried out:

- a geometry as the one illustrated on Figure 3.1 has been created;
- equations (3.5), (3.6), (3.7), (3.8), (3.9), (3.10) and (3.11) have been reformulated in two different ways according as the precursors are considered or not; that is, if these ones are not taken into account so as that:

$$\underline{\underline{e_a}} = \left\{ \begin{array}{cc} 0 & 0 \\ 0 & 0 \end{array} \right\} \tag{3.42}$$

$$\underline{\underline{d_a}} = \left\{ \begin{array}{cc} \dfrac{1}{v_1} & 0 \\ 0 & \dfrac{1}{v_2} \end{array} \right\} \tag{3.43}$$

$$\underline{\underline{c}} = \left\{ \begin{array}{cc} \mathcal{D}_{C1} & 0 \\ 0 & \mathcal{D}_{C2} \end{array} \right\} \tag{3.44}$$

$$\underline{\underline{\alpha}} = \left\{ \begin{array}{cc} 0 & 0 \\ 0 & 0 \end{array} \right\} \tag{3.45}$$

$$\underline{\gamma} = \left\{ \begin{array}{c} 0 \\ 0 \end{array} \right\} \tag{3.46}$$

$$\underline{\underline{a}} = \left\{ \begin{array}{cc} \left[+\mathcal{D}_{C1}\, B^2 + \Sigma_{C1a} + \Sigma_{Ct} - (\nu\Sigma_f)_{C1}\right] & \left[-\left(1 - b_{2_i}\right)\, (\nu\Sigma_f)_{C2}\right] \\ (-\Sigma_{Ct}) & (+\mathcal{D}_{C2}\, B^2 + \Sigma_{C2a}) \end{array} \right\} \tag{3.47}$$

$$\underline{\underline{\beta}} = \left\{ \begin{array}{cc} 0 & 0 \\ 0 & 0 \end{array} \right\} \tag{3.48}$$

$$\underline{f} = \left\{ \begin{array}{c} 0 \\ 0 \end{array} \right\} \tag{3.49}$$

for the core and:

$$\underline{\underline{e_a}} = \left\{ \begin{array}{cc} 0 & 0 \\ 0 & 0 \end{array} \right\} \tag{3.50}$$

$$\underline{\underline{d_a}} = \left\{ \begin{array}{cc} \dfrac{1}{v_1} & 0 \\ 0 & \dfrac{1}{v_2} \end{array} \right\} \tag{3.51}$$

$$\underline{\underline{c}} = \left\{ \begin{array}{cc} \mathcal{D}_{R1} & 0 \\ 0 & \mathcal{D}_{R2} \end{array} \right\} \tag{3.52}$$

$$\underline{\underline{\alpha}} = \left\{ \begin{array}{cc} 0 & 0 \\ 0 & 0 \end{array} \right\} \tag{3.53}$$

$$\underline{\gamma} = \left\{ \begin{array}{c} 0 \\ 0 \end{array} \right\} \tag{3.54}$$

$$\underline{\underline{a}} = \left\{ \begin{array}{cc} (+\mathcal{D}_{R1}\, B^2 + \Sigma_{R1a} + \Sigma_{Rt}) & 0 \\ (-\Sigma_{Rt}) & (+\mathcal{D}_{R2}\, B^2 + \Sigma_{R2a}) \end{array} \right\} \tag{3.55}$$

$$\underline{\underline{\beta}} = \left\{ \begin{array}{cc} 0 & 0 \\ 0 & 0 \end{array} \right\} \tag{3.56}$$

$$\underline{f} = \left\{ \begin{array}{c} 0 \\ 0 \end{array} \right\} \tag{3.57}$$

for the reflector, whereas on the contrary so as that:

$$\underline{\underline{e_a}} = \left\{ \begin{array}{ccccc} 0 & 0 & 0 & ... & 0 \\ 0 & 0 & 0 & ... & 0 \\ 0 & 0 & 0 & ... & 0 \\ ... & & & & \\ 0 & 0 & 0 & ... & 0 \end{array} \right\} \tag{3.58}$$

$$\underline{\underline{d_a}} = \left\{ \begin{array}{ccccc} \frac{1}{v_1} & 0 & 0 & ... & 0 \\ 0 & \frac{1}{v_2} & 0 & ... & 0 \\ 0 & 0 & 1 & ... & 0 \\ ... & & & & \\ 0 & 0 & 0 & ... & 1 \end{array} \right\} \tag{3.59}$$

$$\underline{\underline{c}} = \left\{ \begin{array}{ccccc} \mathcal{D}_{C1} & 0 & 0 & ... & 0 \\ 0 & \mathcal{D}_{C2} & 0 & ... & 0 \\ 0 & 0 & 0 & ... & 0 \\ ... & & & & \\ 0 & 0 & 0 & ... & 0 \end{array} \right\} \tag{3.60}$$

$$\underline{\underline{\alpha}} = \left\{ \begin{array}{ccccc} 0 & 0 & 0 & ... & 0 \\ 0 & 0 & 0 & ... & 0 \\ 0 & 0 & 0 & ... & 0 \\ ... & & & & \\ 0 & 0 & 0 & ... & 0 \end{array} \right\} \tag{3.61}$$

$$\underline{\gamma} = \left\{ \begin{array}{c} 0 \\ 0 \\ 0 \\ ... \\ 0 \end{array} \right\} \tag{3.62}$$

$$\underline{\underline{a}} = \begin{Bmatrix} \left[+\mathcal{D}_{C1}\, B^2 + \Sigma_{C1a} + \Sigma_{Ct} - \left(\nu\Sigma_f\right)_{C1}\right] & \left[-\left(\nu\Sigma_f\right)_{C2}\,(1-b_{2_1})\right] & -\lambda_1 & ... & -\lambda_1 \\ \left(-\Sigma_{Ct}\right) & \left(+\mathcal{D}_{C2}\, B^2 + \Sigma_{C2a}\right) & 0 & ... & 0 \\ 0 & -\left(\nu\Sigma_f\right)_{C2}\, b_{2_1} & +\lambda_1 & ... & 0 \\ ... & & & & \\ 0 & -\left(\nu\Sigma_f\right)_{C2}\, b_{2_1} & 0 & ... & +\lambda_N \end{Bmatrix} \tag{3.63}$$

$$\underline{\underline{\beta}} = \begin{Bmatrix} 0 & 0 & 0 & ... & 0 \\ 0 & 0 & 0 & ... & 0 \\ 0 & 0 & 0 & ... & 0 \\ ... & & & & \\ 0 & 0 & 0 & ... & 0 \end{Bmatrix} \tag{3.64}$$

$$\underline{f} = \begin{Bmatrix} 0 \\ 0 \\ 0 \\ ... \\ 0 \end{Bmatrix} \tag{3.65}$$

for the core and:

$$\underline{\underline{e_a}} = \begin{Bmatrix} 0 & 0 & 0 & ... & 0 \\ 0 & 0 & 0 & ... & 0 \\ 0 & 0 & 0 & ... & 0 \\ ... & & & & \\ 0 & 0 & 0 & ... & 0 \end{Bmatrix} \tag{3.66}$$

$$\underline{\underline{d_a}} = \begin{Bmatrix} \frac{1}{v_1} & 0 & 0 & ... & 0 \\ 0 & \frac{1}{v_2} & 0 & ... & 0 \\ 0 & 0 & 1 & ... & 0 \\ ... & & & & \\ 0 & 0 & 0 & ... & 1 \end{Bmatrix} \tag{3.67}$$

$$\underline{\underline{c}} = \begin{Bmatrix} \mathcal{D}_{R1} & 0 & 0 & ... & 0 \\ 0 & \mathcal{D}_{R2} & 0 & ... & 0 \\ 0 & 0 & 0 & ... & 0 \\ ... & & & & \\ 0 & 0 & 0 & ... & 0 \end{Bmatrix} \tag{3.68}$$

$$\underline{\underline{\alpha}} = \begin{Bmatrix} 0 & 0 & 0 & ... & 0 \\ 0 & 0 & 0 & ... & 0 \\ 0 & 0 & 0 & ... & 0 \\ ... & & & & \\ 0 & 0 & 0 & ... & 0 \end{Bmatrix} \tag{3.69}$$

$$\underline{\gamma} = \begin{Bmatrix} 0 \\ 0 \\ 0 \\ ... \\ 0 \end{Bmatrix} \tag{3.70}$$

$$\underline{\underline{a}} = \begin{Bmatrix} \left(+\mathcal{D}_{R1}\, B^2 + \Sigma_{R1a} + \Sigma_{Rt}\right) & 0 & 0 & ... & 0 \\ \left(-\Sigma_{Rt}\right) & \left(+\mathcal{D}_{R2}\, B^2 + \Sigma_{R2a}\right) & 0 & ... & 0 \\ 0 & 0 & 1 & ... & 0 \\ ... & & & & \\ 0 & 0 & 0 & ... & 1 \end{Bmatrix} \tag{3.71}$$

$$\underline{\underline{\beta}} = \begin{Bmatrix} 0 & 0 & 0 & ... & 0 \\ 0 & 0 & 0 & ... & 0 \\ 0 & 0 & 0 & ... & 0 \\ ... & & & & \\ 0 & 0 & 0 & ... & 0 \end{Bmatrix} \tag{3.72}$$

$$\underline{f} = \begin{Bmatrix} 0 \\ 0 \\ 0 \\ ... \\ 0 \end{Bmatrix} \tag{3.73}$$

for the reflector;

- boundary and initial conditions (3.12), (3.13), (3.14), (3.16) and (3.17) have been imposed;
- all the values choice for the neutronic properties have been loaded.

First of all, the initial spatial distributions of the fast thermal flux and the thermal one in MARS have been determined. To do that and remembering that the solution of the equations (3.5), (3.6), (3.9) and (3.10) is defined for less than a

Parameter	Value	Measure unit
Uranium 235 nucleus density	5.29×10^{26}	m^-3
Uranium 238 nucleus density	2.25×10^{28}	m^-3
Fast fission microscopic cross section for uranium 235	1.287	barn
Thermal fission microscopic cross section for uranium 235	531.021	barn
Fast fission microscopic cross section for uranium 238	1.287	barn
Energy produced by a nuclear fission reaction of uranium 235 and uranium 238	200	MeV

Table 3.4: MARS uranium properties

multiplicative constant, their relative values Φ_1 and Φ_2 have been calculated running a stationary simulation since arbitrary initial conditions with the formulation without precursors; then, their absolute values ϕ_1 and ϕ_2 have been calculated fixing such a value of the multiplicative constant Φ_{ref} that they are able to guarantee a nominal thermal power production, that is they are able to verify the following equations:

$$P_{nom} = \int_V \left(\phi_1 N_{U_{238}} \sigma_{U_{238}} + \phi_1 N_{U_{235}} \sigma_{U_{235f}} + \phi_1 N_{U_{235}} \sigma_{U_{235t}}\right) E_f \, dV = \\ = \int_V \left(\Phi_1 \Phi_{ref} N_{U_{238}} \sigma_{U_{238}} + \Phi_1 \Phi_{ref} N_{U_{235}} \sigma_{U_{235f}} + \Phi_1 \Phi_{ref} N_{U_{235}} \sigma_{U_{235t}}\right) E_f \, dV \tag{3.74}$$

So doing and using the values of the uranium properties reported on Table 3.4, a multiplicative constant of $1.7164 \times 10^{17}\, 1/(m^2\, s)$ and the nominal spatial distributions of the fast neutron flux and the thermal one illustrated on Figure 3.6.

On Figures 3.7 and 3.8 the result of the first analysis are illustrated: they show the MARS responses in a zero power condition since the initial state referred above to a succession of a negative core absorption macroscopic cross section step given 5 s after the beginning of the simulation and a positive one given 7 s after this time determined respectively not considering and considering the precursors; in

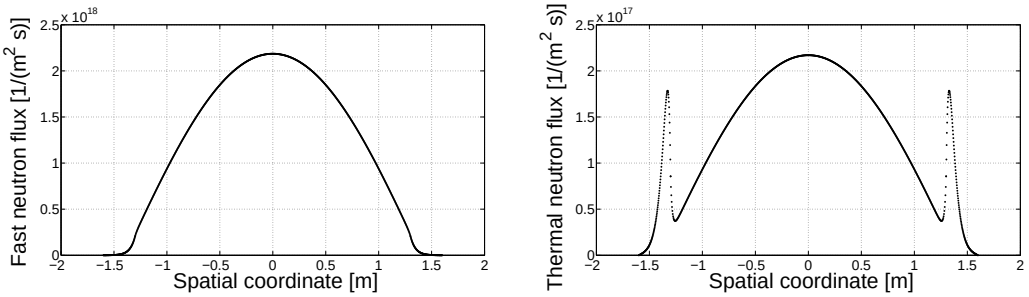

(a) Fast neutron flux **(b)** Thermal neutron flux

Figure 3.6: Nominal spatial distributions of the MARS neutron fluxes

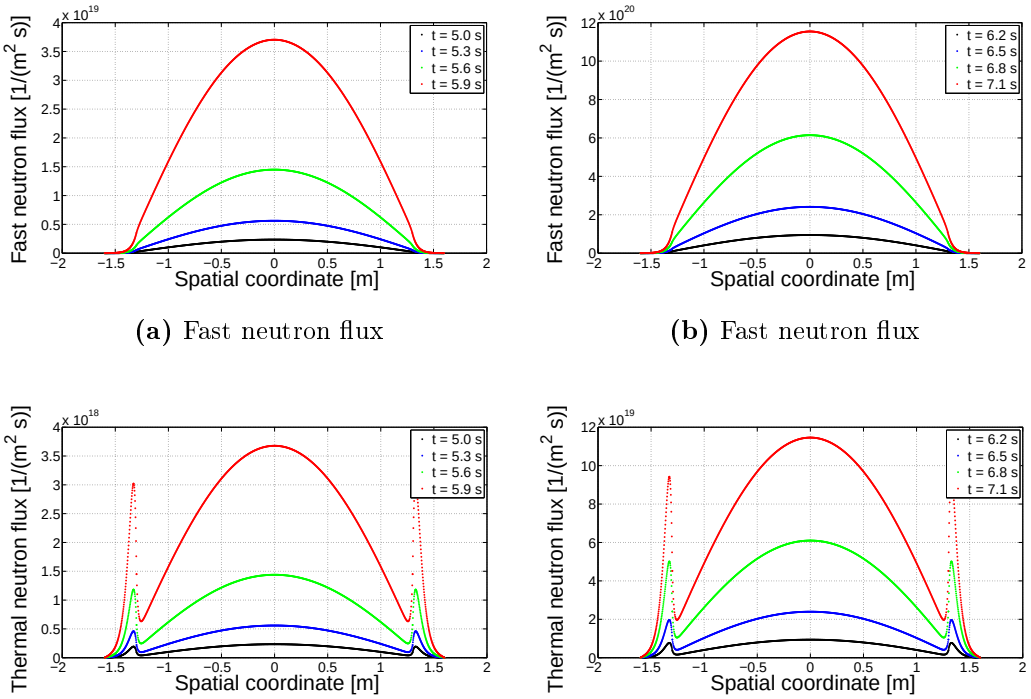

(a) Fast neutron flux **(b)** Fast neutron flux

(c) Thermal neutron flux **(d)** Thermal neutron flux

Figure 3.7: MARS response in a zero power condition to a negative core absorption macroscopic cross section step of 0.01 % given 5 s after the beginning of the simulation and a positive one of 0.01 % given 7 s after this time without the precursors

particular, in the first case a perturbation size of 0.01 %, about 6.8 pcm, has been fixed whereas in the second case a step of 0.1 %, about 68.3 pcm, has been chosen. Moreover, Figure 3.9 illustrates the stationary state reached by MARS in a zero power condition when, since the initial state referred above, it is stimulated with

a succession of steps as the one described but characterized by a perturbation size of 0.1 % determined not considering the precursors.

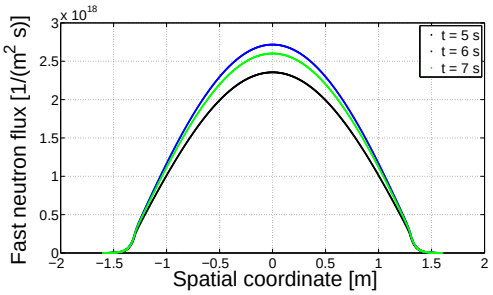

(a) Fast neutron flux

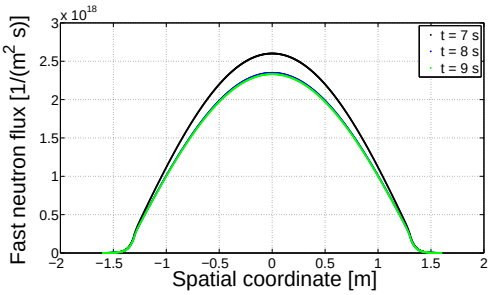

(b) Fast neutron flux

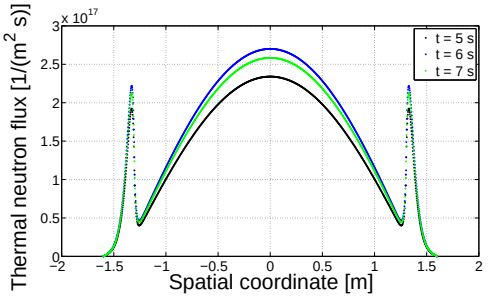

(c) Thermal neutron flux

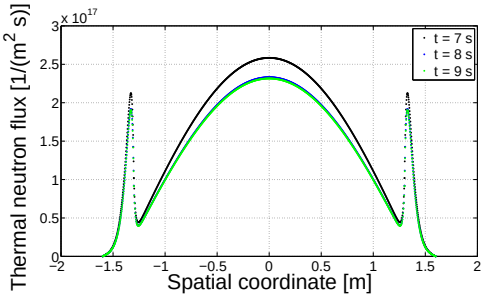

(d) Thermal neutron flux

Figure 3.8: MARS response in a zero power condition to a negative core absorption macroscopic cross section step of 0.1 % given 5 s after the beginning of the simulation and a positive one of 0.1 % given 7 s after this time with the precursors

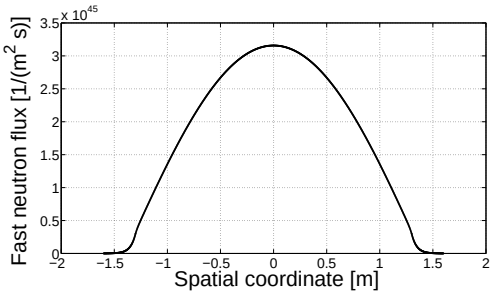

(a) Fast neutron flux

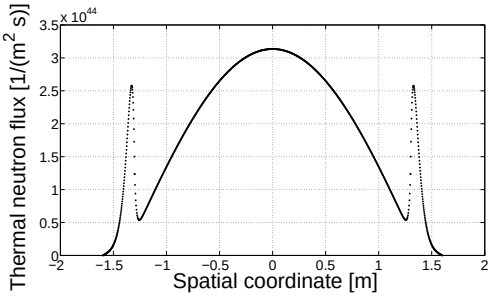

(b) Thermal neutron flux

Figure 3.9: Stationary state reached by MARS after a negative core absorption macroscopic cross section step of 0.1 % and a positive one given 5 s and 7 s after the beginning of the simulation without the precursors

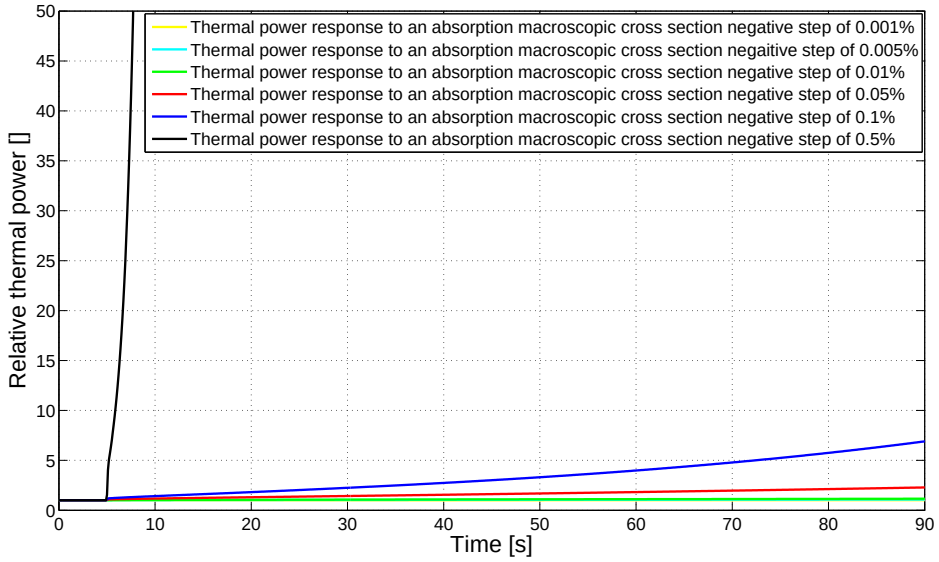

Figure 3.10: MARS response in a zero power condition to negative core absorption macroscopic cross section steps of different entities with the precursor

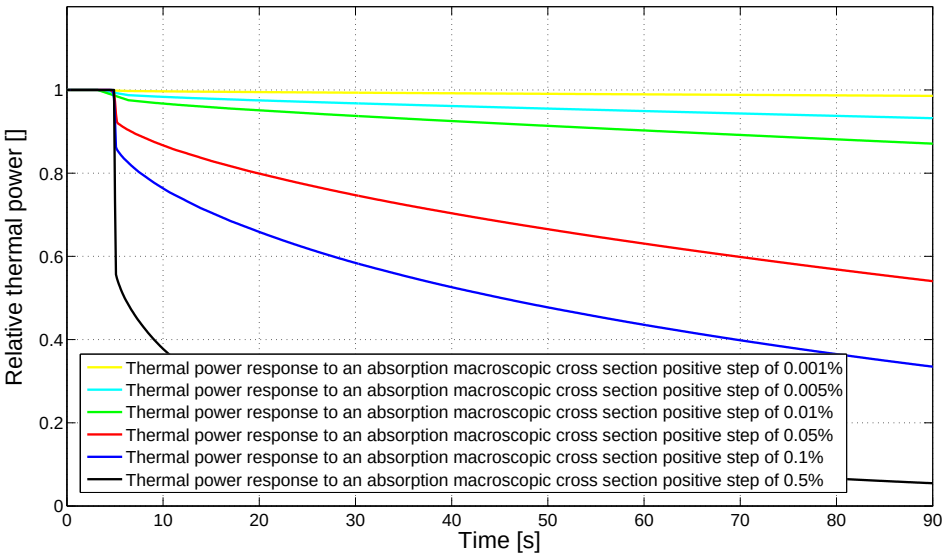

Figure 3.11: MARS response in a zero power condition to positive core absorption macroscopic cross section steps of different entities with the precursor

The result is exactly the same one obtained with the zero-dimensional model deduced on the previous chapter for SURE: indeed, it being understood a zero power condition, whereas if the precursors are not considered a modest reactivity insertion induces an increase of the neutron fluxes of some magnitude orders, if

they are taken into account the same perturbation is just perceptible. This result is physically valid and underlines, besides the fundamental role played by the precursors, the reliability of the neutronics model just described.

Instead, Figures 3.10 and 3.10 show the result of the second analysis: the MARS response in a zero power condition since the initial state referred above to positive or negative core absorption macroscopic cross section steps of different entities determined considering the precursors.

Both on Figure 3.10 and on Figure 3.11 the prompt jump and the exponential trend typical of the zero power reactor dynamics are present, further confirmation of the validity of the neutronics model just described.

3.4 The neutronics and thermo-hydraulics model

During this third part of the work a second step has been the development of a one-dimensional neutronics and thermo-hydraulics model for MARS in a normal operating condition.

To do that the neutronics one just described and the one-dimensional thermo-hydraulics one deduced on the first chapter have been used by means of an appropriate coupling.

As for the zero-dimensional model of SURE, two phases have been tackled: at first, the thermo-hydraulics model referred above has been opportunely changed so as to make it applicable to MARS and at second this one and the neutronics one just described have been coupled deducing apposite coupling equations. In particular the realization of this second phase has been rather complex in this case because of the necessity to deduce the trend of the core macroscopic cross sections and of the core the diffusion coefficients with the thermo-hydraulics properties, in particular with the fuel temperature and the coolant one; to this aim an interesting procedure suggested by [1] based on the determination of the effective multiplicative factor corresponding to different core compositions, that is corresponding to different values of the temperatures mentioned, has been used.

Later on, a section is dedicated to each of these phases. Moreover, the verify

Parameter	Value	Measure unit
Hydraulic perimeter	7.676×10^2	m
Hydraulic area	1.852	m^2
Hydraulic diameter	9.650×10^{-2}	m
Thermal perimeter	7.012×10^2	m
Thermal area	1.823×10^3	m^2

Table 3.5: MARS geometrical features

of the validity of the model so developed are reported.

3.4.1 The application of the one-dimensional thermo-hydraulics model to MARS

The application of the one-dimensional thermo-hydraulics model deduced on the first chapter required first of all the definition of three different domains: the down reflector, the core and the up reflector. Then, on each of them some changes have been done: the equations on which this model is based have been opportunely reformulated, the correct geometric features have been imposed and an equation able to take the fuel presence into account, only for the second one, has been introduced.

Let us considerer the first change. Equations (1.12), (1.13) and (1.17) and all the constitute and closure equations associated to these ones, choosing as correlations the Mac Adams and the Jones ones, have been imposed in the form deduced on the first chapter in the core domain; instead, for the down and up reflector, in which there are not fuel materials, the term representing the introduction of thermal power in energy balance equation has been eliminated.

About the second change, the values of the geometric features have been calculated by the ones illustrated on Table 3.1 and are reported on Table 3.5.

Finally let us considerer the third change. The equation introduced for the core domain is a fuel energy balance equation taking, as in a zero-dimensional formulation, the following form:

$$\frac{\partial}{\partial t}\left(m_{fuel}\,\chi_{fuel}\,T_{fuel}\right) = q^{'''}\,m_{fuel}\,\rho_{fuel} - q^{''}\,A_t \tag{3.75}$$

where for the specific heat the value suggested by [7], that is 292.88 J/(kg℃), has been chosen and the volume has been calculated since the values reported on Tables 3.1 and 3.2.

Both to the coolant equations defined on the down reflector, on the core and on the up reflector and to the fuel equation defined only on the second one appropriate initial conditions have to be associated and to do that, as just done for the fast neutron flux and for the thermal one, a nominal thermal power production can be fixed. Moreover, boundary conditions are required to solve the first ones; it can be done imposing that:

- at the first extremity of the down reflector the coolant pressure, the mass flux and the dynamic enthalpy assume the inlet values, that is:

$$\begin{aligned} p(0,t)|_R &= p_{in} \\ g_m(0,t)|_R &= g_{m_{in}} \\ h_m^+(0,t)|_R &= h_{in} \end{aligned} \tag{3.76}$$

- at the first interface between the down reflector and the core the flux terms preserve their values, that is:

$$\begin{aligned} g_m(L_{R_{down}},t)|_R &= g_m(L_{R_{down}},t)|_C \\ \left.\frac{g_m^2(L_{R_{down}},t)}{\rho_m^+(L_{R_{down}},t)}\right|_R &= \left.\frac{g_m^2(L_{R_{down}},t)}{\rho_m^+(L_{R_{down}},t)}\right|_C \\ g_m(L_{R_{down}},t)\,h_m(L_{R_{down}},t)|_R &= g_m(L_{R_{down}},t)\,h_m(L_{R_{down}},t)|_C \end{aligned} \tag{3.77}$$

- at the second interface between the down reflector and the core the flux terms preserve their values, that is:

$$\begin{aligned} g_m(L_{R_{down}}+L_C,t)|_R &= g_m(L_{R_{down}}+L_C,t)|_C \\ \left.\frac{g_m^2(L_{R_{down}}+L_C,t)}{\rho_m^+(L_{R_{down}}+L_C,t)}\right|_R &= \left.\frac{g_m^2(L_{R_{down}}+L_C,t)}{\rho_m^+(L_{R_{down}}+L_C,t)}\right|_C \\ g_m(L_{R_{down}}+L_C,t)\,h_m(L_{R_{down}}+L_C,t)|_R &= \\ = g_m(L_{R_{down}}+L_C,t)\,h_m(L_{R_{down}}+L_C,t)|_C & \end{aligned} \tag{3.78}$$

- at the second extremity of the up reflector the coolant pressure, the mass flux and the dynamic enthalpy assume such values that:

$$\begin{aligned}
\Gamma_1(L_{R_{down}} + L_C + L_{R_{up}}, t)\big|_R &= -g_m(L_{R_{down}} + L_C + L_{R_{up}}, t)\big|_R \\
\Gamma_2(L_{R_{down}} + L_C + L_{R_{up}}, t)\big|_R &= -\frac{g_m(L_{R_{down}} + L_C + L_{R_{up}}, t)^2}{\rho_m^+(L_{R_{down}} + L_C + L_{R_{up}}, t)}\Big|_R \\
\Gamma_3(L_{R_{down}} + L_C + L_{R_{up}}, t)\big|_R &= \\
= -\, g_m(L_{R_{down}} + L_C + L_{R_{up}}, t)\, h_m^+(L_{R_{down}} + L_C + L_{R_{up}}, t)\big|_R &
\end{aligned} \tag{3.79}$$

3.4.2 The deduction of coupling equations between the neutronics model and the thermo-hydraulics one

Two different kinds of equation are necessary to couple the neutronics model just described and the thermo-hydraulics one deduced on the first chapter and here corrected: those ones expressing the effect of the fuel temperature variations and the coolant temperature ones on the neutronics and vice versa those one expressing the effect of the core neutron fluxes variations on the thermo-hydraulics.

The first ones are equations in which the trend of the core macroscopic cross sections and diffusion coefficients with the fuel and coolant temperature are expressed.

Their deduction is rather complex and requires at first the assumption of specific hypothesis and at second the assumption of a precise procedure. So, the following hypothesis have been assumed:

- two feedback effects are taken into account: those one due to the fuel temperature variations and those one due to the coolant temperature ones;

- the fuel temperature variations induce only linear variations of the core transfer macroscopic cross section from the fast group to the thermal one: this choice is justified by the fact that physically to fuel temperature variations the broadening or the tightening of the uranium 238 absorption macroscopic cross section resonances and, consequently, the increase or the decrease of the fast neutrons reaching the thermal energy achieve; these variations take the following form:

$$\Sigma_{Ct}(T_{fuel}) = \Sigma_{Ct}(T_{fuel_{nom}}) + C_{fuel}\,(T_{fuel} - T_{fuel_{nom}}) \tag{3.80}$$

where:

$$C_{fuel} = \frac{\delta \Sigma_{Ct}}{\delta T_{fuel}} \tag{3.81}$$

- the coolant temperature variations induce linear variation of the core transfer macroscopic cross section from the fast group to the thermal one and diffusion coefficients characterized by a certain angular coefficient and linear variations of the core absorption macroscopic cross sections characterized by a different angular coefficient: indeed, although physically to coolant temperature variations the increase or the decrease of the water nucleus density achieve, this increase or this decrease weighs upon the whole core features differently because of the higher value of the scattering microscopic cross section, on which the first three parameters depend, as regards the absorption one, on which instead the last two parameters depend;

- the variations of the core transfer macroscopic cross section from the fast group to the thermal one and diffusion coefficients with the coolant temperature can be expressed by the following formula:

$$\Sigma_{Ct}(T_{cool}) = \Sigma_{Ct}(T_{cool_{nom}}) + C_{cool_{scat}} \left(T_{cool} - T_{cool_{nom}}\right) \tag{3.82}$$

$$\mathcal{D}_{C1}(T_{cool}) = \mathcal{D}_{C1}(T_{cool_{nom}}) - \left[\mathcal{D}_{C1}(T_{cool_{nom}})\right]^2 C_{cool_{scat}} \left(T_{cool} - T_{cool_{nom}}\right) \tag{3.83}$$

$$\mathcal{D}_{C2}(T_{cool}) = \mathcal{D}_{C2}(T_{cool_{nom}}) - \left[\mathcal{D}_{C2}(T_{cool_{nom}})\right]^2 C_{cool_{scat}} \left(T_{cool} - T_{cool_{nom}}\right) \tag{3.84}$$

where:

$$C_{cool_{scat}} = \frac{\delta \Sigma_{cool1scat}}{\delta T_{cool}} = \frac{\delta \Sigma_{cool2scat}}{\delta T_{cool}} \tag{3.85}$$

indeed, it can be assumed that the first one is proportional to the coolant scattering macroscopic cross section at fast energy whereas the second ones are proportional to the inverse of this cross section respectively at fast energy and thermal energy, that is:

$$\Sigma_{Ct} \propto \Sigma_{cool1scat} \tag{3.86}$$

$$\mathcal{D}_{C1} \propto \frac{1}{\Sigma_{cool1scat}} \tag{3.87}$$

$$\mathcal{D}_{C2} \propto \frac{1}{\Sigma_{cool2scat}} \tag{3.88}$$

and consequently:

$$\begin{aligned}\Sigma_{Ct}(T_{cool}) &= \Sigma_{Ct}(T_{cool_{nom}}) + \frac{\delta\Sigma_{Ct}}{\delta T_{cool}}\left(T_{cool} - T_{cool_{nom}}\right) = \\ &= \Sigma_{Ct}(T_{cool_{nom}}) + C_{cool_{scat}}\left(T_{cool} - T_{cool_{nom}}\right) =\end{aligned} \tag{3.89}$$

$$\begin{aligned}\mathcal{D}_{C1}(T_{cool}) &= \mathcal{D}_{C1}(T_{cool_{nom}}) + \frac{\delta\mathcal{D}_{C1}}{\delta T_{cool}}\left(T_{cool} - T_{cool_{nom}}\right) = \\ &= \mathcal{D}_{C1}(T_{cool_{nom}}) - \left[D_{C1}(T_{cool_{nom}})\right]^2 C_{cool_{scat}}\left(T_{cool} - T_{cool_{nom}}\right)\end{aligned} \tag{3.90}$$

$$\begin{aligned}\mathcal{D}_{C2}(T_{cool}) &= \mathcal{D}_{C2}(T_{cool_{nom}}) + \frac{\delta\mathcal{D}_{C2}}{\delta T_{cool}}\left(T_{cool} - T_{cool_{nom}}\right) = \\ &= \mathcal{D}_{C2}(T_{cool_{nom}}) - \left[D_{C2}(T_{cool_{nom}})\right]^2 C_{cool_{scat}}\left(T_{cool} - T_{cool_{nom}}\right)\end{aligned} \tag{3.91}$$

- the variations of the core absorption macroscopic cross sections can be expressed by the following formula:

$$\Sigma_{C1a}(T_{cool}) = \Sigma_{C1a}(T_{cool_{nom}}) + C_{cool_{abs}}\left(T_{cool} - T_{cool_{nom}}\right) \tag{3.92}$$

$$\Sigma_{C2a}(T_{cool}) = \Sigma_{C2a}(T_{cool_{nom}}) + C_{cool_{abs}}\left(T_{cool} - T_{cool_{nom}}\right) \tag{3.93}$$

where:

$$C_{cool_{abs}} = \frac{\delta\Sigma_{cool1abs}}{\delta T_{cool}} = \frac{\delta\Sigma_{cool2abs}}{\delta T_{cool}} \tag{3.94}$$

indeed, it can be assumed that these ones are proportional to the coolant absorption macroscopic cross section respectively at fast energy and thermal energy, that is:

$$\Sigma_{C1a} \propto \Sigma_{cool1abs} \tag{3.95}$$

$$\Sigma_{C2a} \propto \Sigma_{cool2abs} \tag{3.96}$$

Moreover, a procedure suggested by [1] has been chosen; it is constituted by the following steps:

- the feedback effect due to the variations of a certain parameters is taken into account;
- an appropriate value of the reactivity feedback coefficient associated to the feedback effect taken into account is chosen;
- two different conditions of the core in term of the parameter the variations of which cause the feedback effect taken into account are fixed;

Fuel feedback coefficient [pcm/℃]	Fuel coefficient [1/(cm℃)]
-1	8.90×10^{-7}
-3	2.67×10^{-6}
-5	4.46×10^{-6}

Table 3.6: Fuel coefficients corresponding to different fuel feedback coefficients

- the value of the effective multiplicative factor k_{eff_1} associated to the first one of the condition fixed is calculated by means of equations (3.18), (3.19), (3.20) and (3.21) as previously explained;

- the value of the effective multiplicative factor k_{eff_2} associated to the second one of the condition fixed is calculated by means of the equation, considered in its differential form, in which the relation between the reactivity and the effective multiplicative factor are expressed, that is:

$$\alpha_x = \frac{\varrho_2 - \varrho_1}{x_2 - x_1} = \frac{1}{x_2 - x_1} \left(\frac{1}{k_{\text{eff}_1}} - \frac{1}{k_{\text{eff}_2}} \right) \tag{3.97}$$

- the values of the core features able to guarantee the value of the effective multiplicative factor calculated are determined by means of equations (3.18), (3.19), (3.20) and (3.21) as previously explained;

- finally the trend of the core features with the parameter the variations of which cause the feedback effect taken into account are determined using the following formula:

$$f(x) = f(x_1) + \frac{f(x_2) - f(x_1)}{x_2 - x_1} (x - x_1) \tag{3.98}$$

Assuming the hypothesis mentioned and using the procedure described by means of *COMSOL Multiphysics PDE Coefficient Form* set on the *Eigenvalue Solver* as described previously, the values for the coefficient C_{fuel} reported in Table 3.6 and those ones for the coefficients $C_{cool_{scat}}$ and $C_{cool_{scat}}$ reported on Table 3.7 has been determined.

Coolant feedback coefficient [pcm/℃]	Coolant scattering coefficient [1/(cm℃)]	Coolant absorption coefficient [1/(cm℃)]
0	0	0
−10	1.00×10^{-5}	2.99×10^{-7}
−20	2.00×10^{-5}	6.09×10^{-7}

Table 3.7: Coolant coefficients corresponding to different coolant feedback coefficients

Instead, the second one is an equation by means of which the thermal power production due to the nuclear fission reactions can be inserted in the fuel energy balance equation and takes the following form:

$$q''' = \left(\Phi_1 \, \Phi_{ref} \, N_{U_{238}} \, \sigma_{U_{238}} + \Phi_1 \, \Phi_{ref} \, N_{U_{235}} \, \sigma_{U_{235f}} + \Phi_1 \, \Phi_{ref} \, N_{U_{235}} \, \sigma_{U_{235t}}\right) \, E_f \, r_{fuel}^2 \tag{3.99}$$

In this equation, the term Φ_{ref} represents the multiplicative constant for less than which the fast flux and the thermal one can be deduced by equations (3.5), (3.6), (3.9) and (3.10) and can be determined by means of equation (3.79) as explained previously; the term R_f represent a fictitious fuel radius and can be calculated by means of the following formula:

$$r_f = \left(\frac{V_f}{\pi \, L_C}\right) \tag{3.100}$$

obtaining a value of 6.176×10^{-1} m; moreover, the uranium properties in it appeared are tho ones reported on Table 3.5.

Besides the equations just illustrated and explained, another one is necessary to couple the fuel dynamics and the coolant one. This equations take the following form:

$$q'' = U \, (T_{fuel} - T_{cool}) \tag{3.101}$$

where the total heat transfer coefficient can be determined by the following formula:

$$U = \frac{1}{R_{fuel} + R_{gap} + R_{clad} + R_{clad-cool}} \frac{1}{2 \, \pi \, r_{clad_{out}}} \tag{3.102}$$

if the fuel temperature is referred to the center of the pellets or the following one:

$$U = \frac{1}{R_{gap} + R_{clad} + R_{clad-cool}} \frac{1}{2 \, \pi \, r_{clad_{ext}}} \tag{3.103}$$

Parameter	Value	Measure unit
Fuel thermal conductivity	2.7	W/(m°C)
Gap thermal conductivity	0.5	W/(m°C)
Clad thermal conductivity	14	W/(m°C)
Heat transfer coefficient between clad and coolant	26 300	W/(m^2°C)
Fuel thermal resistance	0.029 47	(m°C)/W
Gap thermal resistance	0.007 82	(m°C)/W
Clad thermal resistance	0.001 617	(m°C)/W
Thermal resistance between clad and coolant	0.001 274	(m°C)/W

Table 3.8: MARS fuel rod thermal conductivity coefficients and thermal resistances

if the fuel temperature is referred to the external diameter of the pellets; however, the thermal resistance appearing in it have been calculated in the following way:

$$R_{fuel} = (4\,\pi\,\kappa_{fuel})^{-1} \tag{3.104}$$

$$R_{gap} = (2\,\pi\,r_{fuel}\,\eta_{gap})^{-1} = \left[2\,\pi\,r_{fuel}\,\frac{\kappa_{gap}}{r_{fuel}\,\ln\left(\frac{r_{clad_{int}}}{r_{fuel}}\right)}\right]^{-1} \tag{3.105}$$

$$R_{clad} = \frac{\ln\frac{r_{clad_{ext}}}{r_{clad_{int}}}}{2\,\pi\,\kappa_{clad}} \tag{3.106}$$

$$R_{clad-coolant} = (2\,\pi\,r_{clad_{ext}}\,\eta_{clad-coolant})^{-1} \tag{3.107}$$

Using the values reported on Table 3.8, the values of the thermal resistances reported on the same one and a value of the total heat transfer coefficient equal to 3127.92 W/(m^{2}K) have been obtained.

3.4.3 The simulation results

As for the neutronics one, a verify of the validity of the neutronics and thermo-hydraulics model developed has been carried out: more precisely, the MARS response in a normal operating condition since its nominal state to perturbations of different kinds and entities has been determined.

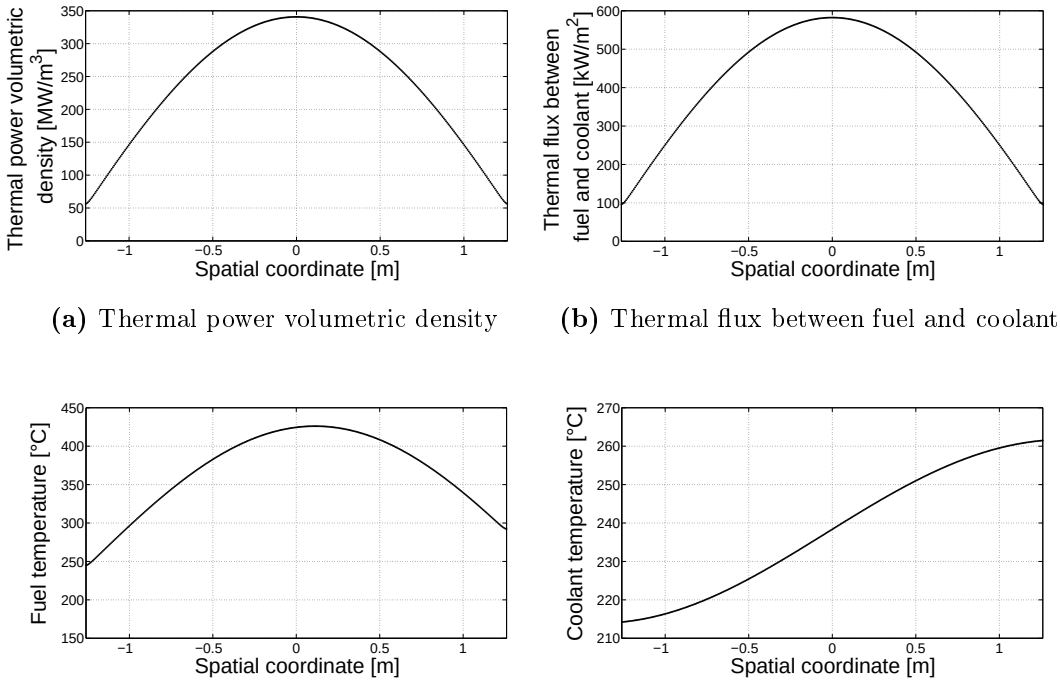

(a) Thermal power volumetric density

(b) Thermal flux between fuel and coolant

(c) Fuel temperature

(d) Coolant temperature

Figure 3.12: MARS nominal thermo-hydraulics condition

To do that, *COMSOL Multiphysics* has been used in the following way: the MARS thermodynamics nominal state has been calculated running a stationary simulation for the thermo-hydraulics model since arbitrary initial values so as to calculate in a second moment its response in a normal operating condition to core absorption macroscopic cross section, inlet coolant mass flux and inlet temperature steps running transient simulations since this nominal state and the neutronics one represented by equations (3.74), (3.16) and (3.18). Obviously, to do that the following steps have been accomplished:

- a geometry as the one illustrated on Figure 3.1 has been created;
- equations (3.5), (3.6), (3.8), (3.9), (3.10) and (3.11) and the relative initial and boundary conditions have been implemented using the *PDE Coefficient Form* module as described previously;
- equations (1.12), (1.13) and (1.17) and the relative constitute equations, closure equations and initial and boundary conditions have been implemented

using the *PDE General Form* module explained on the first chapter and the procedure illustrated on the first chapter;

- coupling equations have been introduced;
- finally, all the values choice for the neutronic properties and the geometric ones have been loaded.

On Figures 3.12 the nominal spatial distributions of the thermal power volumetric density, the thermal flux between fuel and coolant, the fuel temperature and the coolant one are illustrated.

As can be see, the thermal power volumetric density and the thermal flux between fuel and coolant are characterized by a spatial distribution symmetric respect the core center, in corresponding of which they assume the highest values of $340.73\,\mathrm{MW/m^3}$ and $580.25\,\mathrm{kW/m^3}$; instead, the fuel temperature takes the expected trend characterized by the reaching of the highest value of $426.0\,^{\circ}\mathrm{C}$ in corresponding of the spatial coordinate $0.115\,\mathrm{m}$; finally, the coolant temperature is characterized by a growing trend from the inlet value of $214.0\,^{\circ}\mathrm{C}$ to the value $261.7\,^{\circ}\mathrm{C}$.

On Figures 3.13, 3.14 and 3.15 the MARS response in a normal operating condition since this nominal state and the neutronics one referred above to different perturbations are reported.

In particular, on Figure 3.14 its response since its nominal state to a positive core absorption macroscopic cross section step of $0.1\,\%$ is illustrated. This perturbation induces a decrease of the thermal power production and consequently a decrease of the fuel temperature and the coolant one the result of which is at first a negative reactivity insertion and then a positive one: so, as can be seen from this figure, as much high are the fuel feedback coefficient and the coolant one as fast is this positive reactivity insertion and therefore as elevated is the thermal power level reached. A similar consideration can be done for a negative core absorption macroscopic cross section step.

Instead, Figure 3.14 illustrates its response since its nominal condition to a positive inlet mass flux of $1\,\%$. This perturbation induces a decrease of the coolant

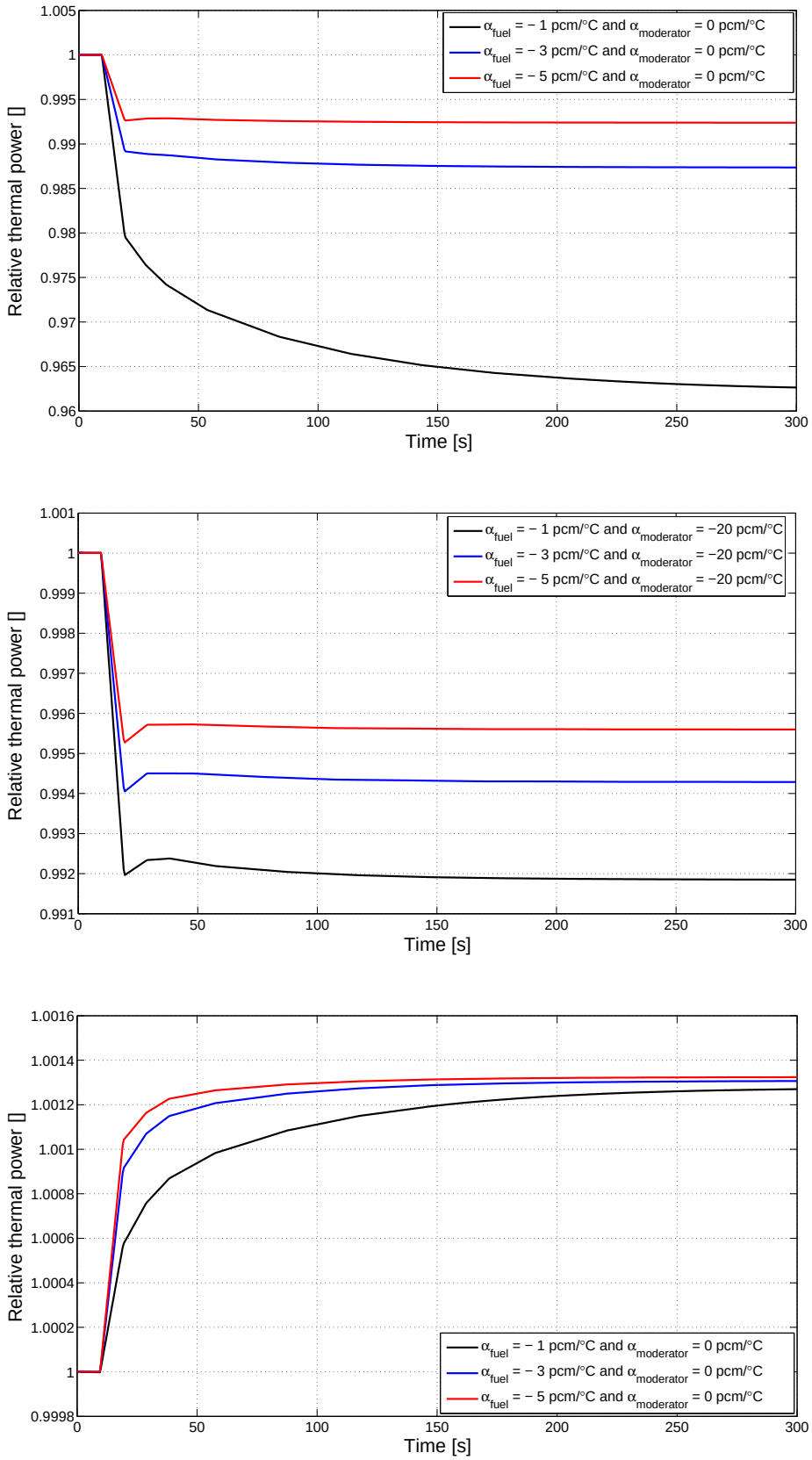

Figure 3.13: MARS response since its nominal condition to a core absorption macroscopic cross section step

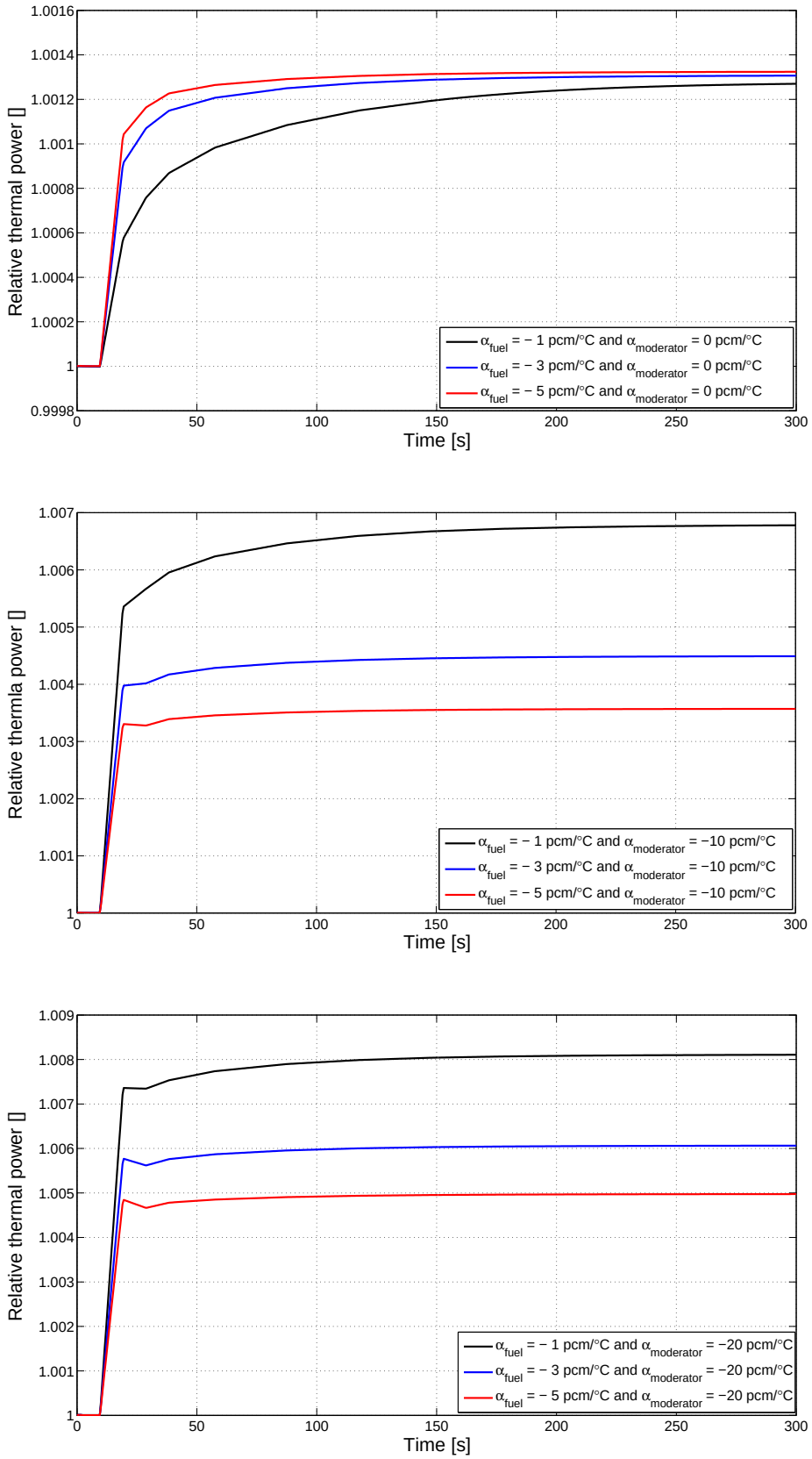

Figure 3.14: MARS response since its nominal condition to a inlet coolant mass flux step

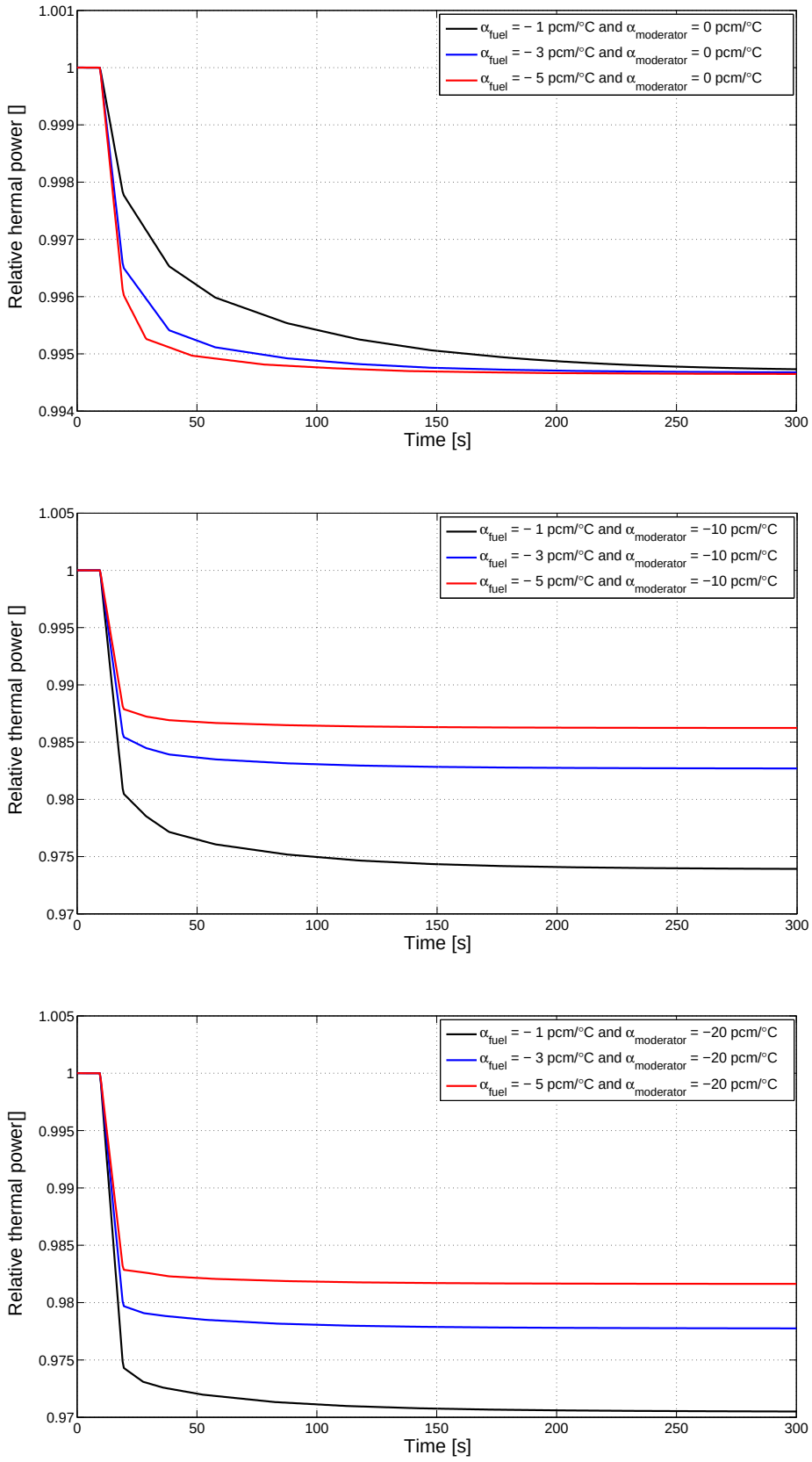

Figure 3.15: MARS response since its nominal condition to a inlet coolant temperature step

temperature the result of which is a positive reactivity insertion that induce in turn an increase of the thermal power production and consequently an increase of the fuel temperature the result of which is a negative reactivity insertion: so, as can be see from this figure, at first as mich high is the coolant feedback corfficient and this positive reactivity insertion as quickly is the thermal power production increase and the fuel temperature one and at second as much high is the fuel feedback coefficient as low is this negative reactivity insertion and the thermal power leval reached. An apart consideration is deserved by the first case: indeed, if the coolant feedback coefficient is null, the positive reactivity insertion and the negative one are due respectively to the fuel temperature decrease that follow the coolant temperature one and to the fuel temperature increase that follow its own decrease with the result that the timetable necessary to reach a stationary state and the corresponding thermal power level depend only on the fuel feedback coefficient. Similar considerations can be done for a negative inlet coolant mass flux step.

Finally, on Figure 3.15 its response since its nominal condition to a positive inlet coolant temperature step of 1 ℃ is illustrated. The same considerations made for the MARS response to a inlet coolant mass flux step can be here repeated: indeed, the first effect produced by such a perturbation is a negative reactivity insertion due to the increase of the coolant temperature if the coolant feedback coefficient is not null or to the increase of the fuel one if this coefficient is null.

To note finally that, unlike what happens in a zero-dimensional model, the inlet perturbation of a certain variable not always reproduces instantly oneself: an example is reported in Figure 3.16 where the inlet coolant enthalpy and the outlet one after a inlet coolant temperature step of 1 ℃ are illustrated.

3.5 Conclusion

Similar considerations to the ones made on the development of the neutronics and thermo-hydraulics model for SURE can be done in this situation for MARS one.

Also this third part of the work pointed out the advantages the modeling and

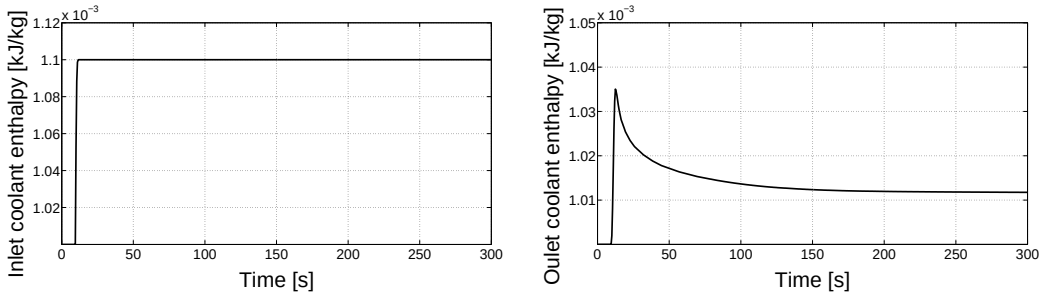

(a) Inlet coolant enthalpy

(b) Outlet coolant enthalpy

Figure 3.16: Coolant enthalpy after a inlet coolant temperature step of 1 °C

the simulating of such a model obtained, both in terms of easiness and in terms of rapidity, if codes as *COMSOL Multiphysics* expressly conceived to solve multi-physics problems are used: indeed, both the *PDE General Form* module used to realize the thermo-hydraulics model and the *PDE Coefficient Form* module used to realize the neutronics one offer the possibility to implement different physics of a multi-dimensional physical systems merely bringing back to an apposite form their partial differential equations and their ordinary ones. What's more such these advantages, as just mentioned, are all the more evident in these case where a one-dimensional approach has been adopted and where the employment of a code based on a different approach should be surely more complex.

Regardless to these implementation aspects, a consideration on the methodology used to developed the MARS neutronics and thermo-hydraulics model and one on the result consequently obtained are necessary to conclude the description of this last part of the work.

The procedure used to determine the core macroscopic cross section and diffusion coefficient trend with the fuel temperature and the coolant one proved to be very efficient: indeed, besides the simplicity in the calculations made more marked by the *COMSOL Multiphysics Eigenvalue Solver* employment, such a procedure allows to take into account at the same time the mathematical aspects and the physical one, representing the eigenvalue found in corresponding of a certain core composition the inverse of the effective multiplicative factor.

Moreover, the results obtained with the MARS neutronics model and the neu-

tronics and thermo-hydraulics one are very good and highlight their reliability: indeed, although also this time no experimental data are available, its simulated responses to certain perturbation both in a zero power condition, determined with the first one, and in a normal operating one, determined with the second one, are physically consistent. More precisely, the simulations performed in a zero power condition underlined once again both the role played by the precursors in the nuclear fission reactor dynamic and the typical trend given by the prompt jump and the exponential growth characterizing it when they are present; instead, those ones performed in a normal operating condition showed, besides the way by means of which the feedback effects due to the fuel temperature and the coolant temperature variations happen, the validity of the procedure used to derive the macroscopic cross section trend with the thermo-hydraulics properties.

To note finally that the limitation appeared in the previous part of the work, that is the not physical instant variation of the outlet properties after a inlet perturbation, seems to be with a one-dimensional approach a little less marked: nevertheless, in such an approach the axial distribution of the properties, and consequently the timetables necessary to them to undergone a change, is taken into account.

Nomenclature

- A area
- b precursor delayed neutron fraction
- B buckling
- c precursor density
- d thermal diffusion coefficient
- D diameter
- $\mathcal{D}$ neutron diffusion coefficient
- E energy
- g mass flux
- h enthalpy
- L channel length

k multiplicative factor

m mass

N nucleus density

p pressure

P perimeter

q'' thermal flux

q''' thermal power volumetric density

r radius

R thermal resistance

t temporal coordinate

T temperature

u internal energy

U total heat transfer coefficient

v neutron velocity

V volume

z spatial coordinate

Greek symbols

α void fraction

α_ϱ reactivity feedback coefficient

η heat transfer coefficient

θ channel slope angle

κ thermal conductivity coefficient

λ precursor decay constant

μ viscosity

ν mean value of the fission neutrons

ρ density

ϱ reactivity

σ microscopic cross section

Σ macroscopic cross section

Φ relative neutron flux

ϕ absolute neutron flux

χ specific heat

Subscripts

abs	absorption
C	core region
$clad$	clad
$cool$	coolant
eff	effective
ext	external
f	fission
$fuel$	fuel
gap	gap
h	hydraulic
i	precursor group
int	internal
m	mixture
nom	nominal
ref	reference
R	reflector region
R_{down},R_{up}	down and up reflector
$scat$	scattering
U	uranium
U_{235}	uranium 235
U_{238}	uranium 238
V	vapor phase
ZrH_x	zyrconium hydride
0	initial
1	fast group
2	thermal group

Bibliography

[1] V. Memoli and A.Cammi. Evaluation of the moderator temperature coefficient of reactivity in a pwr. In *COMSOL User Conference 2007 Grenoble*, 2007.

[2] James J. Duderstadt and Louis J. Hamilton. *Nuclear reactor analysis*. John Wiley&sons, 1976.

[3] Gianfranco Caruso. *Esercitazioni di Impianti Nucleari*. Aracne, 2003.

[4] Enrico Mainardi and Ugo Spezia. Orizzonti della tecnologia nucleare in italia. In *Giornata di studio AIN 2004*, 2004.

[5] Sandro Salsa, Federico M.G. Vegni, Anna Zaretti, and Paolo Zunino. *Invito alle equazioni a derivate parziali*. Springer, 2009.

[6] *COMSOL Multiphysics User's Guide*.

[7] Gilberto Rinaldi. *Materiali e combustibili nucleari*. Siderea, 2006.

Conclusion

Some final considerations.

By the first part of the work, described on the first chapter, two important aspects of the thermo-hydraulics modeling emerged.

The first one concerns the difference between a zero-dimensional formulation and a one-dimensional one outlined by the simulation performed. More precisely, on one hand the pressure distributions determined with the zero-dimensional model, not so consistent with the experimental data, demonstrate its scarce aptitude for describe all those physical phenomena, like the fluid-dynamics ones, in which the pressure and the velocity play a fundamental role. Although, on the other hand, its capability to reproduce the temperature distributions, practically overlapped with the ones determined with the one-dimensional model, makes it very suitable, in view also of its simplicity, to face problems in which on the contrary the quantities of interest are the energetic ones, like the thermodynamical ones.

The second one concerns the employing of *COMSOL Multiphysics* in the implementation and the simulation of both the models built up: that which the first part of the work underlined about it is, independently of all the considerations made on the multi-physics modeling and simulating, its qualify for solve with easiness and rapidity single sets of partial or ordinary differential equations.

Instead, the development of the neutronics and the thermo-hydraulics models for SURE and for MARS, described respectively on the second chapter and on the third one, remarks just the advantages that the modeling and the simulating of such physical systems can obtained if a multi-physics approach and, consequently, code as this one is used.

The fairness of the results obtained is indicative of such a feature: indeed, even if no experimental data were available neither on SURE neither on MARS, their simulated responses to different kinds of perturbations are physically coherent both in a zero power condition and in a normal operating one. To note moreover that, whereas the consistency demonstrated in a zero-power condition is due only to well-chosen values of the reactivity feedback coefficients, the reason of the fairness reached in the one-dimensional formulation has to be search in the procedure, widely described on the third chapter, used to determine the core macroscopic cross section trend with the fuel temperature and the coolant one.

Future developments of the present work can be so imagined. A possible one, based only on the one-dimensional thermo-hydraulics model developed, could be the modeling of the natural circulation taking place in closed channels a first section of which is heated and a second section of which is cooled: indeed, such an issue is of great importance in the study of the accidental situation that could happen in a core. Nevertheless, a one-dimensional model for BWRs could be realized by means of the one developed for MARS if a rigorous calculation of the macroscopic cross sections will be carried out.

Appendix A

The one-dimensional thermo-hydraulics model

Conservation equations

$$\frac{\partial}{\partial t}(\rho_m) + \frac{\partial}{\partial z}(g_m) = 0 \tag{A.1}$$

$$\frac{\partial}{\partial t}(g_m) + \frac{\partial}{\partial z}\left(\frac{g_m^2}{\rho_m^+}\right) = -a_g \sin\theta\, \rho_m - \frac{dp}{dz} - \left(\frac{\partial p}{\partial z}\right)_F \tag{A.2}$$

$$\frac{\partial}{\partial t}\left(\rho_m h_m - p\right) + \frac{\partial}{\partial z}\left(g_m h_m^+\right) = + \left(\frac{\partial p}{\partial z}\right)_F \frac{g_m}{\rho_m} + \left(\frac{\partial p}{\partial z}\right) \frac{g_m}{\rho_m} + q'' \frac{P_t}{A_h} \tag{A.3}$$

Constitutive equations

$$\rho_L = \begin{cases} \rho_L(p,h) & \text{if} \quad v_C \leq 0 \\ \rho_L(p) & \text{if} \quad 0 \leq v_C \leq 1 \end{cases} \tag{A.4}$$

$$\rho_V = \begin{cases} \rho_V(p) & \text{if} \quad 0 \leq v_C \leq 1 \\ \rho_V(p,h) & \text{if} \quad v_C \geq 1 \end{cases} \tag{A.5}$$

$$h_L = h_L(p) \quad \text{if} \quad 0 \leq v_C \leq 1 \tag{A.6}$$

$$h_V = h_V(p) \quad \text{if} \quad 0 \leq v_C \leq 1 \tag{A.7}$$

$$\mu_L = \begin{cases} \mu_L(p,h) & \text{if} \quad v_C \leq 0 \\ \mu_L(p) & \text{if} \quad 0 \leq v_C \leq 1 \end{cases} \tag{A.8}$$

$$\mu_V = \begin{cases} \mu_V(p) & \text{if} \quad 0 \le v_C \le 1 \\ \mu_V(p,h) & \text{if} \quad v_C \ge 1 \end{cases} \tag{A.9}$$

$$s = s(p) \quad \text{if} \quad 0 \le v_C \le 1 \tag{A.10}$$

Closure equations

$$\rho_m = \begin{cases} \rho_m^+ = \rho_L & \text{if} \quad v_C \le 0 \\ \alpha\,\rho_L + (1-\alpha)\,\rho_V & \text{if} \quad 0 \le v_C \le 1 \\ \rho_m^+ = \rho_V & \text{if} \quad v_C \ge 1 \end{cases} \tag{A.11}$$

$$\rho_m^+ = \begin{cases} \rho_m = \rho_L & \text{if} \quad v_C \le 0 \\ \left[\dfrac{x^2}{\alpha\,\rho_V} + \dfrac{(1-x)^2}{(1-\alpha)\,\rho_L}\right]^{-1} & \text{if} \quad 0 \le v_C \le 1 \\ \rho_m = \rho_V & \text{if} \quad v_C \ge 1 \end{cases} \tag{A.12}$$

$$h_m = \begin{cases} h_m^+ = h_L & \text{if} \quad v_C \le 0 \\ \dfrac{\alpha\,\rho_V\,h_L + (1-\alpha)\,\rho_L\,h_L}{\rho_m} & \text{if} \quad 0 \le v_C \le 1 \\ h_m^+ = h_V & \text{if} \quad v_C \ge 1 \end{cases} \tag{A.13}$$

$$-\left(\frac{\partial p}{\partial z}\right)_F = \begin{cases} -\left(\dfrac{\partial p}{\partial z}\right)_F^L = -\dfrac{f_M^L}{D_h}\,\dfrac{g_m^2}{2\,\rho_L} & \text{if} \quad v_C \le 0 \\ -\left(\dfrac{\partial p}{\partial z}\right)_F^{TP} = -\phi_{LO}^2\,\dfrac{f_M^{TP-LO}}{D_h}\,\dfrac{g_m^2}{2\,\rho_L} & \text{if} \quad 0 \le v_C \le 1 \\ -\left(\dfrac{\partial p}{\partial z}\right)_F^V = -\dfrac{f_M^V}{D_h}\,\dfrac{g_m^2}{2\,\rho_V} & \text{if} \quad v_C \ge 1 \end{cases} \tag{A.14}$$

$$f_M^L = f\,(Re_L) \tag{A.15}$$

$$f_M^{TP-LO} = f\,(Re_{TP-LO}) \tag{A.16}$$

$$f_M^V = f\,(Re_V) \tag{A.17}$$

$$Re_L = \frac{g_m\,D_h}{A_h\,\mu_L} \tag{A.18}$$

$$Re_{TP-LO} = \frac{g_m\,D_h}{A_h\,\mu_L} \tag{A.19}$$

$$Re_V = \frac{g_m\,D_h}{A_h\,\mu_V} \tag{A.20}$$

$$\phi_{LO}^2 = f\,(thermo - hydraulics\,properties) \tag{A.21}$$

$$\alpha = \begin{cases} 0 & \text{if} \quad v_C \leq 0 \\ \left[1 + \dfrac{1-x}{x}\,\dfrac{\rho_V}{\rho_L}\,S\right]^{-1} & \text{if} \quad 0 \leq v_C \leq 1 \\ 1 & \text{if} \quad v_C \geq 1 \end{cases} \tag{A.22}$$

$$\beta = \begin{cases} 0 & \text{if} \quad v_C \leq 0 \\ \left[1 + \dfrac{1-x}{x}\,\dfrac{\rho_V}{\rho_L}\right]^{-1} & \text{if} \quad 0 \leq v_C \leq 1 \\ 1 & \text{if} \quad v_C \geq 1 \end{cases} \tag{A.23}$$

$$x = \begin{cases} 0 & \text{if} \quad v_C \leq 0 \\ \dfrac{h_m^+ - h_L}{h_V - h_L} & \text{if} \quad 0 \leq v_C \leq 1 \\ 1 & \text{if} \quad v_C \geq 1 \end{cases} \tag{A.24}$$

$$S = C_0 + \frac{(C_0 - 1)\,x\,\rho_L}{(1-x)\,\rho_V} \tag{A.25}$$

$$C_0 = \beta\,\left[1 + \left(\frac{1}{\beta} - 1\right)^B\right] \tag{A.26}$$

$$B = \left(\frac{\rho_V}{\rho_L}\right)^{0.1} \tag{A.27}$$

Initial conditions

$$p(z,0) = p_{in} \tag{A.28}$$

$$g_m(z,0) = g_{m_{in}} \tag{A.29}$$

$$h_m^+(z,0) = h_{in} \tag{A.30}$$

Boundary conditions

$$p(0,t) = p_{in} \tag{A.31}$$

$$g_m(0,t) = g_{m_{in}} \tag{A.32}$$

$$h_m^+(0,t) = h_{in} \tag{A.33}$$

$$\Gamma_1(L,t) = -g_m(L,t) \tag{A.34}$$

$$\Gamma_2(L,t) = -\frac{g_m^2(L,t)}{\rho_m^+(L,t)} \tag{A.35}$$

$$\Gamma_3(L,t) = -g_m(L,t)\,h_m^+(L,t) \tag{A.36}$$

Appendix B

The zero-dimensional thermo-hydraulics model

Conservation equations for the subcooled region

$$\frac{d}{dt}\left(\langle\rho\rangle_1\ A_h\, L_1\right) = G_{in} + \rho_{12}\, A_h\, \frac{dL_1}{dt} - G_{12} \tag{B.1}$$

$$\begin{aligned}\frac{d}{dt}\left(\langle G\rangle_1\ L_1\right) = \frac{G_{in}^2}{\rho_{in}\, A_h} + G_{12}\, \frac{dL_1}{dt} - \frac{G_{12}^2}{\rho_{12}\, A_h} + p_{in}\, A_h - p_{12}\, A_h + \\ -a_g\ \langle\rho\rangle_1\ A_h\, L_1 - \frac{f_{M_1}}{2\, D_h} \left\langle \frac{G^2}{\rho\, A_h} \right\rangle_1 L_1\end{aligned} \tag{B.2}$$

$$\begin{aligned}\frac{d}{dt}\left(\langle\rho\, h\rangle_1\ A_h\, L_1 - \langle p\rangle_1\ A_h\, L_1\right) = G_{in}\, h_{in} + \rho_{12}\, u_{12}\, A_h\, \frac{dL_1}{dt} \\ -G_{12}\, h_{12} + q^{''}\, P_t\, L_1\end{aligned} \tag{B.3}$$

Conservation equations for the saturated region

$$\frac{d}{dt}\left(\langle\rho\rangle_2\ A_h\, L_2\right) = G_{12} - \rho_{12}\, A_h\, \frac{dL_1}{dt} - G_{23} + \rho_{23}\, A_h\, \frac{d\left(L_1 + L_2\right)}{dt} \tag{B.4}$$

$$\begin{aligned}\frac{d}{dt}\left(\langle G\rangle_2\ L_2\right) = \frac{G_{12}^2}{\rho_{12}\, A_h} - G_{12}\, \frac{dL_1}{dt} - \frac{G_{23}^2}{\rho_{23}\, A_h} + G_{23}\, \frac{d\left(L_1 + L_2\right)}{dt} + p_{12}\, A_h + \\ -p_{23}\, A_h - a_g\ \langle\rho\rangle_2\ A_h\, L_2 - \phi_{LO_2}\, \frac{f_{M_2}}{2\, D_h} \left\langle \frac{G^2}{\rho_L\, A_h} \right\rangle_2 L_2\end{aligned} \tag{B.5}$$

$$\begin{aligned}\frac{d}{dt}\left(\langle\rho\, h\rangle_2\ A_h\, L_2 - \langle p\rangle_2\ A_h\, L_2\right) = G_{12}\, h_{12} - \rho_{12}\, u_{12}\, A_h\, \frac{dL_1}{dt} + \\ +\rho_{23}\, u_{23}\, A_h\, \frac{d\left(L_1 + L_2\right)}{dt} - G_{23}\, h_{23} + q^{''}\, P_t\, L_2\end{aligned} \tag{B.6}$$

Conservation equations for the superheated region

$$\frac{d}{dt}\left(\langle\rho_3\rangle\ A_h\, L_3\right) = G_{23} - \rho_{23}\, A_h\, \frac{d\left(L_1 + L_2\right)}{dt} - G_{out} \tag{B.7}$$

$$\begin{aligned}\frac{d}{dt}\left(\langle G_3\rangle\ L_3\right) = \frac{G_{23}^2}{\rho_{23}\, A_h} - G_{23}\, \frac{d\left(L_1 + L_2\right)}{dt} - \frac{G_{out}^2}{\rho_{out}\, A_h} + p_{23}\, A_h - p_{out}\, A_h \\ -a_g\ \langle\rho\rangle_3\ A_h\, L_3 - \frac{f_{M_3}}{2\, D_h}\left\langle \frac{G^2}{\rho\, A_h}\right\rangle_3 L_3\end{aligned} \tag{B.8}$$

$$\begin{aligned}\frac{d}{dt}\left(\langle\rho\, h\rangle_3\ A_h\, L_3 - \langle p\rangle_3\ A_h\, L_3\right) = G_{23}\, h_{23} - \rho_{23}\, u_{23}\, A_h\, \frac{d\left(L_1 + L_2\right)}{dt} + \\ -G_{out}\, h_{out} + q^{''}\, P_t\, L_3\end{aligned} \tag{B.9}$$

Constitutive equations for the subcooled region

$$\rho_{12} = \rho_L(p_{12}) \tag{B.10}$$

$$h_{12} = h_L(p_{12}) \tag{B.11}$$

$$u_{12} = u_L(p_{12}) \tag{B.12}$$

$$\mu_{12} = \mu_L(p_{12}) \tag{B.13}$$

Constitutive equations for the saturated region

$$\rho_{23} = \rho_V(p_{23}) \tag{B.14}$$

$$h_{23} = h_V(p_{23}) \tag{B.15}$$

$$u_{23} = u_V(p_{23}) \tag{B.16}$$

$$\mu_{23} = \mu_V(p_{23}) \tag{B.17}$$

$$\rho_{LO} = \rho_L(p_{23}) \tag{B.18}$$

$$\mu_{LO} = \mu_L(p_{23}) \tag{B.19}$$

Constitutive equations for the superheated region

$$\rho_{out} = \rho(p_{out}, h_{out}) \tag{B.20}$$

$$\mu_{out} = \mu(p_{out}, h_{out}) \tag{B.21}$$

Closure equations for the subcooled region

$$\langle \rho \rangle_1 = \frac{\rho_{in} + \rho_{12}}{2} \tag{B.22}$$

$$\langle G \rangle_1 = \frac{G_{in} + G_{12}}{2} \tag{B.23}$$

$$\left\langle \frac{G^2}{\rho\, A_h} \right\rangle_1 = \frac{\dfrac{G_{in}^2}{\rho_{in}\, A_h} + \dfrac{G_{12}^2}{\rho_{12}\, A_h}}{2} \tag{B.24}$$

$$\langle \mu \rangle_1 = \frac{\mu_{in} + \mu_{12}}{2} \tag{B.25}$$

$$\langle \rho\, h \rangle_1 = \frac{(\rho\, h)_{in} + (\rho\, h)_{12}}{2} \tag{B.26}$$

$$\langle p \rangle_1 = \frac{p_{in} + p_{12}}{2} \tag{B.27}$$

$$f_{M_1} = f\left(Re_1\right) \tag{B.28}$$

$$Re_1 = \frac{\langle G \rangle_1\, D_h}{A_h\, \langle \mu \rangle_1} \tag{B.29}$$

Closure equations for the saturated region

$$\langle \rho \rangle_2 = \frac{\rho_{12} + \rho_{23}}{2} \tag{B.30}$$

$$\langle G \rangle_2 = \frac{G_{12} + G_{23}}{2} \tag{B.31}$$

$$\left\langle \frac{G^2}{\rho\, A_h} \right\rangle_2 = \frac{\dfrac{G_{12}^2}{\rho_{12}\, A_h} + \dfrac{G_{23}^2}{\rho_{LO}\, A_h}}{2} \tag{B.32}$$

$$\langle \mu \rangle_2 = \frac{\mu_{12} + \mu_{LO}}{2} \tag{B.33}$$

$$\langle \rho\, h \rangle_2 = \frac{(\rho\, h)_{12} + (\rho\, h)_{23}}{2} \tag{B.34}$$

$$\langle p \rangle_2 = \frac{p_{12} + p_{23}}{2} \tag{B.35}$$

$$f_{M_2} = f\left(Re_2\right) \tag{B.36}$$

$$Re_2 = \frac{\langle G \rangle_2\, D_h}{A_h\, \langle \mu \rangle_2} \tag{B.37}$$

$$\phi_{LO_2} = f\left(thermo - hydraulics\, properties\right) \tag{B.38}$$

Closure equations for the superheated region

$$\langle \rho \rangle_3 = \frac{\rho_{23} + \rho_{out}}{2} \tag{B.39}$$

$$\langle G \rangle_3 = \frac{G_{23} + G_{out}}{2} \tag{B.40}$$

$$\left\langle \frac{G^2}{\rho\, A_h} \right\rangle_3 = \frac{\dfrac{G_{23}^2}{\rho_{23}\, A_h} + \dfrac{G_{out}^2}{\rho_{out}\, A_h}}{2} \tag{B.41}$$

$$\langle \mu \rangle_3 = \frac{\mu_{23} + \mu_{out}}{2} \tag{B.42}$$

$$\langle \rho\, h \rangle_3 = \frac{(\rho\, h)_{23} + (\rho\, h)_{out}}{2} \tag{B.43}$$

$$\langle p \rangle_3 = \frac{p_{23} + p_{out}}{2} \tag{B.44}$$

$$f_{M_3} = f\left(Re_3\right) \tag{B.45}$$

$$Re_3 = \frac{\langle G \rangle_3\, D_h}{A_h\, \langle \mu \rangle_3} \tag{B.46}$$

Bond conditions

$$L = L_1 + L_2 + L_3 \tag{B.47}$$

Initial conditions

$$G_{12}\left(0\right) = G_{12_0} \tag{B.48}$$

$$G_{23}\left(0\right) = G_{23_0} \tag{B.49}$$

$$G_{out}\left(0\right) = G_{out_0} \tag{B.50}$$

$$p_{12}\left(0\right) = p_{12_0} \tag{B.51}$$

$$p_{23}\left(0\right) = p_{23_0} \tag{B.52}$$

$$p_{out}\left(0\right) = p_{out_0} \tag{B.53}$$

$$L_1\left(0\right) = L_{1_0} \tag{B.54}$$

$$L_2\left(0\right) = L_{1_0} \tag{B.55}$$

$$h_{out}\left(0\right) = h_{out_0} \tag{B.56}$$

Appendix C

The zero-dimensional neutronics model

Core neutron balance equation

$$\frac{dn_C}{dt} = \frac{\varrho - b - f(1-b)}{f}\,\frac{n_C}{\Lambda_C} + f_{RC}\,\frac{1-\varrho}{1-f}\,\frac{n_R}{\Lambda_R} + \sum_{i=1}^{N} \lambda_i c_i \tag{C.1}$$

Reflector neutron balance equation

$$\frac{dn_R}{dt} = f_{CR}\,\frac{1-\varrho}{1-f}\,\frac{n_C}{\Lambda_C} - \frac{1-\varrho}{1-f}\,\frac{n_R}{\Lambda_R} \tag{C.2}$$

Core precursor balance equation

$$\frac{dc_i}{dt} = b_i\,\Lambda_C\,n_C - \lambda_i\,c_i \qquad i = 1, 2, ..., N_i \tag{C.3}$$

Initial conditions

$$n_C\,(0) = n_{C_0} \tag{C.4}$$

$$n_R\,(0) = \frac{1}{f_{CR}\,\Lambda_C\,\Lambda_R}\,n_{C_0} \tag{C.5}$$

$$c_i\,(0) = \frac{b_i\,\Lambda_C}{\lambda_i}\,n_{C_0} \qquad i = 1, 2, ..., N_i \tag{C.6}$$

Appendix D

The zero-dimensional neutronics and thermo-hydraulics model

Neutronics equations

$$\frac{dn_C}{dt} = \frac{\varrho - b - f(1-b)}{f}\,\frac{n_C}{\Lambda_C} + f_{RC}\,\frac{1-\varrho}{1-f}\,\frac{n_R}{\Lambda_R} + \sum_{i=1}^{N}\lambda_i c_i \tag{D.1}$$

$$\frac{dn_R}{dt} = f_{CR}\,\frac{1-\varrho}{1-f}\,\frac{n_C}{\Lambda_C} - \frac{1-\varrho}{1-f}\,\frac{n_R}{\Lambda_R} \tag{D.2}$$

$$\frac{dc_i}{dt} = b_i\,\Lambda_C\,n_C - \lambda_i\,c_i \qquad i = 1, 2, ..., N_i \tag{D.3}$$

$$n_C\,(0) = n_{C_0} \tag{D.4}$$

$$n_R\,(0) = \frac{1}{f_{CR}\,\Lambda_C\,\Lambda_R}\,n_{C_0} \tag{D.5}$$

$$c_i\,(0) = \frac{b_i\,\Lambda_C}{\lambda_i}\,n_{C_0} \qquad i = 1, 2, ..., N_i \tag{D.6}$$

Thermo-hydraulics equations

$$\frac{d}{dt}\left(\langle\rho\rangle_1\;A_h\,L_1\right) = G_{in} + \rho_{12}\,A_h\,\frac{dL_1}{dt} - G_{12} \tag{D.7}$$

$$\begin{aligned}\frac{d}{dt}\left(\langle G\rangle_1\;L_1\right) = {} & \frac{G_{in}^2}{\rho_{in}\,A_h} + G_{12}\,\frac{dL_1}{dt} - \frac{G_{12}^2}{\rho_{12}\,A_h} + p_{in}\,A_h - p_{12}\,A_h \\ & -a_g\;\langle\rho\rangle_1\;A_h\,L_1 - \frac{f_{M_1}}{2\,D_h}\left\langle\frac{G^2}{\rho\,A_h}\right\rangle_1 L_1\end{aligned} \tag{D.8}$$

$$\frac{d}{dt}\left(\langle\rho\,h\rangle_1\ A_h\,L_1 - \langle p\rangle_1\ A_h\,L_1\right) = G_{in}\,h_{in} + \rho_{12}\,u_{12}\,A_h\,\frac{dL_1}{dt} + \\ -G_{12}\,h_{12} + U\left(T_{fuel} - T_{cool}\right)P_t\,L_1 \tag{D.9}$$

$$\rho_{12} = \rho_L(p_{12}) \tag{D.10}$$

$$h_{12} = h_L(p_{12}) \tag{D.11}$$

$$u_{12} = u_L(p_{12}) \tag{D.12}$$

$$\mu_{12} = \mu_L(p_{12}) \tag{D.13}$$

$$\langle\rho\rangle_1 = \frac{\rho_{in} + \rho_{12}}{2} \tag{D.14}$$

$$\langle G\rangle_1 = \frac{G_{in} + G_{12}}{2} \tag{D.15}$$

$$\left\langle \frac{G^2}{\rho\,A_h} \right\rangle_1 = \frac{\dfrac{G_{in}^2}{\rho_{in}\,A_h} + \dfrac{G_{12}^2}{\rho_{12}\,A_h}}{2} \tag{D.16}$$

$$\langle\mu\rangle_1 = \frac{\mu_{in} + \mu_{12}}{2} \tag{D.17}$$

$$\langle\rho\,h\rangle_1 = \frac{(\rho\,h)_{in} + (\rho\,h)_{12}}{2} \tag{D.18}$$

$$\langle p\rangle_1 = \frac{p_{in} + p_{12}}{2} \tag{D.19}$$

$$f_{M_1} = f\left(Re_1\right) \tag{D.20}$$

$$Re_1 = \frac{\langle G\rangle_1\ D_h}{A_h\ \langle\mu\rangle_1} \tag{D.21}$$

$$\frac{d}{dt}\left(\langle\rho\rangle_2\ A_h\,L_2\right) = G_{12} - \rho_{12}\,A_h\,\frac{dL_1}{dt} - G_{23} + \rho_{23}A_h\frac{d\left(L_1 + L_2\right)}{dt} \tag{D.22}$$

$$\frac{d}{dt}\left(\langle G\rangle_2\ L_2\right) = \frac{G_{12}^2}{\rho_{12}\,A_h} - G_{12}\,\frac{dL_1}{dt} - \frac{G_{23}^2}{\rho_{23}\,A_h} + G_{23}\,\frac{d\left(L_1 + L_2\right)}{dt} + p_{12}\,A_h + -p_{23}\,A_h - a_g\,\rho_2\,A_h\,L_2 - \tag{D.23}$$

$$\frac{d}{dt}\left(\langle\rho\,h\rangle_2\ A_h\,L_2 - \langle p\rangle_2\ A_h\,L_2\right) = G_{12}\,h_{12} - \rho_{12}\,u_{12}\,A_h\,\frac{dL_1}{dt} + \\ +\rho_{23}\,u_{23}\,A_h\,\frac{d\left(L_1 + L_2\right)}{dt} - G_{23}\,h_{23} + U\left(T_{fuel} - T_{cool}\right)P_t\,L_2 \tag{D.24}$$

$$\rho_{L_{out}} = \rho_L(p_{out}) \tag{D.25}$$

$$\rho_{V_{out}} = \rho_V(p_{out}) \tag{D.26}$$

$$h_{L_{out}} = h_L(p_{out}) \tag{D.27}$$

$$h_{V_{out}} = h_V(p_{out}) \tag{D.28}$$

$$\mu_{L_{out}} = \mu_L(p_{out}) \tag{D.29}$$

$$\langle \rho \rangle_2 = \frac{\rho_{12} + \rho_{out}}{2} \tag{D.30}$$

$$\langle G \rangle_2 = \frac{G_{12} + G_{out}}{2} \tag{D.31}$$

$$\left\langle \frac{G^2}{\rho\, A_h} \right\rangle_2 = \frac{\dfrac{G_{12}^2}{\rho_{12}\, A_h} + \dfrac{G_{out}^2}{\rho_{out}\, A_h}}{2} \tag{D.32}$$

$$\langle \mu \rangle_2 = \frac{\mu_{12} + \mu_{out}}{2} \tag{D.33}$$

$$\langle \rho\, h \rangle_2 = \frac{(\rho\, h)_{12} + (\rho\, h)_{out}}{2} \tag{D.34}$$

$$\langle p \rangle_2 = \frac{p_{12} + p_{out}}{2} \tag{D.35}$$

$$f_{M_2} = f\left(Re_2\right) \tag{D.36}$$

$$Re_2 = \frac{\langle G \rangle_2\, D_h}{A_h\, \langle \mu \rangle_2} \tag{D.37}$$

$$\phi_{LO_2} = f\left(thermo - hydraulics\, properties\right) \tag{D.38}$$

$$\rho_{out} = \rho_{L_{out}}\left(1 - \alpha_{out}\right) + \rho_{V_{out}}\, \alpha_{out} \tag{D.39}$$

$$h_{out} = h_{L_{out}}\left(1 - x_{out}\right) + h_{V_{out}}\, x_{out} \tag{D.40}$$

$$\alpha_{out} = \frac{1}{1 + \dfrac{1 - x_{out}}{x_{out}}\, \dfrac{\rho_{V_{out}}}{\rho_{L_{out}}}\, S_{out}} \tag{D.41}$$

$$\beta_{out} = \frac{1}{1 + \dfrac{1 - x_{out}}{x_{out}}\, \dfrac{\rho_{V_{out}}}{\rho_{L_{out}}}} \tag{D.42}$$

$$S_{out} = C_{0_{out}} + \frac{\left(C_{0_{out}} - 1\right) x_{out}\, \rho_{L_{out}}}{\left(1 - x_{out}\right) \rho_{V_{out}}} \tag{D.43}$$

$$C_{0_{out}} = B_{out}\left[1 + \left(\frac{1}{\beta_{out}} - 1\right)^{B_{out}}\right] \tag{D.44}$$

$$B_{out} = \left(\frac{\rho_{V_{out}}}{\rho_{L_{out}}}\right)^{0.1} \tag{D.45}$$

$$\frac{d}{dt}(m_{fuel}\, \chi_{fuel}\, T_{fuel}) = q'''\, m_{fuel}\, \rho_{fuel} - U\left(T_{fuel} - T_{cool}\right) A_t \tag{D.46}$$

$$\rho_{cool_{nom}} = \frac{\langle \rho \rangle_1\, L_1 + \langle \rho \rangle_2\, L_2}{L_1 + L_2} \tag{D.47}$$

$$T_{cool} = \frac{\langle T \rangle_1\, L_1 + \langle T \rangle_2\, L_2}{L_1 + L_2} \tag{D.48}$$

$$G_{12}\left(0\right) = G_{12_0} \tag{D.49}$$

$$G_{out}(0) = G_{out_0} \tag{D.50}$$

$$p_{12}(0) = p_{12_0} \tag{D.51}$$

$$p_{out}(0) = p_{out_0} \tag{D.52}$$

$$L_1(0) = L_{1_0} \tag{D.53}$$

$$x_{out}(0) = x_{out_0} \tag{D.54}$$

$$T_{fuel}(0) = T_{fuel_0} \tag{D.55}$$

Coupling equations between neutronics and thermo-hydraulics

$$\varrho = \alpha_{\varrho_{T_{fuel}}}(T_{fuel} - T_{fuel_{nom}}) - \alpha_{\varrho_{\rho_{cool}}}(\rho_{cool} - \rho_{cool_{nom}}) \tag{D.56}$$

$$q''' = n_C\, v_n\, \sigma_{U_{235}}\, N_{U_{235}}\, E_{U_{235}} \tag{D.57}$$

Appendix E

The one-dimensional neutronics model

Fast neutron balance equation in the core

$$\frac{1}{v_1}\frac{\partial \Phi_1}{\partial t} + \frac{\partial}{\partial z}\left(-\mathcal{D}_{C1}\frac{\partial \Phi_1}{\partial z}\right) = \left[-\mathcal{D}_{C1}\,B^2 - \Sigma_{C1a} - \Sigma_{Ct} + (\nu\,\Sigma_f)_{C1}\right]\,\Phi_1 + \left[+\,(\nu\,\Sigma_f)_{C2}\,(1-b_2)\right]\,\Phi_2 + \textstyle\sum_{i=1}^{N}\lambda_i\,c_i \tag{E.1}$$

Fast neutron balance equation in the reflector

$$\frac{1}{v_1}\frac{\partial \Phi_1}{\partial t} + \frac{\partial}{\partial z}\left(-\mathcal{D}_{R1}\frac{\partial \Phi_1}{\partial z}\right) = \left(-\mathcal{D}_{R1}\,B^2 - \Sigma_{R1a} - \Sigma_{Rt}\right)\,\Phi_1 \tag{E.2}$$

Thermal neutron balance equation in the core

$$\frac{1}{v_2}\frac{\partial \Phi_2}{\partial t} + \frac{\partial}{\partial z}\left(-\mathcal{D}_{C2}\frac{\partial \Phi_2}{\partial z}\right) = (+\Sigma_{Ct})\,\Phi_1 + \left(-\mathcal{D}_{C2}\,B^2 - \Sigma_{C2a}\right)\,\Phi_2 \tag{E.3}$$

Thermal neutron balance equation in the reflector

$$\frac{1}{v_2}\frac{\partial \Phi_2}{\partial t} + \frac{\partial}{\partial z}\left(-\mathcal{D}_{R2}\frac{\partial \Phi_2}{\partial z}\right) = (+\Sigma_{Rt})\,\Phi_1 + \left(-\mathcal{D}_{R2}\,B^2 - \Sigma_{R2a}\right)\,\Phi_2 \tag{E.4}$$

Precursor balance equation in the core

$$\frac{\partial c_i}{\partial t} = (\nu\,\Sigma_f)_{C2}\;b_i\,\Phi_2 - \lambda_i\,c_i \qquad i = 1, 2, ..., N_i \tag{E.5}$$

Initial conditions

$$\Phi_1(z, t=0) = \Phi_{1_0}(z) \tag{E.6}$$

$$\Phi_2(z, t=0) = \Phi_{2_0}(z) \tag{E.7}$$

$$c_{i_0} = \frac{(\nu \Sigma_f)_{C1}\,(1-b_i)}{\lambda_i}\,\Phi_{1_0} \qquad i = 1, 2, ..., N_i \tag{E.8}$$

Boundary conditions

$$\Phi_1(0, t) = 0 \tag{E.9}$$

$$\Phi_1(L_{R_{down}} + L_C + L_{R_{up}}, t) = 0 \tag{E.10}$$

$$\Phi_2(0, t) = 0 \tag{E.11}$$

$$\Phi_2(L_{R_{down}} + L_C + L_{R_{up}}, t) = 0 \tag{E.12}$$

$$-\mathcal{D}_{R1}\ \frac{\partial \Phi_1(L_{R_{down}}, t)}{\partial z}\bigg|_R = -\mathcal{D}_{C1}\ \frac{\partial \Phi_1(L_{R_{down}}, t)}{\partial z}\bigg|_C \tag{E.13}$$

$$-\mathcal{D}_{C1}\ \frac{\partial \Phi_1(L_{R_{down}} + L_C, t)}{\partial z}\bigg|_R = -\mathcal{D}_{R1}\ \frac{\partial \Phi_1(L_{R_{down}} + L_C, t)}{\partial z}\bigg|_C \tag{E.14}$$

$$-\mathcal{D}_{R2}\ \frac{\partial \Phi_2(L_{R_{down}}, t)}{\partial z}\bigg|_R = -\mathcal{D}_{C2}\ \frac{\partial \Phi_2(L_{R_{down}}, t)}{\partial z}\bigg|_C \tag{E.15}$$

$$-\mathcal{D}_{C2}\ \frac{\partial \Phi_2(L_{R_{down}} + L_C, t)}{\partial z}\bigg|_R = -\mathcal{D}_{R2}\ \frac{\partial \Phi_2(L_{R_{down}} + L_C, t)}{\partial z}\bigg|_C \tag{E.16}$$

$$c_i(L_{R_{down}}, t) = 0 \qquad i = 1, 2, ..., N_i \tag{E.17}$$

$$c_i(L_{R_{down}} + L_C, t) = 0 \tag{E.18}$$

Appendix F

The one-dimensional neutronics and thermo-hydraulics model

Neutronics equations

$$\frac{1}{v_1}\frac{\partial \Phi_1}{\partial t}+\frac{\partial}{\partial z}\left(-\mathcal{D}_{C1}\frac{\partial \Phi_1}{\partial z}\right)=\left[-\mathcal{D}_{C1}B^2-\Sigma_{C1a}-\Sigma_{Ct}+(\nu\Sigma_f)_{C1}\right]\Phi_1 + \left[+(\nu\Sigma_f)_{C2}(1-b_2)\right]\Phi_2+\sum_{i=1}^{N}\lambda_i c_i \tag{F.1}$$

$$\frac{1}{v_1}\frac{\partial \Phi_1}{\partial t}+\frac{\partial}{\partial z}\left(-\mathcal{D}_{R1}\frac{\partial \Phi_1}{\partial z}\right)=\left(-\mathcal{D}_{R1}B^2-\Sigma_{R1a}-\Sigma_{Rt}\right)\Phi_1 \tag{F.2}$$

$$\frac{1}{v_2}\frac{\partial \Phi_2}{\partial t}+\frac{\partial}{\partial z}\left(-\mathcal{D}_{C2}\frac{\partial \Phi_2}{\partial z}\right)=(+\Sigma_{Ct})\Phi_1+\left(-\mathcal{D}_{C2}B^2-\Sigma_{C2a}\right)\Phi_2 \tag{F.3}$$

$$\frac{1}{v_2}\frac{\partial \Phi_2}{\partial t}+\frac{\partial}{\partial z}\left(-\mathcal{D}_{R2}\frac{\partial \Phi_2}{\partial z}\right)=(+\Sigma_{Rt})\Phi_1+\left(-\mathcal{D}_{R2}B^2-\Sigma_{R2a}\right)\Phi_2 \tag{F.4}$$

$$\frac{\partial c_i}{\partial t}=(\nu\Sigma_f)_{C2}\,b_i\,\Phi_2-\lambda_i c_i \qquad i=1,2,...,N_i \tag{F.5}$$

$$\Phi_1(z,t=0)=\Phi_{1_0}(z) \tag{F.6}$$

$$\Phi_2(z,t=0)=\Phi_{2_0}(z) \tag{F.7}$$

$$c_{i_0}=\frac{(\nu\Sigma_f)_{C1}(1-b_i)}{\lambda_i}\Phi_{1_0} \qquad i=1,2,...,N_i \tag{F.8}$$

$$\Phi_1(0,t)=0 \tag{F.9}$$

$$\Phi_1(L_{R_{down}}+L_C+L_{R_{up}},t)=0 \tag{F.10}$$

$$\Phi_2(0,t)=0 \tag{F.11}$$

$$\Phi_2(L_{R_{down}} + L_C + L_{R_{up}}, t) = 0 \tag{F.12}$$

$$-\mathcal{D}_{R1} \left.\frac{\partial \Phi_1(L_{R_{down}}, t)}{\partial z}\right|_R = -\mathcal{D}_{C1} \left.\frac{\partial \Phi_1(L_{R_{down}}, t)}{\partial z}\right|_C \tag{F.13}$$

$$-\mathcal{D}_{C1} \left.\frac{\partial \Phi_1(L_{R_{down}} + L_C, t)}{\partial z}\right|_R = -\mathcal{D}_{R1} \left.\frac{\partial \Phi_1(L_{R_{down}} + L_C, t)}{\partial z}\right|_C \tag{F.14}$$

$$-\mathcal{D}_{R2} \left.\frac{\partial \Phi_2(L_{R_{down}}, t)}{\partial z}\right|_R = -\mathcal{D}_{C2} \left.\frac{\partial \Phi_2(L_{R_{down}}, t)}{\partial z}\right|_C \tag{F.15}$$

$$-\mathcal{D}_{C2} \left.\frac{\partial \Phi_2(L_{R_{down}} + L_C, t)}{\partial z}\right|_R = -\mathcal{D}_{R2} \left.\frac{\partial \Phi_2(L_{R_{down}} + L_C, t)}{\partial z}\right|_C \tag{F.16}$$

$$c_i(L_{R_{down}}, t) = 0 \qquad i = 1, 2, ..., N_i \tag{F.17}$$

$$c_i(L_{R_{down}} + L_C, t) = 0 \qquad i = 1, 2, ..., N_i \tag{F.18}$$

Thermo-hydraulics equations

$$\frac{\partial}{\partial t}(\rho_m) + \frac{\partial}{\partial z}(g_m) = 0 \tag{F.19}$$

$$\frac{\partial}{\partial t}(g_m) + \frac{\partial}{\partial z}\left(\frac{g_m^2}{\rho_m^+}\right) = -a_g \sin\theta\, \rho_m - \frac{dp}{dz} - \left(\frac{\partial p}{\partial z}\right)_F \tag{F.20}$$

$$\frac{\partial}{\partial t}\left(\rho_m h_m - p\right) + \frac{\partial}{\partial z}\left(g_m h_m^+\right) = + \left(\frac{\partial p}{\partial z}\right)_F \frac{g_m}{\rho_m} + \left(\frac{\partial p}{\partial z}\right) \frac{g_m}{\rho_m} + q'' \frac{P_t}{A_h} \tag{F.21}$$

$$T_{cool} = \begin{cases} T\,(p,h) & \text{if} \quad v_C \leq 0 \\ T\,(p) & \text{if} \quad 0 \leq v_C \leq 1 \\ T\,(p,h) & \text{if} \quad v_C \geq 1 \end{cases} \tag{F.22}$$

$$\rho_L = \begin{cases} \rho_L(p,h) & \text{if} \quad v_C \leq 0 \\ \rho_L(p) & \text{if} \quad 0 \leq v_C \leq 1 \end{cases} \tag{F.23}$$

$$\rho_V = \begin{cases} \rho_V(p) & \text{if} \quad 0 \leq v_C \leq 1 \\ \rho_V(p,h) & \text{if} \quad v_C \geq 1 \end{cases} \tag{F.24}$$

$$\mu_L = \begin{cases} \mu_L(p,h) & \text{if} \quad v_C \leq 0 \\ \mu_L(p) & \text{if} \quad 0 \leq v_C \leq 1 \end{cases} \tag{F.25}$$

$$\mu_V = \begin{cases} \mu_V(p) & \text{if} \quad 0 \leq v_C \geq 1 \\ \mu_V(p,h) & \text{if} \quad v_C \geq 1 \end{cases} \tag{F.26}$$

$$h_L = h_L(p) \quad \text{if} \quad 0 \leq v_C \leq 1 \tag{F.27}$$

$$h_V = h_V(p) \quad \text{if} \quad 0 \leq v_C \leq 1 \tag{F.28}$$

$$s = s(p) \quad \text{if} \quad 0 \leq v_C \leq 1 \tag{F.29}$$

$$\rho_m = \begin{cases} \rho_m^+ = \rho_L & \text{if} \quad v_C \leq 0 \\ \alpha\,\rho_L + (1-\alpha)\,\rho_V & \text{if} \quad 0 \leq v_C \leq 1 \\ \rho_m^+ = \rho_V & \text{if} \quad v_C \geq 1 \end{cases} \tag{F.30}$$

$$\rho_m^+ = \begin{cases} \rho_m = \rho_L & \text{if} \quad v_C \leq 0 \\ \left[\dfrac{x^2}{\alpha\,\rho_V} + \dfrac{(1-x)^2}{(1-\alpha)\,\rho_L}\right]^{-1} & \text{if} \quad 0 \leq v_C \leq 1 \\ \rho_m = \rho_V & \text{if} \quad v_C \geq 1 \end{cases} \tag{F.31}$$

$$h_m = \begin{cases} h_m^+ = h_L & \text{if} \quad v_C \leq 0 \\ \dfrac{\alpha\,\rho_V\,h_L + (1-\alpha)\,\rho_L\,h_L}{\rho_m} & \text{if} \quad 0 \leq v_C \leq 1 \\ h_m^+ = h_V & \text{if} \quad v_C \geq 1 \end{cases} \tag{F.32}$$

$$-\left(\frac{\partial p}{\partial z}\right)_F = \begin{cases} -\left(\dfrac{\partial p}{\partial z}\right)_F^L = -\dfrac{f_M^L}{D_h}\,\dfrac{g_m^2}{2\,\rho_L} & \text{if} \quad v_C \leq 0 \\ -\left(\dfrac{\partial p}{\partial z}\right)_F^{TP} = -\phi_{LO}^2\,\dfrac{f_M^{TP-LO}}{D_h}\,\dfrac{g_m^2}{2\,\rho_m^+} & \text{if} \quad 0 \leq v_C \leq 1 \\ -\left(\dfrac{\partial p}{\partial z}\right)_F^V = -\dfrac{f_M^V}{D_h}\,\dfrac{g_m^2}{2\,\rho_V} & \text{if} \quad v_C \geq 1 \end{cases} \tag{F.33}$$

$$f_M^L = f\left(Re_L\right) \tag{F.34}$$

$$f_M^{TP-LO} = f\left(Re_{TP-LO}\right) \tag{F.35}$$

$$f_M^V = f\left(Re_V\right) \tag{F.36}$$

$$Re_L = \frac{g_m\,D_h}{A_h\,\mu_L} \tag{F.37}$$

$$Re_{TP-LO} = \frac{g_m\,D_h}{A_h\,\mu_L} \tag{F.38}$$

$$Re_V = \frac{g_m\,D_h}{A_h\,\mu_V} \tag{F.39}$$

$$\phi_{LO}^2 = f\left(thermo - hydraulics\,properties\right) \tag{F.40}$$

$$\alpha = \begin{cases} 0 & \text{if} \quad v_C \leq 0 \\ \left[1 + \dfrac{1-x}{x}\,\dfrac{\rho_V}{\rho_L}\,S\right]^{-1} & \text{if} \quad 0 \leq v_C \leq 1 \\ 1 & \text{if} \quad v_C \geq 1 \end{cases} \tag{F.41}$$

$$\beta = \begin{cases} 0 & \text{if} \quad v_C \leq 0 \\ \left[1 + \dfrac{1-x}{x}\,\dfrac{\rho_V}{\rho_L}\right]^{-1} & \text{if} \quad 0 \leq v_C \leq 1 \\ 1 & \text{if} \quad v_C \geq 1 \end{cases} \tag{F.42}$$

$$x = \begin{cases} 0 & \text{if} \quad v_C \leq 0 \\ \dfrac{h_m^+ - h_L}{h_V - h_L} & \text{if} \quad 0 \leq v_C \leq 1 \\ 1 & \text{if} \quad v_C \geq 1 \end{cases} \tag{F.43}$$

$$S = C_0 + \frac{(C_0 - 1)\, x\, \rho_L}{(1-x)\, \rho_V} \tag{F.44}$$

$$C_0 = \beta \left[1 + \left(\frac{1}{\beta} - 1\right)^B\right] \tag{F.45}$$

$$B = \left(\frac{\rho_V}{\rho_L}\right)^{0.1} \tag{F.46}$$

all valid both for the reflector domains and for the core domain if the following condition is imposed:

$$q^{''} = \begin{cases} 0 & \text{if} \quad 0 \leq z \leq L_{R_{down}} \\ U\ (T_{fuel} - T_{cool}) & \text{if} \quad L_{R_{down}} \leq z \leq L_{R_{down}} + L_C \\ 0 & \text{if} \quad L_{R_{down}} + L_C \leq z \leq L_{R_{down}} + L_C + L_{R_{up}} \end{cases} \tag{F.47}$$

$$p(z,0) = p_{in} \tag{F.48}$$

$$g_m(z,0) = g_{m_{in}} \tag{F.49}$$

$$h_m^+(z,0) = h_{in} \tag{F.50}$$

$$T_{fuel}\,(z,0) = T_{fuel_0}\,(z) \tag{F.51}$$

$$p(0,t)|_R = p_{in} \tag{F.52}$$

$$g_m(0,t)|_R = g_{m_{in}} \tag{F.53}$$

$$h(0,t)|_R = h_{in} \tag{F.54}$$

$$g_m(L_{R_{down}},t)|_R = g_m(L_{R_{down}},t)|_C \tag{F.55}$$

$$\left.\frac{g_m^2(L_{R_{down}},t)}{\rho_m^+(L_{R_{down}},t)}\right|_R = \left.\frac{g_m^2(L_{R_{down}},t)}{\rho_m^+(L_{R_{down}},t)}\right|_C \tag{F.56}$$

$$g_m(L_{R_{down}},t)\, h_m(L_{R_{down}},t)|_R = g_m(L_{R_{down}},t)\, h_m(L_{R_{down}},t)|_C \tag{F.57}$$

$$g_m(L_{R_{down}} + L_C, t)\big|_R = g_m(L_{R_{down}} + L_C, t)\big|_C \tag{F.58}$$

$$\left.\frac{g_m^2(L_{R_{down}} + L_C, t)}{\rho_m^+(L_{R_{down}} + L_C, t)}\right|_R = \left.\frac{g_m^2(L_{R_{down}} + L_C, t)}{\rho_m^+(L_{R_{down}} + L_C, t)}\right|_C \tag{F.59}$$

$$\begin{aligned} &g_m(L_{R_{down}} + L_C, t)\, h_m(L_{R_{down}} + L_C, t)\big|_R = \\ &= g_m(L_{R_{down}} + L_C, t)\, h_m(L_{R_{down}} + L_C, t)\big|_C \end{aligned} \tag{F.60}$$

$$\Gamma_1(L_{R_{down}} + L_C + L_{R_{up}}, t)\big|_R = -g_m(L_{R_{down}} + L_C + L_{R_{up}}, t)\big|_R \tag{F.61}$$

$$\Gamma_2(L_{R_{down}} + L_C + L_{R_{up}}, t)\big|_R = -\left.\frac{g_m^2(L_{R_{down}} + L_C + L_{R_{up}}, t)}{\rho_m^+(L_{R_{down}} + L_C + L_{R_{up}}, t)}\right|_R \tag{F.62}$$

$$\begin{aligned} &\Gamma_3(L_{R_{down}} + L_C + L_{R_{up}}, t)\big|_R = \\ &= - g_m(L_{R_{down}} + L_C + L_{R_{up}}, t)\, h_m^+(L_{R_{down}} + L_C + L_{R_{up}}, t)\big|_R \end{aligned} \tag{F.63}$$

$$\frac{\partial}{\partial t}\left(m_{fuel}\, \chi_{fuel}\, T_{fuel}\right) = q^{'''}\, m_{fuel}\, \rho_{fuel} - q^{''}\, A_t \tag{F.64}$$

Coupling equations between neutronics and thermo-hydraulics

$$\Sigma_{C1a} = \Sigma_{C1a}(T_{fuel}, T_{cool}) \tag{F.65}$$

$$\Sigma_{C2a} = \Sigma_{C2a}(T_{fuel}, T_{cool}) \tag{F.66}$$

$$\Sigma_{Ct} = \Sigma_{Ct}(T_{fuel}, T_{cool}) \tag{F.67}$$

$$\mathcal{D}_{C1} = \mathcal{D}_{C1}(T_{fuel}, T_{cool}) \tag{F.68}$$

$$\mathcal{D}_{C2} = \mathcal{D}_{C2}(T_{fuel}, T_{cool}) \tag{F.69}$$

$$q^{'''} = \left(\Phi_1\, \Phi_{ref}\, N_{U_{238}}\, \sigma_{U_{238}} + \Phi_1\, \Phi_{ref}\, N_{U_{235}}\, \sigma_{U_{235f}} + \Phi_1\, \Phi_{ref}\, N_{U_{235}}\, \sigma_{U_{235t}}\right)\, E_f\, r_{fuel}^2 \tag{F.70}$$

Nomenclature

A	area
a_g	gravitational acceleration
b	precursor delayed neutron fraction
B	buckling
c	precursor density
d	thermal diffusion coefficient
D	diameter
$\mathcal{D}$	neutron diffusion coefficient
E	energy
f	neutron transfer probability
f_m	mass fraction
f_M	Moody's factor
f_v	volume fraction
Fr	Froude number
g	mass flux
G	integrated mass flow rate (referred to the thermohydraulics 0-D model)
h	enthalpy
l	surface protusion depth
L	channel length
k	multiplicative factor
m	mass
M	integrated mass (referred to the thermohydraulics 0-D model)
n	neutron density
N	nucleus density

p	pressure
P	perimeter
q''	thermal flux
q'''	thermal power volumetric density
r	radius
R	thermal resistance
Re	Reynolds number
s	surface vapor tension
S	slip ratio
t	temporal coordinate
T	temperature
u	internal energy
U	total heat transfer coefficient
v	neutron velocity
V	volume
We	Webber number
x	dynamic quality
z	spatial coordinate

Greek symbols

α	void fraction
α_ϱ	reactivity feedback coefficient
β	volumetric ratio
η	heat transfer coefficient
θ	channel slope angle
κ	thermal conductivity coefficient
λ	precursor decay constant
Λ	neutron generation time
μ	viscosity
ν	mean value of the fission neutrons
ξ	volumetric expansion coefficient
ρ	density
ϱ	reactivity

σ	microscopic cross section
Σ	macroscopic cross section
τ	neutron life time
Φ	relative neutron flux
ϕ	absolute neutron flux
$\phi_{LO,L}$	two phase multiplier
χ	specific heat

Subscripts

abs	absorption
C	core region
$clad$	clad
$cool$	coolant
eff	effective
ext	external
f	fission
$fuel$	fuel
F	frictional
gap	gap
h	hydraulic
i	precursor group
in	channel inlet
int	internal
L	liquid phase
m	mixture
nom	nominal
out	channel outlet
ref	reference
R	reflector region
R_{down}	down reflector
R_{up}	up reflector
sat	saturation
$scat$	scattering

t	thermal
U	uranium
U_{235}	uranium 235
U_{238}	uranium 238
V	vapor phase
ZrH_x	zyrconium hydride
0	initial
1	fast group (referred to the 1-D neutronics model)
	subcooled region (referred to the 0-D thermohydraulics models)
2	thermal group (referred to the 1-D neutronics model)
	saturated region (referred to the 0-D thermohydraulics model)
3	superheated region (referred to the 0-D thermohydraulics model)
12	moving boundary between the subcooled region and the saturated one (referred to the 0-D thermohydraulics model)
23	moving boundary between the saturated region and the superheated one (referred to the 0-D thermohydraulics model)

Superscripts

SP	single phase
TP	two phase
$+$	dynamic (referred to the 1-D thermohydraulics model)

Mathematical symbols

$\langle\rangle$	mean value on a certain length

Bibliography

Gianfranco Caruso. *Esercitazioni di Impianti Nucleari.* Aracne, 2003.

Gilberto Rinaldi. *Materiali e combustibili nucleari.* Siderea, 2006.

James J. Duderstadt and Louis J. Hamilton. *Nuclear reactor analysis.* John Wiley&sons, 1976.

Neil E. Todreas and Mujid S. Kazimi. *NUCLEAR SYSTEMS I - Thermal Hydraulic Fundamentals.* Taylor&Francis, 1989.

Sandro Salsa and Federico M.G. Vegni and Anna Zaretti and Paolo Zunino. *Invito alle equazioni a derivate parziali.* Springer, 2009.

Cammi, A. Cammi and F. Finzi and C. Lombardi and M. E. Ricotti and L. Santini. *A "Generation III+" nuclear reactor for space needs.* Progress in nuclear energy, 2009.

Gregory D. Spriggs and Robert D. Busch and John G. William. *Two-region kinetic model for reflected reactor.* Annals of nuclear energy, 1997.

M. T. Simnad. *The U-ZrH_x alloy: its properties and use in Triga fuel.* Nuclear Engineering and design, 1981.

Enrico Mainardi and Ugo Spezia. *Orizzonti della tecnologia nucleare in Italia.* Giornata di studio AIN 2004.

V. Memoli and A.Cammi. *Evaluation of the moderator temperature coefficient of reactivity in a PWR.* COMSOL User Conference 2007 Grenoble.

Vito Memoli and Andrea Bigoni and Antonio Cammi and Marco Colombo and Carlo Lombardi and Davide Papini and Marco Enrico Ricotti. *Preliminar feasibility study of a water space reactor with an innovative reactivity control system.* PHYSOR 2010 - Advances in Reactor Physics to Power the Nuclear Renaissance.

Vito Memoli. *Modeling approaches for analysis of innovative nuclear reactors.* PhD Thesys, 2010.

COMSOL Multiphysics User's Guide